0051714

DOE/RL-99-11
Rev. 0

200-BP-1 Prototype Barrier Treatability Test Report

SEP 1999
RECEIVED
EDMC

United States
Department of Energy

TRADEMARK DISCLAIMER

Reference herein to any specific commercial product, process, or service by trade name, trademark, manufacturer, or otherwise, does not necessarily constitute or imply its endorsement, recommendation, or favoring by the United States Government or any agency thereof or its contractors or subcontractors.

This report has been reproduced from the best available copy.
Available in paper copy and microfiche.

Available to the U.S. Department of Energy
and its contractors from
Office of Scientific and Technical Information
P.O. Box 62
Oak Ridge, TN 37831
(615) 576-8401

Available to the public from the U.S. Department of Commerce
National Technical Information Service
5285 Port Royal Road
Springfield, VA 22161
(703) 487-4650

Printed in the United States of America

DISCLM-5.CHP (8-91)

DOE/RL-99-11
Rev. 0

200-BP-1 Prototype Barrier Treatability Test Report

August 1999

United States Department of Energy

P.O. Box 550, Richland, Washington 99352

EXECUTIVE SUMMARY

A 4-year (fiscal years 1995 through 1998) treatability test has been successfully completed on a prototype of the Hanford Barrier constructed in fiscal year 1994 over the 216-B-57 Crib in the 200-BP-1 Operable Unit. The primary purpose of the test was to document surface barrier constructability, construction costs, and physical and hydrologic performance in support of the remediation of the remaining waste sites within the 200-BP-1 Operable Unit. In addition to satisfying data needs specific to the 200-BP-1 Operable Unit, treatability test results will also support the evaluation and potential application of surface barriers at other waste sites on the Hanford Site.

The principal surface barrier performance parameters evaluated during the treatability test included water balance within the barrier under ambient and extreme precipitation conditions; surface wind and water erosion; stability of the barrier foundation, surface, and riprap side slope; surface vegetation dynamics; and animal intrusion. Using irrigation techniques, extreme precipitation conditions were simulated by applying water up to three times normal, including 1,000-year storms. Treatability test objectives have been achieved or exceeded by the 4 years of testing. Results demonstrate that the barrier is easily constructed with standard construction equipment, performance criteria have been met or exceeded, and the Hanford Barrier and associated design components are highly effective.

This report summarizes the results of the treatability test, and provides recommendations for future monitoring of the prototype Hanford Barrier, remediation of the operable unit, optimizing barrier design components, and additional barrier development needs.

CONTENTS

1.0 INTRODUCTION 1-1
1.1 PURPOSE AND SCOPE 1-1
1.2 SITE BACKGROUND 1-3
1.3 TECHNOLOGY DESCRIPTION 1-4
1.3.1 Barrier Development Program 1-4
1.3.2 Hanford Barrier 1-5

2.0 TREATABILITY STUDY APPROACH 2-1
2.1 TEST OBJECTIVES 2-1
2.2 EXPERIMENTAL DESIGN 2-2
2.2.1 Phase I Barrier Constructability Evaluation and Cost 2-2
2.2.2 Phase II Barrier Performance Testing and Monitoring 2-3

3.0 RESULTS AND DISCUSSION 3-1
3.1 PHASE I BARRIER CONSTRUCTABILITY AND COST 3-1
3.1.1 Cost Data 3-2
3.1.2 RCRA Equivalency: Asphalt Layer 3-2
3.2 PHASE II BARRIER PERFORMANCE TESTING AND MONITORING 3-5
3.2.1 Water Balance 3-5
3.2.2 Water and Wind Erosion 3-25
3.2.3 Stability 3-34
3.2.4 Vegetation 3-40
3.2.5 Animal Intrusion 3-51
3.2.6 Summary of Vegetation and Animal Intrusion Observations 3-51
3.3 DEVIATIONS FROM TEST PLAN/COMPARISON OF TEST OBJECTIVES 3-52
3.4 QUALITY ASSURANCE 3-52

4.0 CONCLUSIONS AND RECOMMENDATIONS 4-1

5.0 REFERENCES 5-1

APPENDICES

A PROTOTYPE HANFORD BARRIER DRAWINGS AND AERIAL PHOTOGRAPH ..... A-i
B SUMMARY OF SOIL WATER STORAGE DATA FOR THE HANFORD BARRIER FOR WY 1995 THROUGH WY 1998 ..... B-i
C SUMMARY OF DRAINAGE DATA FOR THE HANFORD BARRIER FOR WY 1995 THROUGH WY 1998 ..... C-i

FIGURES

1-1. Location of the 200-BP-1 Operable Unit and 216-B-57 Crib 1-2
1-2. Hanford Prototype Surface Barrier Cross Section. 1-6
1-3. Hanford Prototype Surface Barrier Cross Section, Basalt Riprap Side Slope. 1-7
1-4. Hanford Prototype Surface Barrier Cross Section, Gravel Side Slope. 1-9
2-1. Plan View of the Prototype Hanford Barrier Showing Layout of the 2 Precipitation Treatments, the 3 Buffer Zones, and the 12 Surface Soil Plots (1W-6W and 1E-6E) 2-4
2-2. Plan View of the Barrier's Surface Showing the Location of the 14 Water Balance Monitoring Stations and Horizontal Neutron Access Tubes. 2-7
2-3. Cross Section of a Typical Water Balance Monitoring Station. 2-8
2-4. Plan View of the Barrier's Surface Showing the 3-m x 3-m Grid and Relative Positions of the Water Balance Monitoring Stations (S1 Through S14). 2-12
2-5. Schematic of Drainage Monitoring System Showing the Siphon Vault and Associated Monitoring Instruments. 2-14
2-6. Schematic of a Creep Gauge. 2-19
2-7. Measurement, Instrumentation, and Data Collection Flow Diagram for the Prototype Surface Barrier. 2-23
3-1. Scheduled Monthly Irrigation Water Application Followed During the First 3 Years of the Treatability Test. 3-7
3-2. Cumulative 4-Year Precipitation Data for the Prototype Barrier 3-7
3-3. Comparison of Water Content $\theta(z)$ Measured with a Seven-Segment Remote Shorting TDR Probe with (a) θ Determined by Gravimetry in a Draining Sand Column, and (b) Field Measurements of θ (by Neutron Probe) in the Silt Loam. 3-8
3-4. Temporal Variation in Soil Water Storage at the Barrier, for Each of the Silt-Loam Plots, from November 1, 1994 through September 30, 1998. 3-10
3-5. Spatiotemporal Variations in Soil Water Content at the Bottom of the Silt-Loam Layer of the Irrigated Treatment of the Barrier. 3-11
3-6. Spatiotemporal Variations in Soil Water Content at the Bottom of the Silt-Loam Layer of the Nonirrigated Treatment of the Barrier. 3-12
3-7. A Comparison of Temporal Variations in Soil Water Content Along Two Transects at the Bottom of Silt-Loam Layer of the Barrier. 3-14
3-8. Cumulative Drainage from the 12 Collection Zones on the Asphalt Pad. 3-15
3-9. Spatiotemporal Variations in Soil Water Content Under the Asphalt Layer. 3-19
3-10. Peak Gust Wind Profiles Measured over the Elevated Surface of the Hanford Barrier on March 30, 1997. 3-29
3-11. Normalized Vertical Profile of Soil Mass Blowing Across the Barrier's Surface Between September 29, 1994 and November 1, 1994. 3-30
3-12. Particle Size Distribution of Soil Material Collected in Dust Traps at the Barrier in WY 1995. 3-31
3-13. Surface Elevations at the Prototype Barrier. 3-35
3-14. Summary of Changes in Settlement Gauge Elevation Between November 1, 1994 and September 1997. 3-37
3-15. Creep Gauge Movement Between December 1994 and September 1995. 3-38
3-16. Creep Gauge Movement Between December 1994 and September 1997. 3-39

3-17. Number of Annual and Perennial Species Including Total Species on the Barrier's Surface. 3-43
3-18. Mean Root Length Density as a Function of Depth in WY 1995, WY 1996, and WY 1997. 3-49
3-19. Mean Survivorship for *Artemisia tridentata* and *Chrysothamnus nauseosus* in WY 1995, WY 1996, and WY 1997 for the Nonirrigated and Irrigated Treatments. ... 3-50

TABLES

2-1. Treatment Structure for the Prototype Surface Barrier. 2-5
2-2. Expected Precision for Major Water Balance, Stability, and Biointrusion Measurements at the Prototype Surface Barrier. 2-15
3-1. Prototype Hanford Barrier Project Costs. 3-2
3-2. Breakdown of Fixed-Price Construction Costs. 3-3
3-3. Unit Costs. 3-4
3-4. Field Asphalt (Without Fluid Application) Permeability Data for the 200-BP-1 Prototype Barrier. 3-4
3-5. Laboratory Asphalt (Without Fluid Application) Permeability Data for the 200-BP-1 Prototype Barrier. 3-4
3-6. Amounts of Water Diverted by the Asphalt Pad (Drainage) at the Prototype Barrier and the Relationship to Precipitation During the Period WY 1995 Through WY 1998. 3-16
3-7. Water Balance Summary for the Hanford Prototype Barrier. 3-24
3-8. Mean % Pea Gravel Content ($\overline{G}$) and the Standard Deviation of the Mean ($\sigma_{\overline{G}}$) of Near-Surface (0-2 cm) and Bulk Samples (0-10 cm) Obtained from the from the Prototype Surface Barrier. 3-32
3-9. Plant Species Observed on the Prototype Surface Barrier. 3-41
3-10. Median and Mode of the Percent Cover Classes. 3-44
3-11. Mann-Whitney Test Results for Cover Class Comparisons Between Years Within Treatments and Between Treatments Within Year. 3-45
3-12. Estimated Leaf Area Index of *Artemisia tridentata* in Each Treatment in WY 1997. 3-48
3-13. Percentage of *Artemisia tridentata* Shrubs with Mature Seed Heads in the Irrigated and Nonirrigated Treatments. 3-50

THIS PAGE INTENTIONALLY
LEFT BLANK

ACRONYMS AND ABBREVIATIONS

ARAR	applicable or relevant and appropriate requirement
ASTM	American Society for Testing and Materials
CERCLA	*Comprehensive Environmental Response, Compensation, and Liability Act*
DOE	U.S. Department of Energy
EDM	electronic distance measurement
EI	erosivity index
EPA	U.S. Environmental Protection Agency
ET	evapotranspiration
FY	fiscal year (October 1 – September 30)
ID	inner diameter
LTA	long-term average
NCP	*National Oil and Hazardous Substances Contingency Plan*
p	significance
PVC	polyvinyl chloride
RCRA	*Resource Conservation and Recovery Act*
RI/FS	remedial investigation/feasibility study
SDRI	sealed double-ring infiltrometer
TDR	time domain reflectrometry
Tri-Party Agreement	*Hanford Federal Facility Agreement and Consent Order*
WY	water year (November 1 – October 31)

1.0 INTRODUCTION

The 200-BP-1 Operable Unit is located in the 200 East Area of the Hanford Site. Results of a feasibility study completed for the source operable unit suggested that a surface barrier would be a viable remedial action alternative for waste sites within the operable unit. Prior to constructing a final barrier over the remaining 216-BY-Cribs, the Tri-Parties agreed on the need for a multi-year treatability study to assess surface barrier constructability and provide cost and performance information needed to fully evaluate and support the selection of a surface barrier as the preferred remedial alternative. This report summarizes the results of a 4-year treatability study completed on a full-scale surface barrier constructed in fiscal year (FY) 1994.

1.1 PURPOSE AND SCOPE

A treatability test was conducted on a full-scale surface barrier constructed over the 216-B-57 Crib within the 200-BP-1 Operable Unit (Figure 1-1). The treatability test was performed as part of the *Comprehensive Environmental Response, Compensation, and Liability Act* (CERCLA) remedial investigation/feasibility study (RI/FS) process for the operable unit to collect performance and cost data needed to fully evaluate surface barriers as a proposed remedial alternative. The report provides conclusions/recommendations on the barrier's constructability, cost, performance, applicability as a remedial alternative, and readiness for implementation. Surface barrier testing and monitoring activities were performed over a 4-year period starting in FY 1995. The treatability test was originally scheduled for 3 years, in accordance with *Hanford Federal Facility Agreement and Consent Order* (Tri-Party Agreement) Change Request M-15-92-5. However, additional funding was obtained for FY 1998 to extend the testing and monitoring activities to nearly 4 years.

The purpose of the test was to demonstrate the physical and hydrologic performance of a prototype of the Hanford Barrier, to document constructability, and to provide cost data to support the implementation of surface barriers as a remedial action for final closure of the remaining waste sites within the 200-BP-1 Operable Unit. In addition to satisfying 200-BP-1-specific data needs, testing of a full-scale barrier will support remedy selection decisions and the remedial design and implementation process for other waste sites on the Hanford Site. Conceptual surface barrier designs, including the Hanford Barrier, have been established through the feasibility study process. A graded approach to cover design has been developed whereby a limited number of barrier designs satisfy the requirements of a broad range of waste sites (DOE-RL 1996, 1999). The 200 Area barrier focused feasibility study (DOE-RL 1996) provides performance and cost comparisons along with an applicable or relevant and appropriate requirement (ARAR) evaluation of these graded barriers (including the Hanford Barrier) and the standard *Resource Conservation and Recovery Act* (RCRA) Subtitle C design. The Hanford Barrier provides the maximum degree of containment and hydrologic protection of the graded barrier designs. Although the application of the Hanford Barrier itself is expected to be limited (e.g., to waste sites with significant transuranic inventories), the Hanford Barrier test results can be used to guide the design of more modest surface barrier designs because they share common

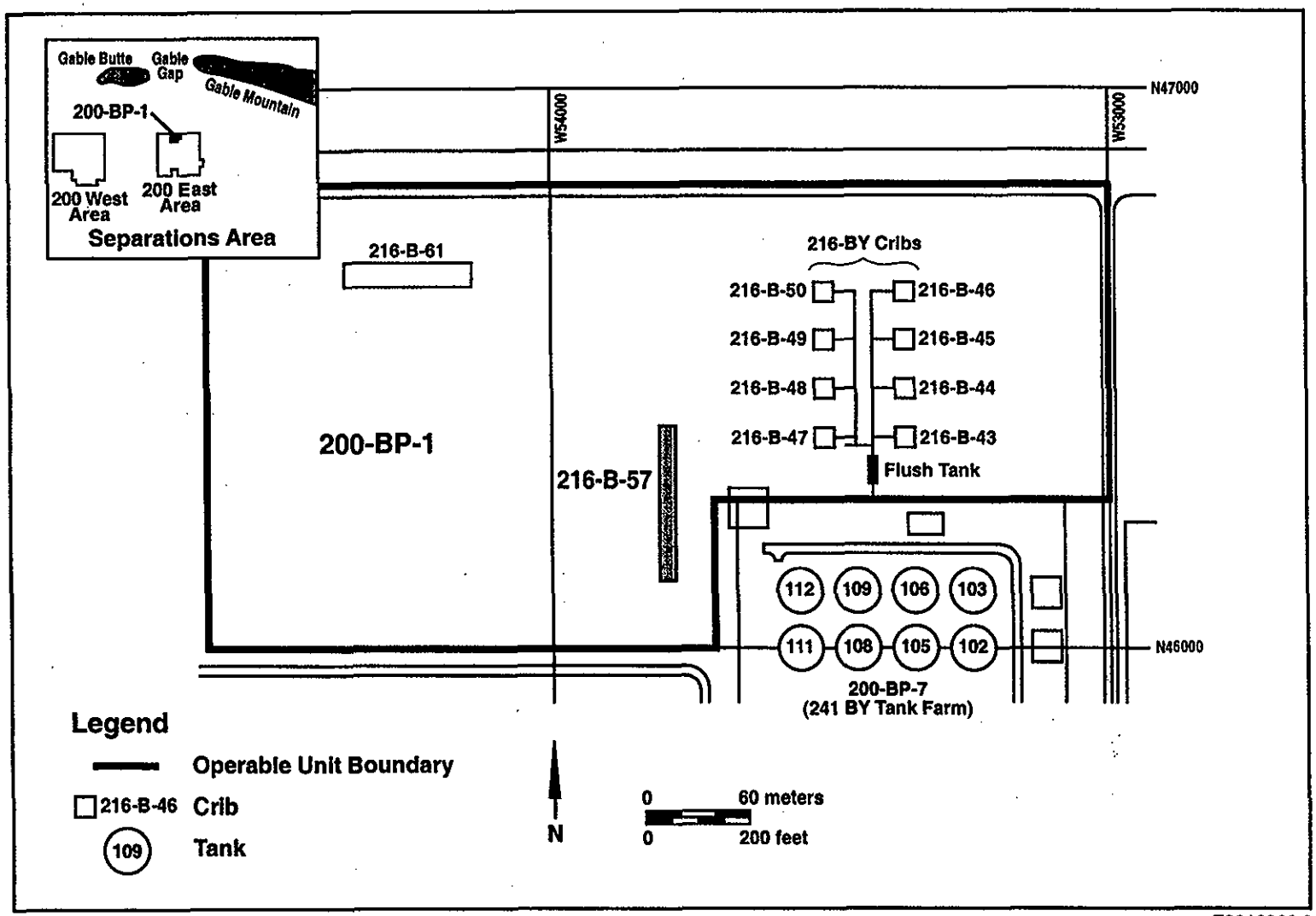

Figure 1-1. Location of the 200-BP-1 Operable Unit and 216-B-57 Crib.

design concepts and components (e.g., capillary break, vegetative components). The remedial design process will be streamlined by having a thoroughly tested set of surface barrier design elements from which site-specific definitive designs can be prepared.

Barrier test performance objectives (see Section 2.1) and requirements were defined in the *Treatability Test Plan for the 200-BP-1 Operable Unit* (DOE-RL 1993a) prepared in FY 1993. In addition to the treatability test plan, a monitoring and testing plan was prepared (Gee et al. 1993b) to provide an additional level of detail to guide the barrier testing program. Yearly summary reports have documented the progress of the testing and monitoring activities (Gee et al. 1995, 1996; Ward et al. 1997).

1.2 SITE BACKGROUND

The 200-BP-1 Operable Unit is located in the approximate center of the Hanford Site, along the northern boundary of the 200 East Area. The operable unit consists of 10 waste sites (cribs) that were used to dispose of low-level radioactive liquid waste from 1955 to 1975. The low-level radioactive waste was a result of U Plant uranium reclamation operations (scavenged supernatant) and waste storage tank condensate from the adjacent 241-BY Tank Farm.

In March 1990, the U.S. Department of Energy (DOE) issued the *Remedial Investigation/ Feasibility Study Work Plan for the 200-BP-1 Operable Unit, Hanford Site, Richland, Washington* (DOE-RL 1990) and initiated site characterization activities. Characterization included a variety of activities that included collection of soil samples from the surface to groundwater (approximately 76.2 m [250 ft] below ground surface).

The results of the study indicated that the majority of high-activity (greater than 1,000,000 pCi/g) contaminated soils are located between 5 and 15 m below ground surface. The primary contaminants of concern remaining in the subsurface soil include strontium-90, cesium-137, plutonium-238, plutonium-239/240, and uranium. Most of the radioactivity is associated with strontium-90 and cesium-137. The contaminants are generally immobile with the exception of uranium, which also has a relatively long half-live (DOE-RL 1993a). Transport modeling results for a surface barrier remediation scenario indicated that uranium would not impact groundwater in excess of proposed drinking water standards within the design life of a barrier (DOE-RL 1994b).

Based on the results of the Phase I remedial investigation, a feasibility study was prepared to examine a range of remedial alternatives and provide a preferred alternative (DOE-RL 1994b). The range of alternatives included no action with institutional controls, three barrier alternatives, four alternatives that involve excavation of the high-activity soils with and without treatment, and one in-situ treatment alternative. A detailed analysis was completed for each of the remedial technologies in accordance with CERCLA and the *National Oil and Hazardous Substances Contingency Plan* (NCP). The results of the comparative analysis suggest that a low-permeability barrier is appropriate for the waste sites within the 200-BP-1 Operable Unit. A draft proposed plan for the operable unit was submitted to the regulators in 1994. Prior to issuance of the proposed plan for public review for the 200-BP-1 waste sites, the U.S. Environmental Protection Agency (EPA) required additional construction and performance data on the proposed barrier collected under this treatability test. Tri-Party Agreement

milestones M-15-02E-T3 through –T7 were established for issuance of a record of decision through completion of remedial activities for the 200-BP-1 Operable Unit. Completion of these milestones is pending the completion of the proposed plan process. The 216-B-57 Crib, within the 200-BP-1 Operable Unit, was the location for conducting this treatability test.

1.3 TECHNOLOGY DESCRIPTION

1.3.1 Barrier Development Program

Surface barriers have been identified as a critical component in management of buried wastes and other sources of subsurface contamination (Daniel 1994b, Daniel et al. 1996). At the Hanford Site, more than 200 past-practice disposal sites have been identified for the possible deployment of surface barriers (DOE-RL 1996). The main function of surface barriers is to ensure that buried wastes are contained and protected from environmental and biotic forces. For waste sites with transuranic constituents, a functional design life of up to 1,000 years is needed (DOE-RL 1996). The 1,000-year design life approaches the upper range of credible and defensible extrapolations of surface barrier performance results. A design life beyond 1,000 years may be beyond normal engineering and scientific capabilities, and tends to be difficult to prove given the great number of uncertainties and assumptions.

Barrier technology, particularly for long-term deployment, remains largely unproven at the field scale. For this reason, the single greatest research and development need related to the use of surface barrier technology in managing hazardous wastes is to document field performance and case histories (Daniel 1994b).

A barrier development program was initiated at the Hanford Site in the mid-1980's as a result of recommendations from the *Final Environmental Impact Statement for the Disposal of Hanford Defense High-Level, Transuranic, and Tank Wastes* (DOE 1987). The barrier program was organized to develop the technology for permanent, long-term containment of near-surface radioactive waste. After nearly 10 years of research, a multilayered earthen barrier was developed and ready for prototype construction and testing.

To obtain representative, supportable cost estimates and authentic performance data, construction of the prototype barrier was recommended over an existing waste site. The 200-BP-1 Operable Unit (216-B-57 Crib) was an ideal location to support outstanding issues from the EPA for remedial action deployment at the 200-BP-1 Operable Unit and provide large-scale barrier performance data. The Hanford Barrier program and remediation activities for the 200-BP-1 Operable Unit were integrated into a single program. Construction and testing was completed under a CERCLA treatability test.

In addition to the Hanford Barrier, additional surface barrier designs have been developed with varying levels of protection (graded approach) for potential application as final remedial actions for the broad range of waste sites present in the 200 Areas (DOE-RL 1996). Completion of this treatability test not only supports the RI/FS process for the 200-BP-1 Operable Unit, but represents a major step in the overall Hanford surface barrier program in demonstrating the performance of the Hanford Barrier design. A path forward for the 200-BP-1 Operable Unit, as

well as general design considerations, priority issues, and future testing needs applicable to an overall barrier development program, are discussed in Section 4.0.

1.3.2 Hanford Barrier

The Hanford Barrier was developed to provide long-term protection (1,000 years) of certain types of waste in semiarid environments and exceed RCRA cover design requirements, including life expectancy and hydraulic conductivity. The surface barrier consists of a variety of natural materials placed in engineered layers. Natural stable construction materials were selected to optimize barrier performance and longevity. The primary function of a surface barrier is to contain waste in place by minimizing (1) the infiltration of precipitation into contaminated soil or debris, thereby minimizing the driving force for downward migration of contaminants; (2) the migration of windblown dust originating from contaminated surface soils; and (3) the intrusion potential for direct exposure to contamination. Key performance objectives for the Hanford Barrier include the following:

- Function in a semiarid to subhumid climate
- A design life of 1,000 years
- Limit drainage through the silt to less than 0.5 mm yr^{-1}
- Limit runoff
- Be maintenance free
- Minimize biotic intrusion
- Minimize erosion
- Meet or exceed RCRA performance criteria.

The barrier design consists of a fine soil (silt-loam) layer overlying other, coarser materials such as sands, gravels, and basalt riprap (Figure 1-3 and Appendix A). Each layer serves a distinct purpose. The silt-loam layer acts as a medium in which moisture is stored until the processes of evaporation and transpiration recycle any excess water back to the atmosphere. The design storage capacity, the total amount of water that can be stored in the silt-loam layer before drainage occurs, is 600 mm based on an assumed available water storage capacity of 0.3 volume water/volume soil estimated from field lysimeter results (0.3% x 2,000 mm silt loam = 600 mm storage capacity). The silt loam is designed to store more than three times the long-term average (LTA) annual precipitation at the Hanford Site. The silt loam also provides a medium for establishing plants, which are necessary for transpiration to take place. In addition, the top 1 m of silt loam had been amended with pea gravel to minimize wind erosion. Coarser materials (sand overlying gravel) placed directly below the silt-loam layer create a capillary break that inhibits the downward percolation of water through the silt (similar to a sponge holding water) and prevent fine soil from filtering downward into the coarse layer. The coarser materials (i.e., basalt riprap) also help deter root penetration, animal burrowing, and inadvertent human intruders (biointrusion) through the barrier profile. An asphalt layer is placed at the bottom of the barrier to provide a low-permeability (hydraulic barrier) and redundant biointrusion layer.

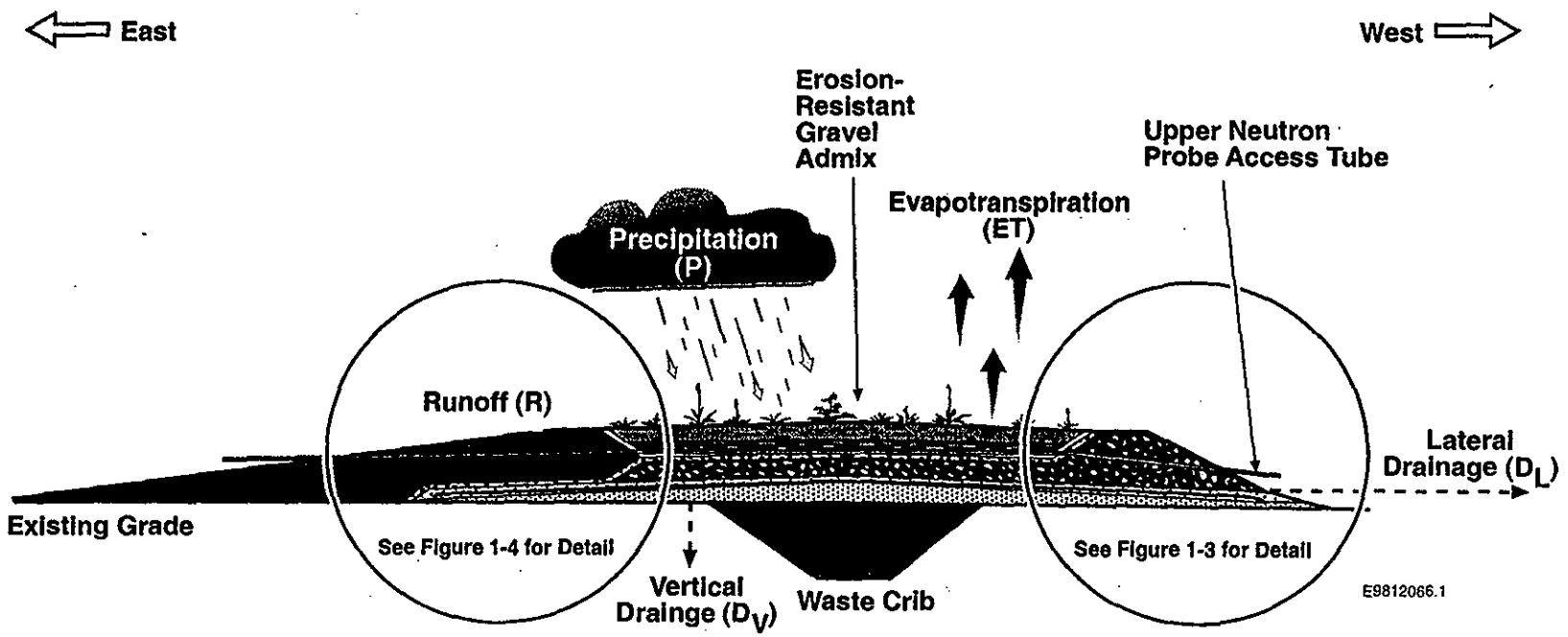

Figure 1-2. Hanford Prototype Surface Barrier Cross Section.

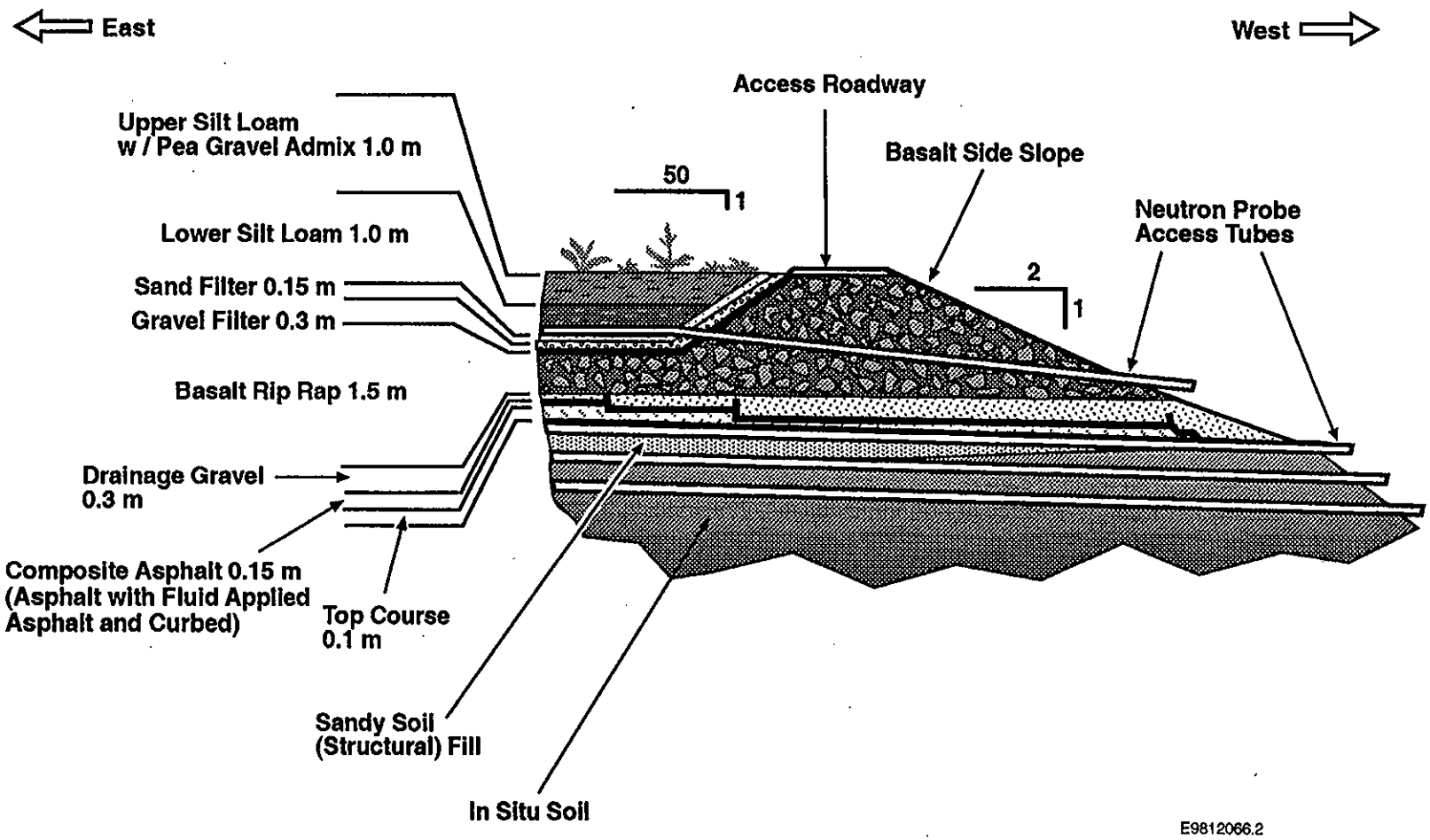

Figure 1-3. Hanford Prototype Surface Barrier Cross Section, Basalt Riprap Side Slope.

Two side-slope configurations are being considered for the Hanford Barrier (Figures 1-3, 1-4, and Appendix A). The first configuration is a relatively steep embankment of basalt riprap (less than 25 cm diameter) placed at approximately a 2:1 slope. The angularity of the riprap provides many interlocking surfaces between adjacent rocks, allowing the creation of a relatively steep yet stable side slope. The second configuration is a relatively flat slope of naturally occurring coarse material (pit run gravel) placed at approximately a 10:1 slope. The flat side slope forms an apron around the periphery of the barrier. This apron provides a gentle transition from the shoulder of the barrier to the surrounding topography.

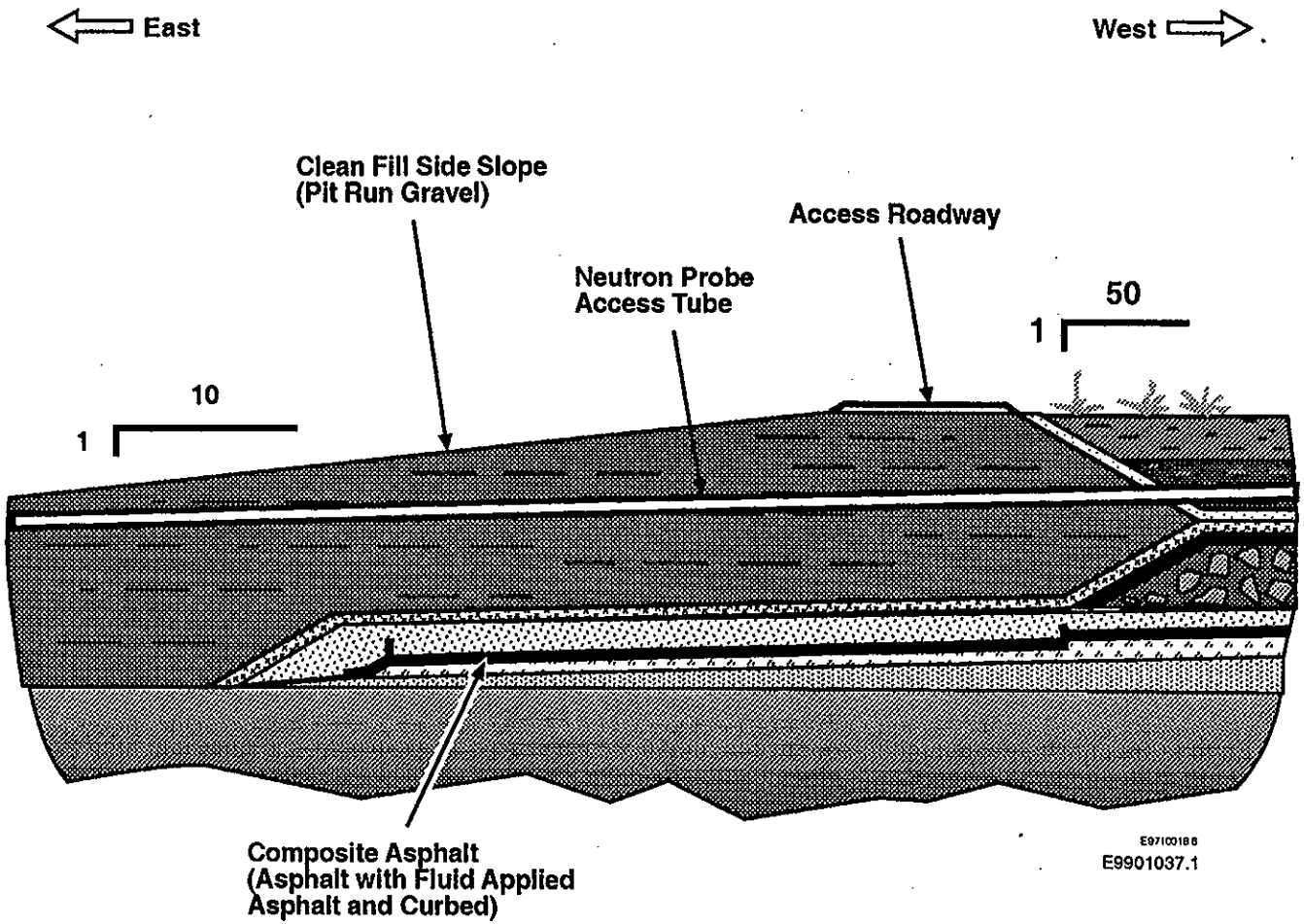

Figure 1-4. Hanford Prototype Surface Barrier Cross Section, Gravel Side Slope.

2.0 TREATABILITY STUDY APPROACH

The Hanford Barrier is a baseline surface barrier design developed for the semiarid climatic conditions at the Hanford Site. The overall objective of the Hanford Barrier design is to provide a highly protective surface barrier system to isolate wastes for an extended period of time using natural materials. Prior to construction of the prototype barrier, barrier performance had been extensively evaluated only through laboratory and small-scale field experiments and computer model simulations. A field-scale experiment was required to enable engineers and scientists to obtain experience in constructing protective barriers and demonstrating their performance.

The treatability test addressed each of the key performance objectives identified in Section 1.3.2 within the time frame of the testing period (4 years). The test did not attempt to project barrier performance over the design life of 1,000 years. The design life of 1,000 years is supported by the use of stable construction materials (largely geologic materials), and previous longevity evaluations completed as part of the barrier development program (see Section 1.3.1). The test did evaluate the performance of the barrier under three times normal precipitation conditions projected as an upper bound for potential climatic change at the Hanford Site, as well as the projected 1,000-year storm.

The treatability test was completed in two phases. Phase I consisted of the design and construction of the prototype Hanford Barrier. Phase I was completed in August 1994. Design and construction activities are briefly discussed in this treatability test report. Detailed information can be found in the *Construction Report for the 200-BP-1 Prototype Surface Barrier* (DOE-RL 1994a). Phase II consisted of a 4-year testing and monitoring program, which is the focus of this report. Additional details can be found in annual reports as required by the Treatability Test Plan (Gee et al. 1995, 1996; Ward et al. 1997).

2.1 TEST OBJECTIVES

The primary goal of the prototype Hanford Barrier treatability test was to assess construction and performance data. Consistent with this goal, the objectives of the treatability test are summarized as follows:

- Evaluate the effectiveness of the barrier components (e.g., the various material layers) individually and as they interact to form a complete/whole engineered system
- Provide large-scale testing of phenomena that are not adequately tested on small-scale plots, in laboratories, or with lysimeters
- Provide a baseline by demonstrating barrier system performance under both stressed and ambient conditions
- Document the testing and monitoring activities for the purpose of peer review and critique, regulatory review, and technology transfer

- Provide a more accurate basis for estimating the costs associated with constructing permanent isolation surface barriers

- Use the information and insights gained from testing activities to direct future barrier development and construction activities.

To ensure that the correct level of detail and data quality was achieved to satisfy these goals and objectives, data quality objectives were defined as follows:

- Collect appropriate data during the construction of the prototype barrier to ensure that the structure has been constructed consistent with the design specifications

- Collect the appropriate data during the monitoring and testing phase of the treatability study to evaluate the performance goals listed above

- Collect sufficient data to support Hanford Site remedial action objectives and regulatory approval.

2.2 EXPERIMENTAL DESIGN

2.2.1 Phase I Barrier Constructability Evaluation and Cost

As part of Phase I testing, constructability data were collected to determine if the barrier could be constructed with standard equipment as designed. A construction quality assurance plan was developed to ensure compliance with design specifications. The plan identified inspection, testing, and verification requirements for individual barrier components (e.g., subgrade, asphalt, drainage gravel, basalt, filter material, and silt loam). Execution of the construction quality assurance was completed by an independent third party. As-built drawings of the barrier were completed after construction. Detailed results of the construction quality assurance can be found in *Construction Quality Assurance Report for the Prototype Surface Barrier* (BHI 1995).

Construction cost data were also identified as an important data need to support decision making for future remedial action activities. Standard project management tools were used to collect cost and schedule data. Mileage to borrow sources was recorded and cycle times documented for material transport.

RCRA equivalency with respect to hydraulic performance of the asphalt (without the fluid-applied asphalt layer) was completed during the construction of the prototype Hanford Barrier. A series of field and laboratory tests were completed on the surface of the barrier's asphalt layer and an adjacent asphalt test pad. The test pad was built just north of the barrier, prior to construction of the barrier to ensure that layout and compaction requirements could be met (DOE-RL 1994a). Asphalt cores were collected from the test pad at the northern end of the barrier after placement of the asphalt layer. Permeability testing was conducted in the laboratory using standard American Society for Testing and Materials (ASTM) methods. A modified falling-head permeameter test was completed on the surface of the barrier's asphalt layer. This method was used to obtain preliminary data prior to installing subsequent layers. The most

accurate hydraulic testing method, ASTM 5093 (ASTM 1990), was conducted on the test pad. Two sealed double-ring infiltrometers (SDRIs) were monitored for nearly 6 months.

2.2.2 Phase II Barrier Performance Testing and Monitoring

As part of Phase II testing, a comprehensive program was designed to test the barrier under both ambient (natural precipitation) and extreme climate (elevated precipitation) conditions for a period of at least 3 years. The program was designed to:

- Evaluate the performance of the barrier using a water-balance approach
- Document the impacts of wind and water erosion on the surface of the barrier
- Evaluate plant community dynamics
- Document the impacts of biointrusion on the barrier.

Descriptions of the experimental design, equipment, and sampling analysis used to assess performance at the prototype Hanford Barrier are provided in the following sections.

2.2.2.1 Experimental Design. For monitoring purposes, the surface of the barrier is divided into two treatments or sections (elevated and ambient), one to the north and the other to the south. The north section was designated to receive an elevated amount of precipitation (natural precipitation plus supplemental irrigation) to simulate extreme climatic conditions (three times the long-term annual precipitation), while the south section received only natural (i.e., ambient) precipitation. To minimize edge effects and interaction between the precipitation treatments, the two sections are separated from each other and from the north and south edges of the barrier by buffer zones. The north section is separated from the south by a 10-m buffer zone. To minimize the impact that the edges could have on monitored processes, the north section is separated from the northern edge by an 18-m buffer zone, whereas a 31-m zone separates the south section from the southern edge. Figure 2-1 is a plan view of the prototype Hanford Barrier showing the layout of the two precipitation treatments.

Each treatment is divided into 6 surface plots (a total of 12), 3 in each quadrant, which coincide with water collection zones of the asphalt layer. The plan view depicted in Figure 2-1 also shows the boundaries of the 12 monitored plots (1W through 6W and 1E through 6E). Each treatment contains two silt-loam-covered plots (14 m by 23 m), two transition plots (4 m by 23 m), and two side-slope plots (one gravel and one basalt riprap). The transition plots separate the soil-covered plots from the riprap and gravel-covered side-slope plots. All of the plots to the north received elevated precipitation, while the plots to the south received only ambient precipitation. Table 2-1 describes each treatment and the associated plots. Each plot was instrumented to permit measurement of physical and biological variables that reflect barrier performance.

During the instrumentation phase, wooden planks were temporarily laid out on the surface to accommodate foot traffic as a precaution against disturbance or compaction of the soil. In addition, a series of concrete stepping stones was installed adjacent to each monitoring transect and along the crown of the barrier to prevent soil disturbance during testing and monitoring activities.

Figure 2-1. Plan View of the Prototype Hanford Barrier Showing Layout of the 2 Precipitation Treatments, the 3 Buffer Zones, and the 12 Surface Soil Plots (1W-6W and 1E-6E).

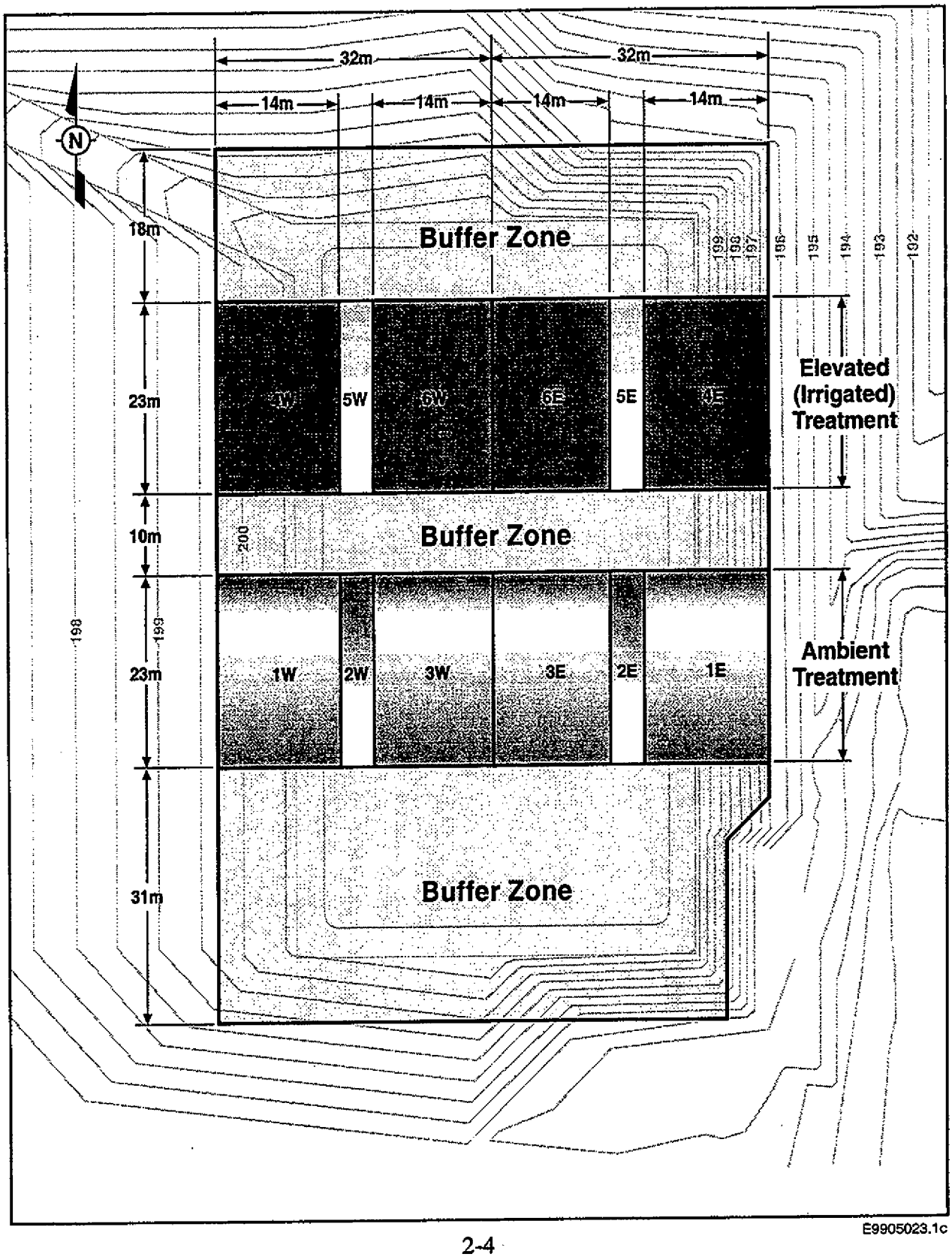

E9905023.1c

Table 2-1. Treatment Structure for the Prototype Surface Barrier.

Section	Precipitation Treatment	Plot Number	Plot Size	Location and Description
North	Ambient precipitation plus irrigation	4W	14 m x 23 m	NW; main gravel-covered plot
		5W	4 m x 23 m	NW; transition silt-loam-covered plot
		6W	14 m x 23 m	NW; main silt-loam-covered plot
		6E	14 m x 23 m	NE; main silt-loam-covered plot
		5E	4 m x 23 m	NE; transition silt-loam-covered plot
		4E	14 m x 23 m	NE; main riprap-covered plot
South	Ambient precipitation	1W	14 m x 23 m	SW; main gravel-covered plot
		2W	4 m x 23 m	SW; transition silt-loam-covered plot
		3W	14 m x 23 m	SW; main silt-loam-covered plot
		3E	14 m x 23 m	SE; main silt-loam-covered plot
		2E	4 m x 23 m	SE; transition silt-loam-covered plot
		1E	14 m x 23 m	SE; main riprap-covered plot

2.2.2.1.1 Water balance. The primary function of the Hanford Barrier is to minimize infiltration of water to buried waste and contaminated soil. Successful performance of the primary function depends on the operation of a series of interactive and dynamic processes that control infiltration, migration, storage, and loss of water. The interactive processes are therefore dependent on the upper 2-m-thick silt-loam layer of the barrier, which is designed to facilitate plant growth and retain water deposited by precipitation until it is recycled, by evapotranspiration (ET), to the atmosphere.

Because these processes all contribute to the water balance, a useful approach to a hydrologic performance evaluation is based on measuring the water-balance components. A schematic cross section of the prototype Hanford Barrier, which includes a depiction of the interactive processes that influence the water balance, was shown in Figure 1-2. The components of the water balance include water inputs by precipitation and irrigation, drainage, surface runoff, changes in water storage (i.e., water content multiplied by the thickness of the soil layer) within the soil profile, and ET. Thus, a major component of the treatability test was the periodic evaluation of the water balance.

A variety of techniques have been developed for measuring the contributions of the different components described above and for evaluating the water balance of soil-water systems. The approach taken in this treatability test is unique in that it is based on the actual measurement of drainage. These data, in combination with measured water inputs from natural precipitation and

irrigation, surface runoff, and soil water storage, permit a more accurate calculation of the final component, ET.

A simplified form of the water-balance equation used to evaluate ET for the Hanford Barrier is written as:

$$ET = (P + I) - (\Delta W + R + D) \tag{2.1}$$

where:

ET	=	evapotranspiration
P	=	natural precipitation
I	=	irrigation
ΔW	=	change in soil water storage
R	=	surface runoff
D	=	drainage out of the soil cover.

The water storage is calculated from soil water content θ by integrating θ over depth profiles. Thus, water storage between the surface and depth L is calculated as follows (Green et al. 1986):

$$W = \int_0^L \theta(z,t)dz \tag{2.2}$$

where:

L	=	maximum depth of measurement.
θ	=	volumetric soil water content
z	=	depth of measurement
t	=	time.

The change in storage, ΔW, is calculated as the difference in water storage measured at different times.

To monitor the hydrologic performance of the top 2-m-thick silt-loam layer under the two precipitation treatments, the surface was fitted with 14 water balance monitoring stations (Figures 2-2 and 2-3). Three stations were installed in each of the silt-loam-covered plots, one station was installed on each of the gravel-covered plots, and none were installed on the transition plots or riprap-covered plots. Figure 2-2 also shows the horizontal neutron access tubes that were used to monitor the distribution of subsurface water content.

Each station is equipped with a precipitation meter (*mini*-lysimeters) to record precipitation events. Additional precipitation data are obtained from six manual rain gauges located in the northern section of the barrier and an automated tipping-bucket gauge located on the gravel-covered side slope. Climatological data are obtained from the Hanford Meteorological Station (HMS), located about 5 km northwest of the barrier.

Figure 2-2. Plan View of the Barrier's Surface Showing the Location of the 14 Water Balance Monitoring Stations and Horizontal Neutron Access Tubes.

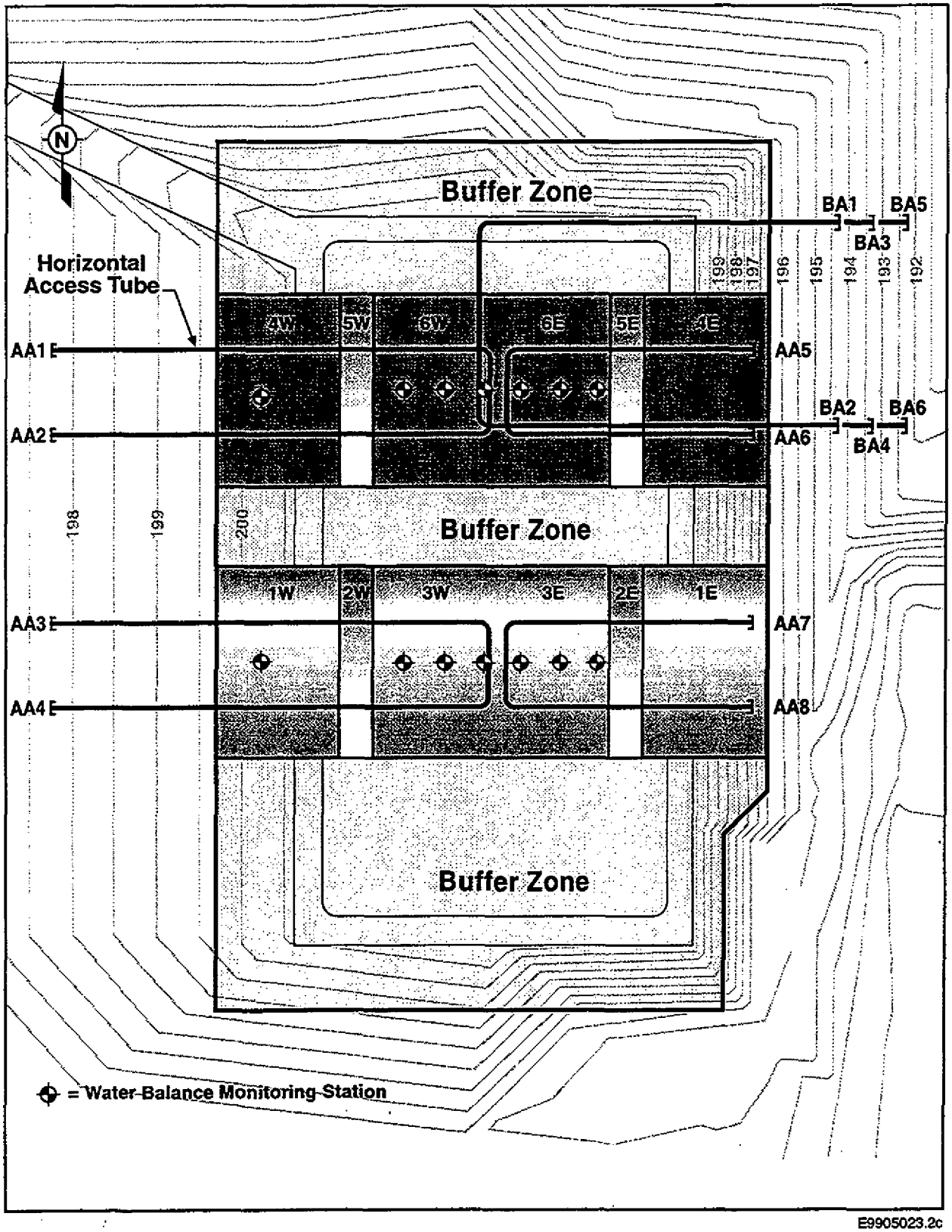

E9905023.2c

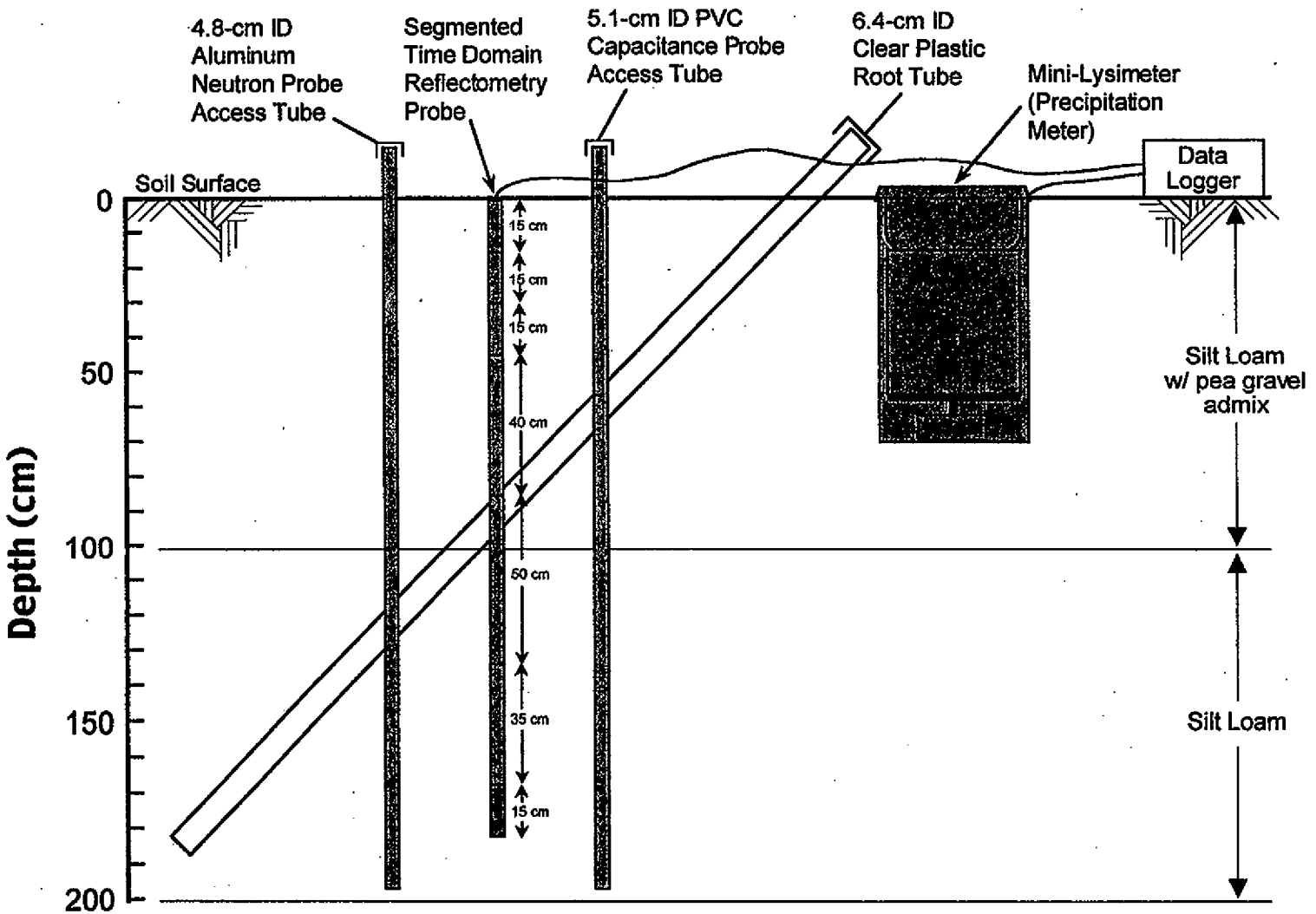

Figure 2-3. Cross Section of a Typical Water Balance Monitoring Station.

To measure water content profiles in the top 2-m-thick silt-loam layer, each monitoring station was fitted with a vertical aluminum access tube for measurements with a neutron probe, a polyvinyl chloride (PVC) access tube for capacitance probe, and a 1.85-m segmented time domain reflectometry (TDR) probe (Figure 2-3). Each surface plot is associated with a water collection system (with boundaries on the asphalt layer) to permit measurement of drainage out of the upper soil layers (Appendix A). Below each treatment, U-shaped horizontal neutron probe access tubes permit measurement of water content above and below the asphalt layer (Figure 2-2 and Appendix A). A pan lysimeter was also installed under the asphalt pad at the northeastern corner of the riprap slope (plot 4E) to permit evaluation of the performance of the asphalt layer (Appendix A).

Detailed descriptions of the various water balance instruments and the procedures governing their use are provided below.

Water inputs. Water received by the barrier was measured by specially constructed mini-lysimeters (Figure 2-3). The lysimeters used a load cell and a collection system that allowed them to act as a rain gauge/snow pillow combination. Thus, rainfall, irrigation, and snow were measured with a single instrument. Fourteen units were installed on the barrier to measure the spatial distribution of precipitation over the surface. These mini-lysimeters, which were controlled by a Campbell Scientific CR-7 datalogger, made measurements once every hour and transmitted data to a base station by telemetry once every 24 hours. The mini-lysimeters were calibrated at least annually to ensure data of the highest quality. Automated measurements of rainfall were supplemented by periodic manual measurements at the barrier and data from the HMS.

Irrigation water was applied with a Lockwood® linear-move, sprinkler irrigation system. The irrigation system spans 42.9 m between road centers and has 10.4-m (34-ft) extension booms beyond the wheels to facilitate irrigation of the side slopes. During irrigation events, the system traveled in a north-to-south direction and back along the roadway. To avoid compaction of the soil surface, movement of the irrigation system was limited to the roadway. The system delivers water at mean rate of about 10 mm hr^{-1} with a coefficient of uniformity of about 96%. Irrigation was initially scheduled to start on November 1, 1994, but was delayed until February 1995 because of water supply problems. Water was usually applied at biweekly intervals, except in winter and depending on the weather. In late March of each year of water years (WY) 1995-1997, a 1,000-year return storm was simulated on the northern section. Although the storm simulated was 68 mm over a 24-hour period, in practice, irrigation was applied at 68 mm over an 8-hour period (Gee et al. 1995).

Soil water content and storage. Soil water content was initially measured using a variety of techniques, including neutron moderation methods, TDR, and frequency domain (capacitance) methods. The three techniques are indirect methods in that they are based on measuring a physical property of the soil that depends on soil water content. All three methods are nondestructive and, except for the TDR method, require manual operation. The neutron method was used as the standard. As treatability testing progressed, the TDR and capacitance probe methods were eliminated from the test because of technical difficulties. Both the TDR and capacitance probe consistently overestimated θ relative to the neutron probe and appeared relatively insensitive to changes in θ at the wetter end of the moisture range (Gee et al. 1995).

The neutron method remained as the only source of water content data. The three methods are briefly reviewed in the following paragraphs

Neutron Method. The neutron method is an indirect method that uses a source of fast neutrons that are slowed down when they interact with the medium surrounding the source. Through collisions with the nuclei of elements in the soil, the neutrons are slowed down. Small atoms are the best for attenuating fast neutrons, and the most efficient is the hydrogen atom. In soils, it is assumed that all of the hydrogen that leads to attenuation of the fast neutrons is due to water molecules present in the soil. Thus, the wetter the soil, the greater the number of slow neutrons.

The equipment used in this test was Campbell Pacific Nuclear hydroprobe (model 503). The hydroprobe consists of a protective shield that houses the nuclear source and the electronic counting system. The probe was deployed in 14 vertical (4.8-cm inner diameter [ID]) aluminum and/or PVC access tubes extending down to 1.9 m from the barrier's surface (Figure 2-3). To permit monitoring of volumetric soil water content, θ, at the capillary break (silt-sand filter interface) and under the asphalt pad, a series of U-shaped access tubes were installed horizontally. Each access tube was constructed from 7.6-cm-ID aluminum tube and installed with the curved section toward the center of the barrier (Figure 2-2 and Appendix A).

At the western side of the prototype surface barrier, a pair of horizontal access tubes was installed at 1.95 m below the surface, near the soil-sand filter interface (AA1, AA2, AA3, AA4; Figure 2-2 and Appendix A). A similar set of tubes (AA5, AA6, AA7, AA8) was also installed at a depth of 1.95 m on the eastern side. Because of the shape of the tubes, a 1-m-wide section on either side of the crown of the barrier is not monitored. Another three sets of tubes were installed under the northeastern section of barrier, below the asphalt layer. Tubes BA1 and BA2 were installed at a depth of 1 m below the asphalt, tubes BA3 and BA4 at 2 m, and tubes BA5 and BA6 at 3 m below the asphalt pad. The northeastern corner of the asphalt pad (under the northern buffer zone) was left uncurbed (Appendix A) to assess the amount of underflow at the edge of the asphalt layer. A 6.5-m by 6.5-m basin lysimeter was also installed beneath the asphalt pad (plot 4E) to assess the permeability of the asphalt layer.

Because of the larger diameter of the horizontal tubes (chosen to minimize the effects of compressive forces), the smaller diameter neutron probe required a carrier to center the tube.

Detailed instructions for using the neutron probe are provided in a surface barrier procedure, PNL-PSB-10.

Time Domain Reflectometry (TDR) Method. The TDR method is an indirect method based on the dependence of the soil's dielectric constant, κ, on volumetric water content. The velocity of a voltage pulse generated along a probe by a TDR unit is used to calculate κ. The dielectric constant for water is 80, while it is between 4 and 8 for the solid phase (e.g., the silt-loam used to construct the surface layer of the barrier), and 1 in air. Because the soil is a mixture of solid, water, and air, with a fixed amount of the solid phase, the value of κ is strongly dependent on the amount of water present. Thus, different combinations of water, air, and soil will lead to different effective values of k, from which θ can be determined with the appropriate calibration relationship. A major advantage of TDR is its insensitivity to textural differences, allowing measurement of θ over a range of soils without the need for extensive calibration.

The main components of the TDR system are a signal generator that produces the voltage pulse and measures the return signal and transit time, transmission lines or probes, and coaxial cable. In the test, specially designed TDR probes (Moisture.Point® system) supplied by Environmental Sensors Inc. were used to measure θ. These probes are of the remote-shorting diode design described by Hook et al. (1992) and were 1.85 m in length. The unique feature of the shorting diode probe is the ability to measure θ profiles at a given location with a single probe. The shorting diode probe was reported to not require a site-specific calibration and as having a linear relationship between θ and $\kappa^{1/2}$ for all soils (Hook and Livingston 1996). The system is fully automated and does not require the use of access tubes. A set of 14 probes was installed, one probe at each monitoring station (Figures 2-2 and 2-3). The probes were connected via 50-m cables to a central multiplexing system and controlled by a Campbell Scientific Inc. CR10 datalogger. Detailed instructions on the TDR measuring procedure are provided in PNL-PSB-7.0.

Frequency Domain (Capacitance) Method. The capacitance method is similar to TDR in that it is also an indirect method based on the dependence of the soil's dielectric constant, κ, on volumetric water content. However, the principle of operation is somewhat different. Troxler manufactured the capacitance probe used in this test. The probe consists of a cylindrical form that houses the electronics, and two metal bands on the periphery of the cylinder act as electrodes. An electric field is formed in the soil around the electrodes, and energy is adsorbed by the soil. The amount of energy adsorbed is dependent on κ and causes a shift in the frequency of the system. The frequency shift can then be converted to θ using the appropriate calibration relationship. The probe was deployed in 14 vertical PVC access tubes extending down to 1.9 m from the barrier's surface (Figure 2-3). Detailed instructions on the measuring procedure are provided in PNL-PSB-6.0.

Surface water runoff. Surface water runoff is a potential source of water loss in the water balance equation. As discussed in Section 2.2.2.1.3, surface runoff can also erode the silt-loam soil layer, thereby reducing the water storage capacity. To quantify the amount of runoff and the conditions under which it occurred, the barrier was fitted with equipment to monitor runoff.

The southwestern corner of the prototype Hanford Barrier was initially fitted with a 6.1-m-wide by 15.2-m-long flume (to permit the monitoring of runoff from a representative length of the barrier. The flume was moved to the northwestern corner after the first year of testing and monitoring to permit monitoring under conditions of elevated precipitation (Figure 2-4). The flume is monitored by an ISCO automated water and sediment sampler. The frequency of monitoring is determined by the intensity of the runoff event.

Drainage. In the context of this treatability test, drainage refers to the water that moves through the surface layers of the barrier onto the asphalt layer. Therefore, it is important to note that drainage measurements in this report do not reflect water movement *through* the asphalt, but only water *diverted* by the asphalt. The diverted water is conveyed through a network of PVC pipes to collection vaults for measurement (Appendix A). This water would likely be discharged along the edge of the asphalt layer and could contribute to recharge unless collected.

Figure 2-4. Plan View of the Barrier's Surface Showing the 3-m x 3-m Grid and Relative Positions of the Water Balance Monitoring Stations (S1 Through S14).

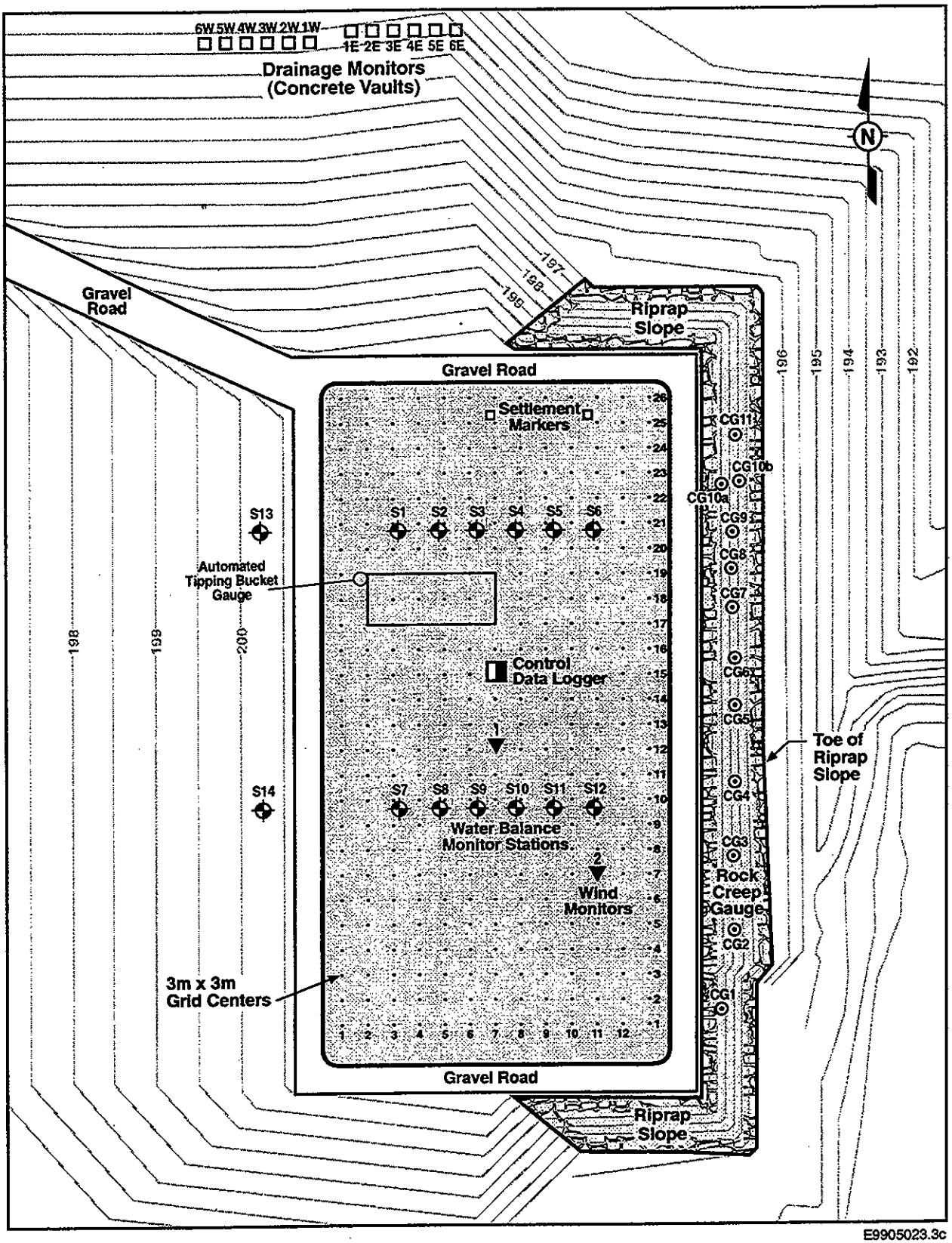

E9905023.3c

Because the Hanford Barrier is designed with a recharge limit of 0.5 mm yr^{-1} or less, measurement of drainage off the asphalt layer is critical for performance assessment.

The low-permeability composite asphalt layer was built with a 2% slope to the east and west of the crown of the barrier, to facilitate lateral water movement. A series of curbs divide the surface of the asphalt into 12 water collection zones (Figure 2-1 and Appendix A). The entire surface of the asphalt pad is covered with a layer of gravel to facilitate lateral drainage toward the lower slope positions of each collection zone. The boundaries of the 12 water collection zones align vertically with each of the 12 surface plots shown in Figure 2-1 and Appendix A, and described in Table 2-1.

The drainage monitoring system is composed of 12 concrete vaults (Figures 2-4 and 2-5 and Appendix A). The vaults were installed to the north and downgradient from the asphalt layer to allow the movement of water by gravity. Drainage water flows into each vault via a datalogger-controlled tipping-bucket raingauge, which allows monitoring of low flows. Each vault is also fitted with a submersed Druck® pressure transducer that continuously monitors the intermediate to high flow rates by recording hydrostatic pressure, which is a function of water height. Measurements are made at intervals ranging from 10 minutes to 1 hour. Also included in each vault is an Orenco® dosing siphon, a passive device for monitoring large flows. The siphon is fitted with a dose counter connected to a datalogger to record dosing events. Each dose is equivalent to 591 ± 40 L of water, or 1.8 mm from the full-sized plots and 6.4 mm from the transition plots. Each vault is also fitted with an evaporometer to monitor the amount of water evaporating from the vault. The measurement precision of the instruments is presented in Table 2-2. Detailed instructions on the measuring procedure are provided in PNL-PSB-4.0.

Pan lysimeter. To monitor the performance of the composite asphalt layer, a pan lysimeter was installed under a section of the asphalt pad that was considered most likely to be stressed by infiltrating water. Consequently, it was installed under the northeastern section of the asphalt layer and lies beneath plot 4E on the riprap side slope (Appendix A). This area was irrigated at three times the long-term annual average precipitation. The 6.5-m by 6.5-m lysimeter, which is shaped like an inverted pyramid, was constructed by sandwiching a geosynthetic composite liner between two geomembranes (Myers and Duranceau 1994). The perimeter of the lysimeter is sealed to the underside of the asphalt, and paired 1.65-mm-diameter stainless steel tubes are used for venting and siphoning water from the bottom of the lysimeter. The siphon tube is connected to a monitoring system, which consists of a pump and tipping-bucket rain gauge controlled by a datalogger.

Evapotranspiration (ET). Evapotranspiration, which is controlled by vegetative cover, soil physical characteristics, and climatic conditions, plays an important role in the performance of vegetated capillary barriers. The Hanford Barrier is designed to maximize ET and thereby limit drainage to the underlying waste zone. For this treatability test, ET was calculated as the difference between water inputs, losses, and storage according to Equation 2.1.

Figure 2-5. Schematic of Drainage Monitoring System Showing the Siphon Vault and Associated Monitoring Instruments.

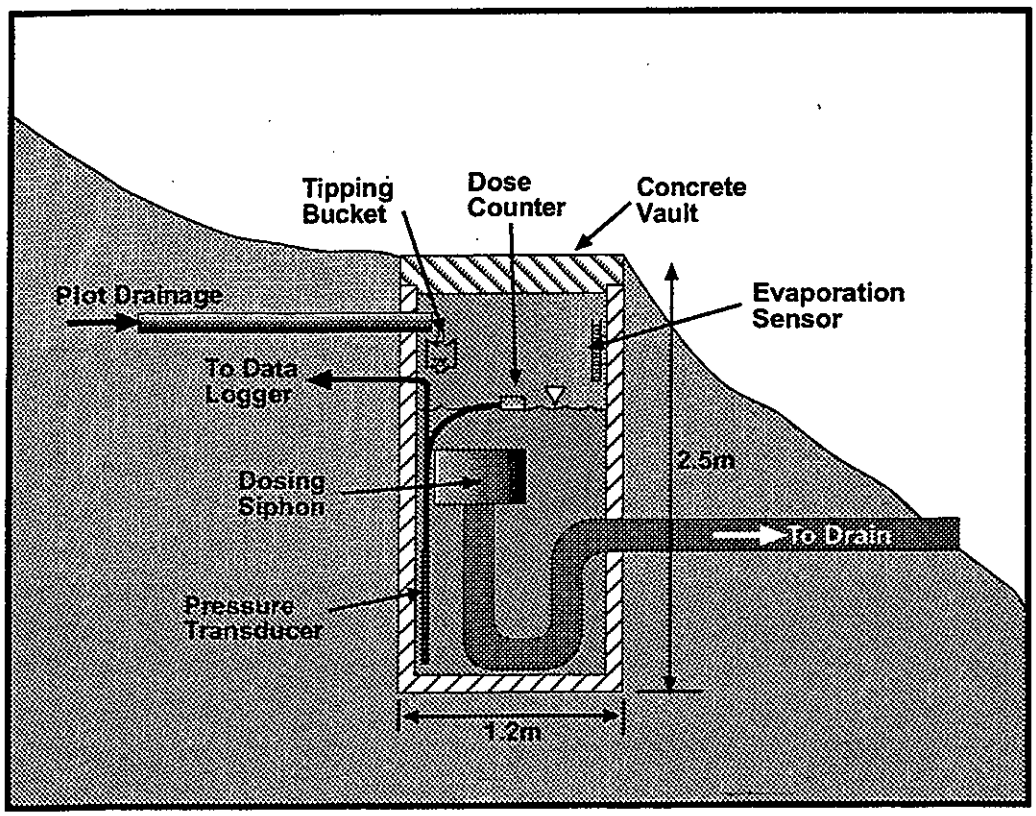

E9901037.2

Table 2-2. Expected Precision for Major Water Balance, Stability, and Biointrusion Measurements at the Prototype Surface Barrier.

Variable	Method	Resolution	Expected Precision
Precipitation (mm)	Manual rain gauge	±0.25 mm	±0.25 mm
	Tipping bucket	±0.25 mm	±0.25 mm
	Mini-lysimeter	±0.20 mm	±0.20 mm
Water Storage (mm)	Neutron probe	±0.005 $m^3\ m^{-3}$	±10 mm over depth L
	TDR	±0.005 $m^3\ m^{-3}$	±10 mm over depth L
	Capacitance probe	±0.010 $m^3\ m^{-3}$	±20 mm over depth L
Surface runoff (mm)	ISCO water sampler	±0.25 mm	±0.25 mm
Drainage (mm)	Tipping bucket	±0.025 mm	Main plot: $3.5 \cdot 10^{-5}$ mm Trans. plot: $7.0 \cdot 10^{-5}$ mm
	Pressure transducer	±0.025 mm	±0.26 mm yr^{-1}; controlled by seepage through vault walls
Evapotranspiration (mm)	By difference: $ET=(P + I)-(\Delta W+R+D)$	Set by least precise component, ΔW	±10 mm
Elevation (m)	Electronic Distance Measurement System	±1 mm over 1 km	±0.05 % of distance
Gravimetric water content (mass of water per unit mass dry soil)	Change in mass of wet soil core after drying	±0.01 g g^{-1}	Subject to spatial variability
Bulk density (g cm^{-3})	Mass of dry soil per unit volume	±0.01 g g^{-1}	Subject to spatial variability
Gravel content (mass of gravel per unit mass dry soil)	Mass of gravel per unit mass of soil	±0.01 g g^{-1}	Subject to spatial variability
Wind stresses	Wind speed (m s^{-1}); anemometer	±0.15 m s^{-1}	±0.15 m s^{-1}
	Blown soil mass (g) (Dust traps/ lab balance)	±0.01 g g^{-1}	±0.01 g g^{-1}
	Piezoelectric sensors	±0.02 g cm^{-3}	±0.02 g cm^{-3}
Plant height, rooting depth; burrow depth (m)	Meter stick	±1.0 mm	±20 mm
Leaf Area	Li-Cor Leaf Area Meter	0.1 mm^2	±4% for 0.25 cm^2
			±0.5% for 10 cm^2
		1 mm^2	±7% for 0.5 cm^2
			±1% for 10 cm^2
Gas Exchange	Li-Cor 6200 System	≤1.7% full scale	≤1.7% full scale
Plant Mass (g)	Laboratory balance	±0.01 g	±0.01 g

2.2.2.1.2 Erosion. The loss of soil by erosion from the surface of protective barriers can reduce the thickness of the soil cover and compromise its ability to control infiltration through a reduction in the designed water storage capacity. The primary agents of soil loss in arid environments are water and wind erosion. To understand the effect of erosion on barriers requires knowledge of how it is affected by different kinds of rain and wind and how erosional processes vary for different soil surface conditions. The barrier was instrumented to monitor water and wind erosion processes.

Water erosion. The amount of water erosion that occurs under a given set of soil conditions is a function of the ability of the rain to cause erosion (erosivity) and the ability of the soil to resist the erosive forces of the rain (erodibility). Erosivity depends primarily on the rainfall characteristics including amount and intensity, whereas erodibility is controlled by soil physical properties and soil conditions at the surface.

The objective of water erosion monitoring was to develop a baseline database for the top silt-loam/admix layer with respect to erosion and soil surface "aging" under natural and elevated precipitation conditions. Measurements were focused on rainfall intensities and amounts; surface runoff and sediment yield; and changes in soil physical properties, including those caused by the establishment of vegetation, disturbance by animals, and from surface topographic changes.

The Hanford Barrier was fitted with an automated tipping-bucket system to monitor rainfall amounts over time, from which intensities were calculated. Monitoring frequency was event-driven, increasing from the regular 1-hour intervals to 1-minute intervals during intense precipitation events. Measures of soil movement by surface runoff were obtained from the 6.1-m-wide by 15.24-m-long flume in the northwestern corner of the prototype barrier (Figure 2-4). The flume is also monitored by an event-driven water and sediment sampler. For the duration of the test, the soil surface was monitored to quantify seasonal and annual changes in soil physical properties, plant population densities, and disturbance by animals. Soil density data were collected at the approximate center of each grid cell (Figure 2-4) using a Troxler® nuclear density gauge. This gauge provides measures of soil water content, as well as the wet and dry bulk densities, ρ_b, of the soil. Measurements related to plant establishment and animal disturbance are discussed below in Section 2.2.2.1.4. Surface topographic changes are discussed below in Section 2.2.2.1.3.

Wind erosion. The amount of wind erosion that occurs under a given set of conditions is a function of the ability of the wind to move the soil particles (erosivity) and the ability of the soil to resist the erosive forces of the wind (erodibility). Erosivity depends primarily on wind velocity, with high winds being able to move more and larger soil particles than slower winds. Erodibility depends on the quantity of vegetation (through its effect on surface roughness); the amount of precipitation; and soil conditions, especially particle diameter and water content. The movement of windblown sand over the surface of the barrier (saltation), especially when free of vegetation, was expected to be an important contributor to eolian stress.

The main objectives of wind erosion monitoring were to quantify the erosive or sheer stresses that impact the barrier, rates of surface deflation or inflation, and abrasive sand particle scouring or saltation. Two additional objectives were proposed for the period after most other monitoring

activities had been discontinued. The objectives were to create a sand dune on the surface and monitor its impact on surface erosion, plant community viability, and soil water storage; and to remove established vegetation by fire or other means to simulate a post-wildfire condition and monitor the impacts on erosion (DOE-RL 1993b). Wind-erosion measurements were therefore focused on measuring the parameters that affect erosivity and erodibility.

Because wind erosion is restricted to dry soils, measurements of wind erosion parameters were focused on the southern, nonirrigated half of the barrier. Three wind boundary layer stations (wind monitoring stations) were installed at the barrier to monitor wind stresses. Station 01 is located south of the center of the barrier, and Station 02 is located in the southeast quadrant, near the riprap side slope (Figure 2-4). To obtain measures of wind stresses over surfaces typical of the Hanford Site for comparison with the stress on the barrier, a third station, Station 03, was established off the barrier at the southwest corner of the site. Each station includes a wind-direction sensor and four wind speed sensors at elevations of 0.25 m, 0.50 m, 1.0 m, and 2.0 m above the soil surface. The resulting data were used to calculate erosivity and surface roughness. Erodibility of the silt-loam-admixture layer was quantified by measures of surface composition, with respect to pea gravel content, and surface layer deflation/inflation. To monitor saltation stresses and sand drift rate, three multi-sensor saltation stations were installed on the eastern side of the southeastern quadrant (Stations 04, 05, 06) at elevations of 0.25, 0.125, 0.50, and 1.0 m. Dust traps were co-located with peizoelectric saltation sensors and allowed collection of the mass of material blowing across the surface as well as calculation of the kinetic energy of sand grains impacting the surface (Gee et al. 1995). The sensors, with cylindrical cross sections to eliminate dependence on wind direction, provided a count record of sand grain impacts and a time record of the total kinetic energy of each erosion event. The dust traps were designed to remain directed into the wind and collect physical samples of silt and sand-sized particles. The sensors were controlled by a datalogger that initiated measurements only when wind speed exceeded 7.5 m s^{-1}. Dust traps were sampled manually after significant windstorms.

2.2.2.1.3 Stability. Barrier stability is important because some of the potential sites for barrier deployment may be susceptible to settlements due to the disintegration of packing materials or the presence of void space. Although theoretical estimates of anticipated settlements can be made, observation of a field-scale barrier allows direct measurement. Barrier stability was tracked by monitoring the degree of vertical deformation of the silt-loam surface and subgrade. Vertical deformation can be caused by consolidation or expansion of the barrier materials and by settlement of the barrier foundation. Settlement and consolidation of the foundation soil and the composite layers of the barrier can compromise barrier performance, particularly through accelerated erosional processes (Walters et al. 1990). Slumping and gullying under the riprap side slope are also important erosional processes that would compromise barrier performance and longevity.

The objectives of this task were to monitor the order and magnitude of the total and differential subsidence in the subgrade below the asphalt and in the layers of the barrier as it ages, and to monitor the stability of the riprap side slope. These processes were quantified by monitoring changes in surface elevation of the respective areas.

Surface topographic changes. To facilitate monitoring of elevation changes, the surface of the barrier was demarcated with a coordinate system established by a 3-m by 3-m grid (Figure 2-4). This grid was established by setting four corner markers to define a 36-m by 75-m rectangle centered within the perimeter of the compacted gravel roadway. Each interior grid point was marked with a wooden survey stake numbered to identify the grid coordinate. Elevation measurements were taken at the location of each stake on the 3-m by 3-m grid using an electronic distance measurement (EDM) system.

Settlement markers. Movement of the asphalt surface is an indicator of subgrade settlements and may be quantified by measuring the change in the elevation of settlement markers attached to the asphalt layer. To enable monitoring of the order and magnitude of settlement in the subgrade below the asphalt layer (i.e., beneath the barrier) and within the barrier, two settlement markers were installed during construction. One marker was installed at the north end of the barrier, near the crown, and the second marker was installed about 14 m to the east of the first marker (Figure 2-4). Each marker consists of a 4.2-m-long galvanized steel rod (25 mm diameter) welded to a 60-cm square plate. The plate is set on the asphalt surface, and the rod extends upward to within 5.0 cm ± 1.0 of the barrier surface. At the surface, the posts are protected with cast iron monument cases whose tops were set 2.5 cm ± 1.0 above the surface (Myers and Duranceau 1994). The 1.95-m portion of each rod that extends downward from the gravel filter to the plate on the asphalt is encased in 10-cm-diameter galvanized steel pipe to prevent binding between the rod and the riprap material. Changes in the elevation of the rods were measured using the EDM. When combined with surface elevation measurements, changes to the thickness of the barrier can be assessed. Surveys were conducted twice per year to document changes in elevation.

Creep gauges. Because of the steepness of the slope (up to 1:1), the riprap side slope was considered to have the greatest potential for movement. Therefore, to monitor stability, creep gauges were installed at 11 locations in the eastern riprap slope during construction (Figure 2-4). Each gauge consisted of 3-m-long steel rebar (1.9 cm diameter) encased in a mortar-filled, 30-cm-long by 7.6-cm-diameter PVC tube (Figure 2-6). The 1.3-cm-diameter head of a large nail embedded in the mortar was used as the benchmark for monitoring creep gauge movement. At each location, a gauge was installed at the mid-slope on the riprap, except for one location near the northeastern corner where two gauges were installed, one at the upper and the other at the lower slope position. Creep gauges were surveyed twice per year to determine their location and elevation.

2.2.2.1.4 Vegetation. Plants are expected to play a crucial role in the hydrologic performance of the Hanford Barrier. In arid environments, plants can be expected to extract, by transpiration, at least twice as much water from the fine silt-loam soils as would be lost by evaporation alone. Not only are plants expected to significantly contribute to the water balance through the direct removal of water, but they can be expected to minimize water and wind erosion (Link et al. 1994). Successful performance of the barrier in the long term is therefore dependent on the establishment of a sustainable plant community on the barrier surfaces. Sustainability is not only a function of successful establishment, but is also a function of biodiversity. Plant communities are generally dynamic, and increasing biodiversity supports the proposition that increased complexity provides increased reliability of the surface to function with changing conditions.

Figure 2-6. Schematic of a Creep Gauge.

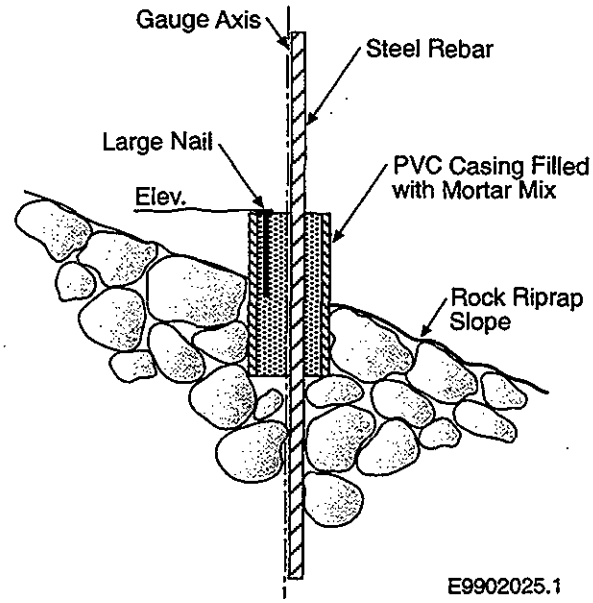

The main objectives of vegetation tests were to evaluate the extent to which plant roots exploit the depth of the silt-loam layer of a field-scale barrier and to determine whether the roots of the established vegetation penetrate the various biointrusion control layers. In light of these objectives, the treatability test included a task to assess plant community dynamics at the prototype barrier. The majority of plant measurements (e.g., plant identification and cover estimates) were typically performed in the spring (April through June).

Plant identification (floristics). Seeds of the shrubs *Artemisia tridentata* (big sagebrush) and *Chrysothamnus nauseosus* (gray rabbitbrush) were collected from McGee Ranch on the Hanford Site on December 23, 1993. The seeds were transported to the Arid Lands Ecology Reserve where they were dried and stored in the dark before being shipped to the Plants of the Wild nursery (Tekoa, Washington) on March 11, 1994. Seeds were cleaned and eventually sown on May 4, 1994 in 164-cm^3 tubes (Gee et al. 1994). Approximately 2,500 seedlings of *C. nauseosus* and 7,500 seedlings of *A. tridentata* germinated.

Shrub planting commenced on November 7, 1995, and was completed the following day. On the surface, 2,700 holes were drilled at a density of 1 hole per square meter, and 2 seedlings were placed in each hole. There were 1,350 *C. nauseosus* and 4,050 *A. tridentata* seedlings planted. *C. nauseosus* and *A. tridenta* were planted uniformly at a 1:3 ratio, respectively. The soil and surrounding gravel surfaces were hydroseeded with a mix of native grass and forb seeds, fertilizer, organics, and a tacking agent on November 11, 1995 (Gee et al. 1995). This seed mixture included *Poa sandbergii* (Sandberg's bluegrass), *Agropyron dasystachyum* (thickspike wheatgrass), *Oryzopsis hymenoides* (Indian ricegrass), *Poa ampla* (Sherman's big bluegrass), *Stipa comata* (needle-and-thread grass), *Pseudoroegneria spicata* (bluebunch wheatgrass), and *Sitanion hystrix* (bottlebrush squirreltail). Following hydroseeding, the shrub seedlings were transplanted to coincide with the grid shown in Figure 2-4.

Vegetation characteristics monitored in the treatability test included floristics composition, ground cover, spatial distribution, plant height, canopy leaf area, gas exchange rate, roots, shrub survivorship, and reproduction. The floristics of the prototype barrier is dynamic, and documentation of floristic composition required periodic visual inspection for the occurrence of various species. The work of Hitchcock and Cronquist (1973) was consulted to aid in the identification of the different species.

Plant cover. Cover estimates of grasses, shrubs, herbaceous forbs, litter, and bare soil were made on each 9-m^2 quadrant patterned after Daubenmire (1959). Cover was estimated by visual inspection of each quadrant.

Plant size. The size of plants in water-limited ecosystems is positively correlated with available water (Link et al. 1990a). Measurements of shoot height were taken to establish whether plants were taller in the irrigated treatment compared with the nonirrigated treatment. Height was measured with a meter stick.

Canopy characteristics. The canopy characteristics such as leaf area and leaf area index are required parameters for calculating plant transpiration rates. Thus, canopy characteristics were measured to estimate leaf area, as described in Link et al. (1990b). The leaf area was measured by double sampling, using a model to relate leaf area to canopy measures. Leaves were stripped from the sampled stems and single-sided green leaf area was determined with a Li-Cor 3100 Leaf Area Meter (Licor, Inc., Lincoln, Nebraska).

Gas exchange. Plant gas exchange data are useful as an indication of the ability of shrubs to remove water from the surface. Comparisons are made for the effect of the irrigation treatment on gas exchange rates for *A. tridentata*. Gas exchange data were gathered with a Li-Cor 6200 gas exchange system.

Root observations. To monitor root intrusion, density, and distribution with depth, 12 clear tubes (minirhizotrons) were installed in the silt-loam layer, extending down to a depth of 1.9 m at a 45° angle (Figure 2-3). Six tubes were placed in the northern section (irrigated) and six in the nonirrigated or southern section. The minirhizotrons were installed near the neutron access tubes so that the correlation between root characteristics and soil water dynamics could be investigated. Root characteristics were observed with a down-well video camera (Circon Agricultural Camera) inserted into the clear tubes. Videos from each root tube were examined to determine root demographics and the number of roots in contact with the rhizotron. Although the root number serves as an indicator for the mechanical state of the soil, root length density provides more information on the efficiency of the root systems at removing water from the silt-loam layer. The calculation of root length density is described in Section 2.2.2.2.4.

Reproduction. The sustainability of a particular species of plant on the barrier is partly dependent on the successful reproduction of that species which, in the long term, could be affected by environmental changes. Data were collected to test the hypothesis that elevated precipitation reduces the percentage of *A. tridentata* shrubs with mature seed heads, compared with the nonirrigated treatment. Data to test the hypothesis were obtained by estimating the percentage of *A. tridentata* shrubs with mature seed heads that were present in both precipitation treatments through visual inspection.

2.2.2.1.5 Animal intrusion. Animals can be expected to colonize the barrier and burrow into the surface. Animal activity often results in pedoturbation, which may directly affect the surface hydrology, plant community dynamics, and erosion by wind and water (Link et al. 1994). Thus, animal activity has the potential to compromise the barrier by deep burrowing. The main objective of the animal intrusion monitoring was to document the occurrence and extent of animal burrows.

No specialized equipment was required for the animal intrusion task. Animal intrusion was determined from visual observation of animal droppings (indicator of animal activity) and burrows. Droppings and burrow counts were recorded annually and mapped in relation to the grid shown in Figure 2-4.

Table 2-2 summarizes the expected measurement precision for major water balance, stability, and biointrusion monitoring elements at the prototype barrier.

2.2.2.2 Sampling and Analysis.

2.2.2.2.1 Water balance. Testing and monitoring activities at the prototype barrier were based on a water year (WY), which ran from November 1 of each year through October 30 of the following year. This format started in WY 1995 and was followed until 1998 when WY 1998 ended on September 30, 1997.

Water inputs. Water input data for evaluation of the water balance were derived primarily from the precipitation meters at the barrier. Hourly measurements were generally made, except during the simulated 1,000-year storm test when measurements were made every 5 minutes. Automated measurements at the barrier were supplemented with manual rain gauge measurements and data from the HMS.

Soil water storage. During the first year of the treatability test, soil water storage (W) was measured using three techniques, TDR, capacitance probe, and neutron probe, with the neutron probe acting as the standard measurement technique. The TDR system is a fully automated and multiplexed system and was generally activated on an hourly basis. Each measurement cycle (7 depths on 14 probes) took 25 minutes. During the first simulated 1,000-year storm event, the TDR system was used to obtain measurements of θ at 0.5-hour intervals. Measured θ was converted to water storage according to Equation 2.2. The expected precision of the TDR system is ±20 mm over depth of the silt-loam layer (Table 2-2).

Neutron probe measurements were first made on September 30, 1994, after which measurements were generally taken twice per month in the vertical access tubes for WY 1995-1997 and decreased to monthly in WY 1998. The frequency of monitoring usually increased to coincide with the extreme precipitation tests (simulated 1,000-year storm events) conducted in late March of WY 1995-1997. During extreme precipitation tests, a once-weekly monitoring frequency was initiated and maintained through the end of April following the storm event.

Neutron probe counts were made at each of the 14 vertical access tubes in 0.15-m increments from the surface down to a depth of 1.9 m and the data stored electronically. Data were downloaded to the database (Figure 2-7) and converted to θ using calibrations derived for the

various barrier materials. Measured θ was converted to soil water storage (W) according to Equation 2.2. A change in storage, ΔW, was calculated as the difference in water storage between the most recent measurement and the previous measurement. The precision in water storage determined from neutron probe measurements at the barrier is ±10 mm over the depth of the silt-loam layer (Table 2-2).

The capacitance probe was deployed manually, and measurements followed the same schedule as the neutron probe. The frequency shift was recorded at each of the 14 vertical access tubes in 0.15-m increments from the surface down to a depth of 1.9 m and the data stored electronically. Data were downloaded to the database (Figure 2-7) and converted to θ using a field-average calibration relationship developed for the silt-loam layer. The resulting θ values were converted to water storage according to Equation 2.2. The expected precision in water storage determined from capacitance probe measurements is ±20 mm (Table 2-2).

Following the first year of testing, the TDR and capacitance were discontinued as a cost-cutting measure. Nevertheless, the data collected were sufficient to evaluate the utility of the techniques for measurements of water storage in engineered covers.

Infiltration and drainage. Sampling for infiltration and drainage included monitoring of changes in θ at the capillary break and under the asphalt pad using the neutron probe through horizontal neutron access tubes. During WY 1995-1997, measurements in the horizontal access tubes at the capillary break were done twice per month, coinciding with the vertical measurements made in the silt loam. The below-asphalt measurements were taken once per month to quantify water dynamics under the asphalt pad and estimate the extent of underflow. In WY 1998, measurements were made once every 2 months. Neutron counts were converted to θ water contents using a calibration function derived for the soil below the asphalt. Drainage out of the upper layers of the barrier was determined from the volume of water diverted by the asphalt pad of each collection zone. The below-asphalt pan lysimeter was also monitored periodically to evaluate the integrity of the asphalt and to document its performance.

Surface runoff. Surface runoff from the flume was monitored continuously using a v-notch weir calibrated to record flow as an equivalent height (mm) of water.

Evapotranspiration. Evapotranspiration was not measured directly, but was obtained as the difference between the water inputs, losses, and storage according to Equation 2.1.

2.2.2.2.2 Water erosion. Water erosion monitoring activities were conducted in WY 1995-1997. Data were collected to determine the rainfall characteristics, surface runoff and sediment yield, soil physical properties, and topographic changes.

Figure 2-7. Measurement, Instrumentation, and Data Collection Flow Diagram for the Prototype Surface Barrier.

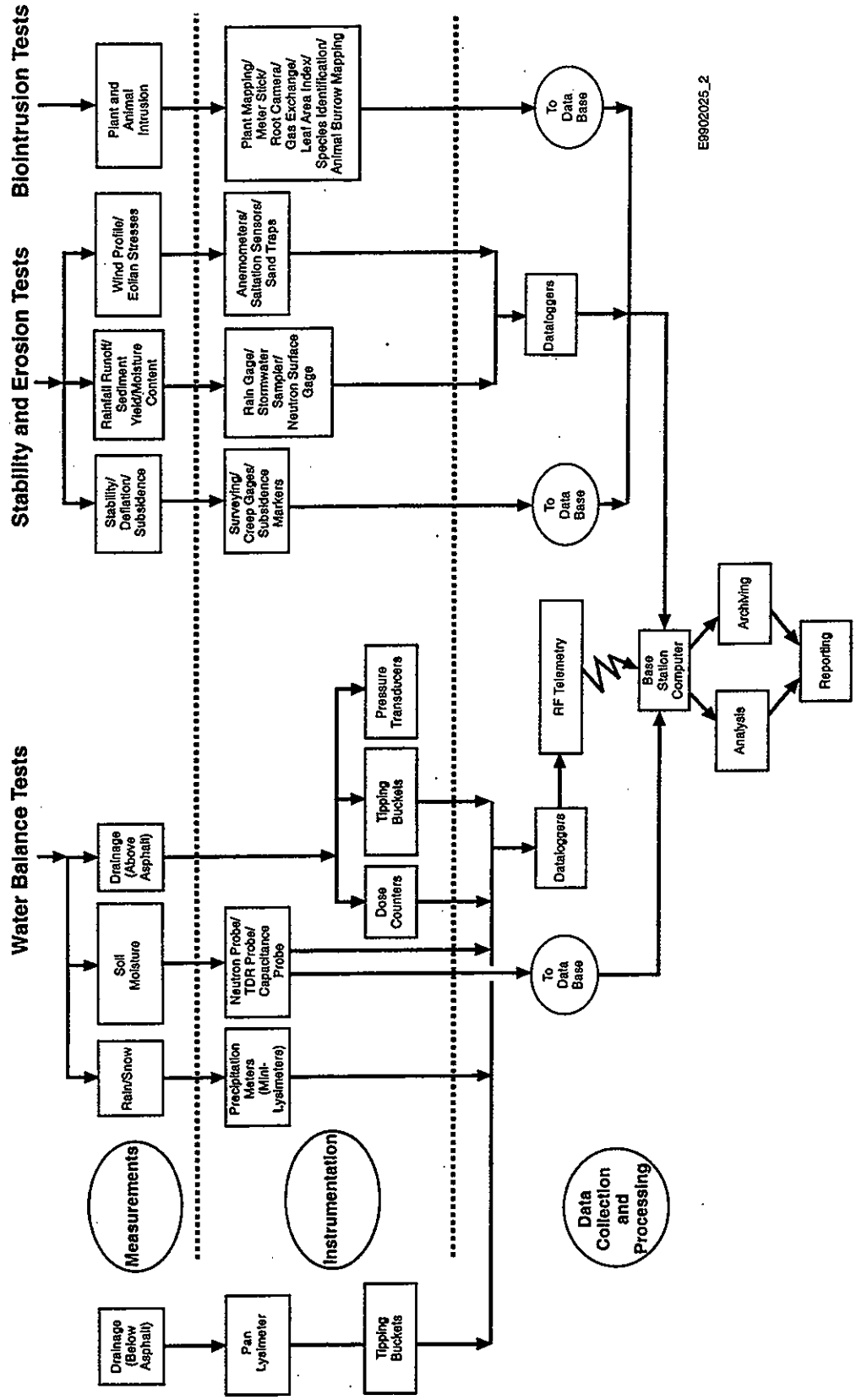

Rainfall characteristics. The best estimator of soil loss is the product of kinetic energy and the 30-minute rainfall intensity, I_{30} (Wischmeier et al. 1958). The I_{30} is the greatest average intensity observed in any 30-minute period during a rainstorm and, when doubled, gives a measure of intensity in mm hr^{-1}. The kinetic energy of rainfall events was calculated according to the energy-intensity equation (Hudson 1981):

$$E = 11.9 + 8.7 \log I \tag{2.3}$$

where E is kinetic energy (J m^{-2} mm^{-1}) and I is rainfall intensity (mm hr^{-1}).

The maximum erosion potential, or erosivity index (EI), was calculated as

$$EI = \frac{E \cdot I_{30}}{1000} \tag{2.4}$$

Surface runoff and sediment yield. The flume was monitored by an automated water and sediment sampler. Subsamples were analyzed in the laboratory to determine sediment concentrations (Gee et al. 1995).

Soil physical properties. Soil property data were collected at the approximate center of each grid cell (Figure 2-4) using a Troxler nuclear density gauge. During the period WY 1995-1997, measurements were generally taken in August of each year. The resulting data allowed calculation of wet and dry bulk densities, ρ_b, of the near-surface silt-loam layer.

Surface composition. Each year, soil samples were obtained by coring the soil column from 0 to 2 cm (surface samples) and from 2 to 10 cm (bulk samples). Samples were taken to the laboratory where wet and dry weights were used to calculate pea gravel content before and after sieving (0.33-cm sieve). Because less than 30 samples were taken at each sampling, the data were analyzed using small sample theory, assuming unequal variances, to identify spatial and temporal differences. Temporal changes in surface composition provide a good measure of changes in erodibility.

Topographic changes. Sampling and analysis for the evaluation of stability consisted mainly of topographic (civil) surveys using an EDM. These are discussed in Section 2.2.2.2.4.

Wind erosion. Wind erosion monitoring activities conducted in WY 1995-1997 focused on wind characteristics, surface and near-surface pea gravel composition, surface layer deflation/inflation, saltation stresses, and sand drift rates. Data were analyzed using the methods summarized below.

The sheer stress parameters of interest are friction velocity (u_*) and roughness height (z_o). The u_* represents a characteristic flow velocity and relates to the effectiveness of turbulent exchange over the surface. The z_o is a measure of the aerodynamic roughness of the surface where the wind speed profile is measured. On an engineered barrier, z_o is influenced by, but is not equal to, the average height of surface roughness elements such as gravel or vegetation. Calculating z_o and u_* from measured airflow boundary layers provides a quantitative method of comparing

different surfaces and surface sheer stresses, respectively. These parameters were calculated from measurements of wind-velocity gradients (change in wind velocity with elevation) near the surface, using the following relationship (Rosenburg et al. 1983):

$$u_* = k\,\Delta u\, ln\left(\frac{z_1 - d}{z_2 - d}\right)^{-1} = kM^{-1} \tag{2.5}$$

where

u_*	=	friction velocity, (m s^{-1})
z_1	=	elevation 1, (m)
z_2	=	elevation 2, (m)
d	=	zero plane displacement
Δu	=	change in velocity between elevations z_1 and z_2, (m)
k	=	von Karman's constant, usually 0.40
M	=	$\Delta u / \ln(z_1\text{-}d/z_2\text{-}d)$.

For an open, level, and relatively smooth surface, such as test surfaces in the wind tunnel (Ligotke 1993) or the barrier shortly after construction, the zero plane displacement, d, in Equation 2.5 is zero and u* is a simple logarithmic function of elevation.

In general, z_o for plants is about an order of magnitude smaller than the plant height, *h*. The empirical relationship between z_o and *h* reported by Szeicz et al. (1969) was rearranged to give *h* as a function of z_o

$$h = \exp(1.003 \ln z_o + 2.039) \tag{2.6}$$

where *h* and z_o are reported in meters.

2.2.2.2.3 Stability. Stability monitoring was performed in WY 1995-1997 and included measures of topographic changes of the surface, creep gauges, settlement gauges, and soil physical properties. No stability measurements were taken in 1998.

Topographic changes. Sampling and analysis for the evaluation of stability consisted mainly of topographic surveys using an EDM system. Surveys were conducted in December 1994, July and September 1995, January and September 1996, and January and September 1997. Each survey included measurement of surface elevation of the two settlement gauges, as well as the elevation and spatial location of the 12 creep gauges on the riprap slope (see Figure 2-4). Surface elevation measurements were taken at the location of each stake on the 3-m by 3-m grid. Vertical control was provided by the use of the four permanent survey monuments that were installed at the outside corners of the site barrier site during construction. The survey data were used to make contour maps with the aid of three-dimensional gridding software.

Creep and settlement gauges. Data from the survey of the settlement and creep gauges were analyzed relative to the first survey. The location of each creep gauge was also surveyed twice

per year. The position of each gauge was described by a northing (x), an easting (y), and an elevation (z) from which a displacement vector was calculated. Changes in x (Δx), y (Δy), and z (Δz) since December 1994 were determined. Changes were used to calculate the resultant (r) and bearing (Θ) of the displacement vector, which were expressed as a polar coordinate P, denoted by (r,Θ).

Soil physical properties. Soil samples were generally taken from the center of each grid cell, and densities were measured at the same location using a Troxler nuclear density gauge. The Troxler gauge provides data on water content as well as the wet and dry bulk densities near the surface (0 to 0.2 m depth).

2.2.2.2.4 Vegetation. Measurements to document vegetation characteristics were made during the period WY 1995-1998. Measurements included floristics composition, ground cover and spatial distribution, plant height, canopy leaf area, gas exchange rate, roots, shrub survivorship, and reproduction. In 1998, vegetation measurements were limited to shrub height, shrub canopy area, and shrub survivorship, and were performed in late August.

Plant identification (floristics). A species plant list was developed for each year of the test period. This list was compiled through several inspections each year. The work of Hitchcock and Cronquist (1973) was consulted to assist in plant species identification. After vegetating the surface with 2 native shrubs and a mixture of 7 grasses and forbs, 34 species were observed in WY 1995. Data analysis focused on documenting the changes in the plant population after the initial survey, with particular interest in the occurrence of new species.

Percent surface cover. To quantify percent cover determined by visual inspection of quadrants, values 1 through 6 were assigned to percentage cover ranges as follows:

1 = 0-5%
2 = 5-25%
3 = 25-50%
4 = 50-75%
5 = 75-95%
6 = 95-100%.

The resulting data are essentially nonparametric, and statistical analysis is based on the techniques of Seigal (1956). Measures of central tendency for these data are given as the median and the mode. The median is the cover class value where half the values are greater; the mode is the cover class with the greatest frequency. Arithmetic means and parametric statistics are invalid for ordinal data because the distance between classes is not equal (Seigal 1956). Note the distance between the midpoints of classes 1 and 2 is 12.5%, and the difference between the midpoints of classes 2 and 3 is 22.5%. Differences between treatments and years for cover data in this study were assessed using the Mann-Whitney test (Seigal 1956). This test ranks values upon which parametric statistics are valid. The Z values given indicate the direction of change, with the larger values indicating the greatest change. Negative values indicate decreases. For ease of interpretation, mapping data were converted to the midpoint of the percentage cover ranges.

Plant size. The size of plants in water-limited ecosystems is positively correlated with available water (Link et al. 1990a). Measurements of shoot height were taken to see if plants were taller in the irrigated treatment compared with the nonirrigated treatment. In WY 1997, canopy shape for *A. tridentata* was measured to relate the treatment to morphological characteristics and to estimate canopy leaf area and leaf area index.

Canopy characteristics and leaf area. To document the observed changes in plant cover with time, leaf area and leaf area index (leaf area compared to the area of the plant canopy projected onto the ground surface) were investigated for *A. tridentata* (sagebrush). The transpiration rates for *A. tridentata* were estimated because it is the dominant shrub on the surface; also, it is expected to account for a large portion of plant transpiration from the surface. Canopy morphological measures were used to estimate canopy leaf area and leaf area index. Observations were taken on April 15, May 15, and June 15, 1997, to describe canopy characteristics, leaf area, and leaf area index dynamics. Canopy characteristics were measured to estimate leaf area, as described in Link et al. (1990b). Details of the leaf area measurements are provided in Ward et al. (1997). Canopy characteristics of the same individual shrubs were measured on the April, May, and June dates. Shrubs were randomly chosen (20 from the nonirrigated treatment and 20 from the irrigated treatment). Leaf area of *A. tridentata* was predicted, based on the day when plants were harvested.

Plant gas exchange. Plant gas exchange data are useful as an indication of the ability of shrubs to remove water from the surface. Gas exchange data were gathered with a Li-Cor 6200 gas exchange system. Measurements were made by placing a chamber over plant stem tips and allowing water vapor and CO_2 to exchange over a few minutes. A 10-cm length of stem was placed in the chamber for plants in the nonirrigated treatment, and a shorter piece (less than 5 cm long) was used in the irrigated treatment. The varying amounts of exposed leaf area were used to maintain similar vapor pressures for the two treatment samples in the chamber. After observations were made, the stem was cut and a single-sided leaf area measured, using a Li-Cor 3100 Leaf Area Meter. All gas exchange observations were taken at mid-day and in full sun.

Root study. Root observations were made using a video camera in the clear mini-rhizotron tubes. Observations were made from July 13 to July 21 in 1995, in June 1996, and on September 18, 1997. In WY 1997, only three tubes were examined in each treatment. The videos of each root tube were examined to calculate root length density. The method was to count each root that intersected with the tube surface and each intersecting branching root from a root already in contact with the tube. In WY 1995 and WY 1996, all roots observed were considered to be alive. In 1997, live roots and dead roots were counted separately. Differentiating live roots from dead roots is subjective. Live roots are white to brown and turgid, and some roots have root hairs. Dead roots are dark in color and contracted within root channels in the soil. Root counts were taken in an area the width of the viewing area (1.55 cm) and 10 cm long. The count data were then divided by the observation area to yield a root length density (Upchurch and Ritchie 1983).

While the root number serves as an indicator for the mechanical state of the soil, root length density provides information on the efficiency of root systems to supply water and nutrients to the whole plant. Thus, the ability of the plants to remove water from the silt-loam layer is highly correlated with root length density. Root length density is normally calculated by dividing the

total root length in contact with the glass tube, determined from root number, by the area of the observation window (Buckland et al. 1993).

Survivorship. A census of live and dead shrubs was conducted in all 300 quadrants during the period WY 1995-1997. The mean survivorship of the shrubs for each year was compared with respect to the precipitation treatment.

Reproduction. Data were collected to test the hypothesis that irrigation reduces the percentage of sagebrush shrubs with mature seed heads, compared to the nonirrigated treatment. Data to test the hypothesis were obtained by estimating the percentage of sagebrush shrubs with mature seed heads that were present in both treatments. The details of the sampling procedures are described by Ward et al. (1997). The percentage of shrubs with mature seed heads (P) was calculated as:

$$P = 100\,(N/T) \tag{2.7}$$

where N is the number of shrubs in each row with mature seed heads and T is the total number of shrubs in the row. Each row is considered an experimental unit where P is the observation. Five replicate experimental units were observed in each treatment. The Student's t-test was used to test the hypothesis.

2.2.2.2.5 Animal intrusion. The 300 quadrants on the surface were inspected for evidence of animal presence (feces and holes) during WY 1995-1998. The first evidence was casually noted in WY 1995, with quantification occurring in the later years. In WY 1996, observations were made between May 24 and June 7, 1996. In WY 1997 observations were made on April 25 and September 12, 1997, and in WY 1998 on August 17 and 18, 1998.

2.2.2.3 Data Management. Figure 2-7 shows an idealized flowchart of the types of measurements, instrumentation, and the flow of data from collection through processing. In practice, the first two levels, Measurements and Instrumentation, were identical to those shown in the flowchart. Data Collection and Processing was somewhat different. Water balance and stability data specific to the Treatability Test Plan and summarized in this report have been transferred to a CD-ROM record. The CD-ROM includes raw data, the calibration functions used to convert them to the final reported values, and the final values summarized in this report. The CD-ROM (PNNL 1999) is in the project file. Vegetation and animal data collected in the field were recorded in laboratory notebooks:

- BNW 55153 (active 07/16/93 to 03/20/95)
- BNW 55910 (active 03/20/95 to 03/08/96)
- BNW 56097 (active 03/08/96 to 10/11/96)
- BNW 56197 (active 10/11/96 to 09/09/97)
- BNW 56337 (active 09/09/97 to 09/30/98).

Copies of the laboratory notebooks are also in the project file.

3.0 RESULTS AND DISCUSSION

Results of the treatability test are discussed for each major phase of activity. Section 3.1 addresses Phase I construction issues including the constructability of the barrier using standard equipment, cost, and hydraulic testing of the asphalt layer. Phase II addresses performance testing and monitoring after construction, the results of which are discussed in Section 3.2.

3.1 PHASE I BARRIER CONSTRUCTABILITY AND COST

Construction of the prototype Hanford Barrier was completed in August 1994. In general, no significant design or construction issues occurred that would compromise the barrier's performance (DOE-RL 1994a). Naturally occurring materials were able to meet the project specifications or provide equivalent performance with minimal processing. The majority of construction issues were related to installation of testing and monitoring equipment. The relevant barrier construction issues included (1) construction schedule, (2) asphalt specifications, (3) application of the fluid-applied asphalt; and (4) borrow source limitations.

Seasonal cycles have a significant impact on the integrity of barrier components. Freezing temperatures made it extremely difficult to meet compaction requirements. Scheduled downtime during the winter months should be planned.

The asphalt mix was developed to minimize permeability while maintaining structural integrity of the overlying materials. During placement of the asphalt, some material was slightly out of specification (the amount of fine material was less than required). Permeability testing was completed to ensure that the performance of the asphalt was acceptable (Section 3.1.2).

The fluid-applied asphalt as applied developed small air bubbles that appeared to be associated with the microcracks in the surface of the asphalt. The application of several thin layers was required to reduce the bubbling effect. Air bubbles in the fluid-applied asphalt were opened by hand while the layer was still hot and allowed to flow into itself. Because of the relatively high line item cost (Section 3.1.1) and construction issues, alternative products may need to be evaluated. In addition, hydraulic conductivity results of the asphalt layer exceed design requirements, which may eliminate the need for the fluid-applied asphalt layer.

Borrow sources for materials used in the construction of the prototype Hanford Barrier were readily available. Large reserves of these materials remain; however, the areas may be culturally and ecologically sensitive, which would require alternate borrow sites. Additional planning is required to secure a reliable source of materials.

All construction-related quality assurance activities are documented in *Construction Quality Assurance Report for the Prototype Surface Barrier* (BHI 1995). As-built drawings (H-2-817484 through H-2-817497) were prepared to document the final Hanford Barrier's configuration.

3.1.1 Cost Data

Tables 3-1 and 3-2 show a breakdown of the actual costs of the prototype Hanford Barrier. It should be noted that many of the line items in Table 3-2 are related to prototype testing. Construction of actual barriers would not require this level of monitoring. Using the asphalt layer as the functional size of the barrier, the approximate unit cost excluding testing and monitoring tasks was $320/m^2$. Extrapolation of these unit costs for estimates of larger barriers, and/or mass construction of barriers, should take into account economy-of-scale factors. Table 3-3 provides unit cost data for individual components of the prototype Hanford Barrier.

3.1.2 RCRA Equivalency: Asphalt Layer

The standard hydraulic performance specification of a RCRA low-permeability soil is 1×10^{-7} cm/s. The smaller the number (i.e., 10^{-8} is better than 10^{-7}), the longer it takes moisture to infiltrate through the layer. Hydraulic performance data were collected from the asphalt layer's surface and from asphalt cores. Tests were completed without the fluid-applied asphalt layer. Modified falling head permeameter data from the asphalt layer's surface are shown in Table 3-4. Data were collected from several areas, including seams, and ranged from 1.08×10^{-7} cm s^{-1} to 1.91×10^{-9} cm s^{-1}. Table 3-5 presents laboratory data from asphalt cores obtained from the asphalt layer during construction activities. The average hydraulic conductivity was 4.7×10^{-10} cm s^{-1}. SDRI data were collected from an adjacent asphalt test pad over the 6-month testing period. Two SDRI tests were completed simultaneously. Test data located over a seam were 9×10^{-9} cm s^{-1} and 2×10^{-8} cm s^{-1} not located over a seam. All hydraulic testing results concluded that the asphalt layer was better than the design standard for a RCRA low-permeability soil.

Table 3-1. Prototype Hanford Barrier Project Costs.

Activity	Actual Cost
Engineering design	$268,400
Engineering inspection	$332,500
Irrigation pipeline/infiltration basin	$262,000
Fixed-price construction	$2,388,500
Construction management	$135,000
Project integration	$95,300
Project total	$3,481,700

Table 3-2. Breakdown of Fixed-Price Construction Costs.

Description	Base Bid
Bond insurance	$27,000
Mobilization	$51,000
Base fill	$160,000
Neutron probe – access tubes	$21,000
Pan lysimeters[a]	$47,000
Collection piping[a]	$35,000
Vaults for siphons[a]	$21,000
Coat inside vaults with bitumastic[a]	$1,000
Dosing siphons and vault piping[a]	$22,000
Asphalt base surface	$47,000
Asphalt layer at terraces and test pad	$285,700
Fluid-applied asphalt	$290,000
Gutters and upper collected system piping[a]	$90,000
Concrete curbing/gutter crickets[a]	$13,000
Drainage gravel	$114,000
Basalt layer and side slope	$293,000
Gravel filter	$67,000
Gravel sideslope, 10:1	$275,000
Sand filter	$40,000
Silt – lower layer	$63,000
Neutron probe – access tubes in silt	$25,000
Pea gravel/silt layer	$128,000
Grade and compact access road[a]	$6,000
Post barricade and gravel stabilization[a]	$15,000
Punchlist/cleanup	$3,500
Demobilize	$2,800
Change orders	$245,500
TOTAL – SUBCONTRACT	$2,388,500

[a]Testing and monitoring components.

Table 3-3. Unit Costs.

Barrier Layer	Total Unit Bid	Cost per Unit	Factors
Sandy soil fill	34,000 yd^3	\$4.32/yd^3	Haul approximately 3.2 km and place
3/4-in. Crushed gravel filter	13,500 tons	\$16.90/ton	Haul approximately 33.8 km and place
Asphalt	3,400 tons	\$84.03/ton	Haul approximately 33.8 km and place
Fluid-applied asphalt	8,050 yd^2	\$36.02/yd^2	Haul approximately 33.8 km and place
Drainage gravel	6,300 tons	\$18.10/ton	Haul approximately 3.2 km and place
Fractured basalt	14,000 yd^3	\$20.93/yd^3	Haul approximately 25.7 km and place
Pit run gravel	40,000 yd^3	\$6.88/yd^3	Haul approximately 3.2 km and place
McGee silt	3,300 yd^3	\$19.09/yd^3	Haul approximately 22.5 km and place
Gravel admix silt	4,600 yd^3	\$32.82/yd^3	Haul, approximately 22.5 km mix and place

Table 3-4. Field Asphalt (Without Fluid Application) Permeability Data for the 200-BP-1 Prototype Barrier.

Sample	Permeability (cm/s)
1 NW Corner	1.91×10^{-09}
2 NW Corner, seam	1.08×10^{-07}
3 N Center	1.47×10^{-08}
4 NE Center	4.33×10^{-08}
5 NE Corner	1.51×10^{-08}

Table 3-5. Laboratory Asphalt (Without Fluid Application) Permeability Data for the 200-BP-1 Prototype Barrier.

Sample	Permeability (cm/s)
1A	1.32×10^{-09}
2A	3.45×10^{-10}
3A	2.42×10^{-10}
4A	1.24×10^{-10}
5A	3.16×10^{-10}

3.2 PHASE II BARRIER PERFORMANCE TESTING AND MONITORING

3.2.1 Water Balance

3.2.1.1 Water Inputs. The LTA is the average amount of natural precipitation expected based on historical Hanford Site meteorological record. Based on records from 1912 through 1980, the LTA equals 160 mm yr^{-1} (Stone et al. 1983). Recent precipitation has been elevated above the LTA with all-time records occurring during the 4-year test, specifically, in calendar year 1995 (313 mm) and 1996 (310 mm) (Hoitink and Burk 1998). Extreme value analysis of Hanford Site precipitation records shows a 60-minute, 100-year return storm of 20.6 mm, whereas the 60-minute, 1,000-year return storm is 28.2 mm. A 24-hour maximum accumulation of 68.1 mm is estimated for the 1,000-year return storm. Although no records are available for periods of less than 60 minutes, analysis of rain gauge charts shows 14 mm falling over a 20-minute period on June 12, 1969, and 11.2 mm falling in only 10 minutes on June 29, 1991. Stratigraphic pollen analysis on sediment cores obtained from Carp Lake (160 km southwest of the Hanford Site) suggests that the mean annual precipitation in the Columbia River Basin, including the Hanford Site, ranged from 50% to 75% of modern levels to as high as 130% of modern levels (Petersen et al. 1993). Based on these findings, the treatability test included an elevated precipitation treatment in which water was applied at three times the LTA, including a simulated 1,000-year storm. Figure 3-1 shows the schedule of water applications followed during the treatability test.

Figure 3-2 shows a plot of cumulative precipitation over the 4-year test for the ambient and irrigated treatments, as well as the LTA. The cumulative LTA for the test period is 640 mm. During the 4 years of testing, the northern, irrigated portion of the barrier received a total (irrigation plus ambient) of 1,609 mm. Irrigation testing ceased in September 1997 after a total of 673 mm of water was applied, and was resumed briefly in May 1998 to facilitate verification of the neutron probe measurements. In contrast, the southern, ambient treatment received 936 mm. This amount was 46% higher than the cumulative LTA for the Hanford Site. In terms of individual test years, natural precipitation in WY 1997 was 1.8 times higher than the LTA, compared to 1.5 times in WY 1996 and 1.8 times in WY 1995. Thus, the ambient treatment was significantly higher stressed than would be expected under the normally drier conditions at the Hanford Site. Since a wetter, rather than drier, climate is expected to place more stress on barrier performance, these results lend support to the expectation of adequate performance under sustained elevated precipitation.

3.2.1.2 Soil Water Storage.

3.2.1.2.1 TDR measurements. There are very few published data that document field performance of remote-shorting diode TDR probes such as those in use at the Hanford Barrier (Gee et al. 1995, Rockhold et al. 1996, Frueh and Hopmans 1997). There were two main problems associated with use of the TDR probes. The data showed several unexplained temporal variations in $\theta(z,t)$, especially in the end segments. Gee et al. (1995) showed that over a 4-hour period the standard deviation in $\theta(z,t)$ ranged from 0.01 $m^3\ m^{-3}$ to 0.10 $m^3\ m^{-3}$, with the error increasing as segment length decreased. Multiple measurements had to be averaged over a longer time to produce meaningful results (Gee et al. 1995). While averaging several readings over a longer time reduced the error, it hampered the resolution of short-term changes in $\theta(z)$.

The second problem related to the assumption of a linear $\theta(\kappa^{1/2})$ relationship for all soils. Laboratory and field measurements show that while this assumption may hold for sandy soils, it does not hold for the silt-loam soil used at the barrier. Figure 3-3(a) compares $\theta(z)$ measured with the remote shorting probe in a coarse sand with that determined in the same soil using soil cores and gravimetry. Figure 3-3(b) compares $\theta(z)$ determined by shorting diode TDR with that determined by neutron probe at one monitoring station at the barrier. There is very good agreement between $\theta(z)$ measured by TDR and gravimetry. However, the discrepancy between TDR and neutron probe measurements is quite large. The $\theta(z)$ profiles shown in Figure 3-3(b) were in response to an application of 70 mm of water to the silt loam over an 8-hour period (WY-1995 1,000-year storm). The change in W determined from the TDR was 55 mm, compared to 69 mm from neutron probe measurements. Although the theoretical maximum uncertainty in θ is $\pm 0.005\ m^3\ m^{-3}$, field measurements show a range of 0.003 to 0.15 $m^3\ m^{-3}$, depending on segment length with the error increasing as segment length decreases. The TDR has much potential for long-term monitoring of engineered covers. However, the problems described above must first be resolved before the technology can be deployed. Limited laboratory calibration shows the $\theta(\kappa^{1/2})$ relationship for the silt loam to be nonlinear. Further improvements in probe design and analytical methods should overcome these problems.

3.2.1.2.2 Capacitance probe measurements. Gee et al. (1995) showed a similarity in the general trend of $\theta(z)$ measured by capacitance probe when compared to neutron probe. However, the capacitance probe proved to be relatively insensitive to changes in θ, especially at the wetter end of the moisture range. The capacitance probe also underestimated θ relative to the neutron probe. This observation is inconsistent with published studies, most of which have shown the capacitance probe to overestimate θ relative to the neutron probe. Results also suggested that use of this technique would require an individual calibration function for each monitoring station. The mean change in water storage estimated from the capacitance probe following the 1,000-year storm of WY 1995 was only 47 ± 15 mm. The error in measurement far exceeds the drainage criterion set for the barrier. Consequently, this technology cannot be recommended for monitoring ΔW.

3.2.1.2.3 Neutron probe measurements. Figure 3-2 shows a summary of soil water storage W for each of the four silt-loam-covered plots. The early data provide some insight into the performance of the barrier at low plant population density and inadequate surface cover. After the shrubs were transplanted on November 7, 1994, a survey on December 2 and 21, 1994 showed that about 80% of the seedlings had lost their green foliage and that no grasses had germinated (Gee et al. 1995). Therefore, the initially slow increase in water storage suggests that evaporation may have played an important role in the early part of WY 1995. Because the silt-loam-covered plots all have a well-developed vegetative cover, the contribution of evaporation is now quite small.

In general, the two precipitation treatments showed similar temporal trends in W. Both treatments showed an annual cycle that peaked in mid-February to early March and reached a minimum by the end of October each year. Primarily, the vegetation on the barrier's surface controls this trend. During the winter months, the plants are dormant and the effect of the main mechanisms for water loss, transpiration, and evaporation is at a minimum.

Figure 3-1. Scheduled Monthly Irrigation Water Application Followed During the First 3 Years of the Treatability Test.

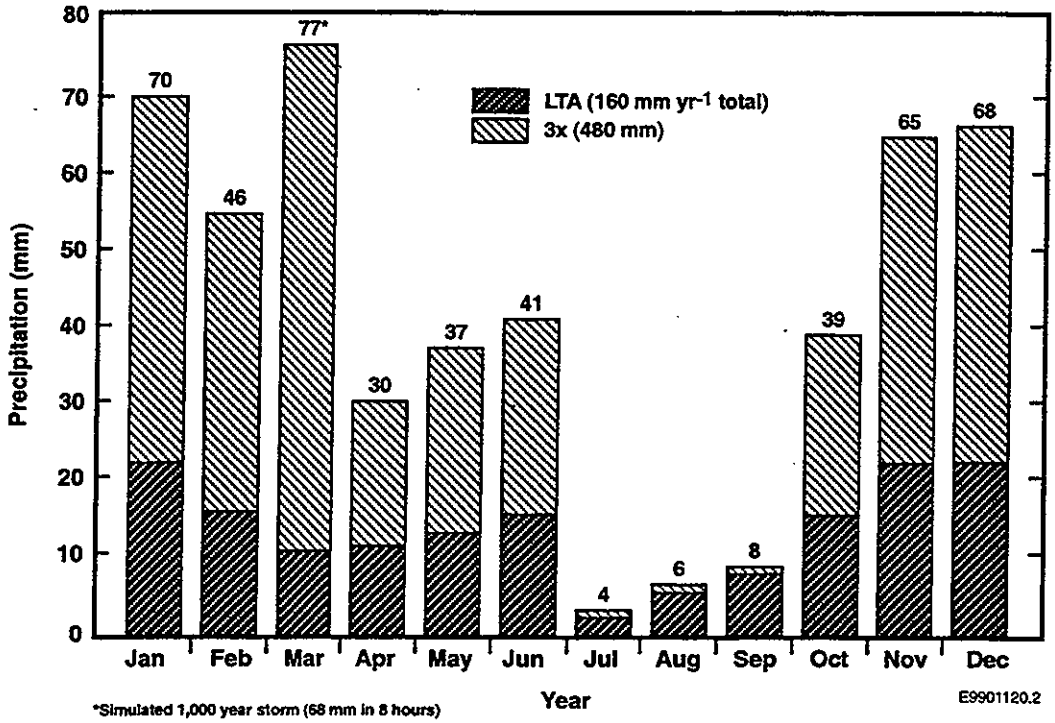

Figure 3-2. Cumulative 4-Year Precipitation Data for the Prototype Barrier. Total Precipitation Includes both Natural Precipitation and Applied Irrigation.

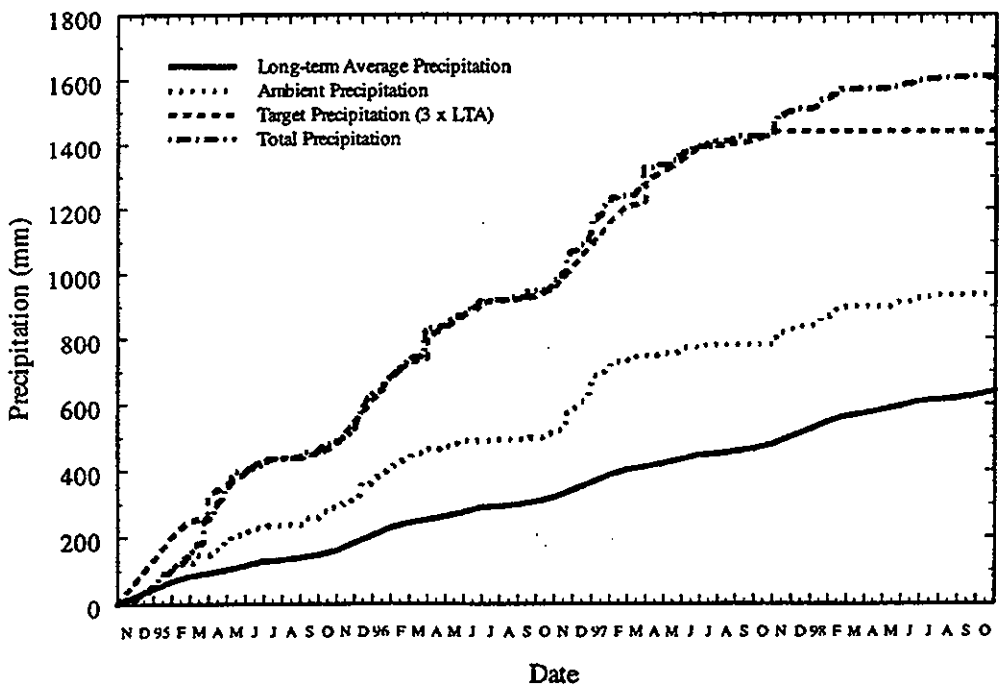

Figure 3-3. Comparison of Water Content θ(z) Measured with a Seven-Segment Remote Shorting TDR Probe with (a) θ Determined by Gravimetry in a Draining Sand Column, and (b) Field Measurements of θ (by Neutron Probe) in the Silt Loam.

(After applying 70 mm of irrigation over 8 hours, the change in storage was 55 mm by TDR measurements compared to 69 mm by neutron probe.)

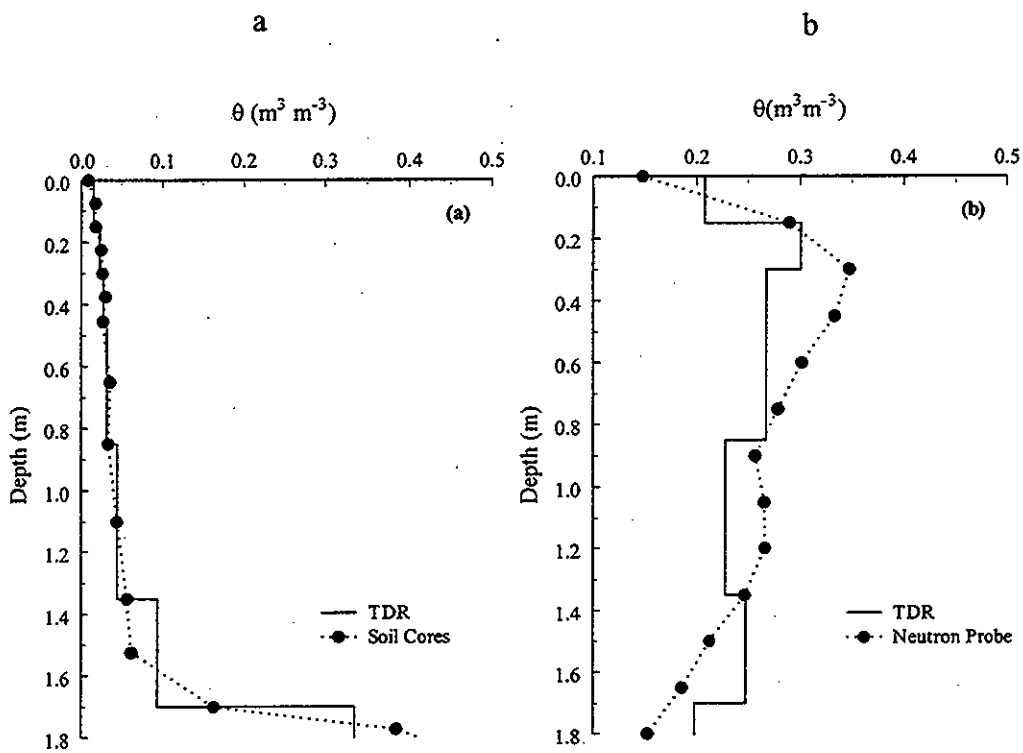

The barrier must therefore store all of the precipitation intercepted. This is reflected in a peak in water storage when winter ends in February. The increase in temperature and the onset of plant transpiration in the spring lead to a rapid decline in water storage. The observed trend in water storage, which reflects a fundamental part of barrier performance, has operated as predicted from previous Hanford Site lysimeter studies (Gee et al. 1993a).

Figure 3-4 shows unusually small peaks in water storage in the winter of WY 1998. There are two explanations: (1) irrigation events were discontinued in September 1997 and briefly resumed in May 1998 to facilitate validation of water storage measurements, and (2) the winter of WY 1998 was unusually dry because of El Niño effects. Precipitation recorded at the barrier in the winter of WY 1998 was 69 mm, compared to 106 mm in WY 1995, 126 mm in WY 1996, and 140 mm in WY 1997. The winter LTA is 60 mm.

3.2.1.3 Infiltration and Drainage.

3.2.1.3.1 Horizontal **neutron measurements-silt-loam capillary break**. Figure 3-5 compares plots of water content as a function of space and time, $\theta(x,t)$, at the northern (irrigated) half of the barrier (neutron tubes AA1 + AA5 and AA2 + AA6) from November 1994 through August 1998. Note that because of the U shape, the tubes are not continuous across the width of the barrier; these plots represent $\theta(x,t)$ measured to within 1 m of the crown of the barrier. Also, because of the location of the tube and the zone of influence of the neutron probe, these data were influenced by the silt-loam layer as well as the underlying layers of sand and gravel (Figure 1-3 and Appendix A). Because the probe was calibrated separately in homogenous sand and in silt loam (not in layered systems), the results are qualitative. Nevertheless, the data provide useful information about the seasonal trends.

The x-axis represents horizontal distance from the center of the barrier, with a positive ordinate to the east of center (toward the riprap side slope) and a negative ordinate to the west of center (toward the gravel side slope). Over the last 4 years, water accumulation showed a clearly defined cycle, with θ increasing in the winter, reaching a maximum in late spring, and decreasing over the summer.

In the 4 years of monitoring, the greatest accumulation of water occurred under the transition surface plots (5W and 5E) of the prototype as shown by the elevated levels at the east and west edges of the graph. It is believed that at the sloped interface between the silt loam and coarser shoulder ballast, a capillary break is formed, facilitating the diagonally downward movement of water. Thus, rather than draining vertically and out via the transition (5E) or side-slope collection area (4E), water collects at the bottom of the silt-loam layer, eventually draining via the silt-loam water collection area (6E). The smaller increase in θ at the northwestern corner (sloped silt-gravel interface) suggests less infiltration may have occurred there than on the eastern side (slope silt-loam-basalt interface).

Figure 3-6 shows similar plots for the southern, nonirrigated section (AA3 and AA4). During the first 2 years, no increase was noted in θ at the capillary break of the nonirrigated treatment. In fact, θ decreased within the first few months of surface revegetation and remained unchanged throughout most of the test period. This trend also showed a dramatic change in WY 1997 when infiltration appeared to have been focused along the edges, as observed in the northern section. There was very limited lateral movement of water.

Figure 3-4. Temporal Variation in Soil Water Storage at the Barrier, for Each of the Silt-Loam Plots, from November 1, 1994 through September 30, 1998. ([a] northwest, 6W; [b] northeast, 6E; [c] southwest, 3W; [d] southeast, 3E).

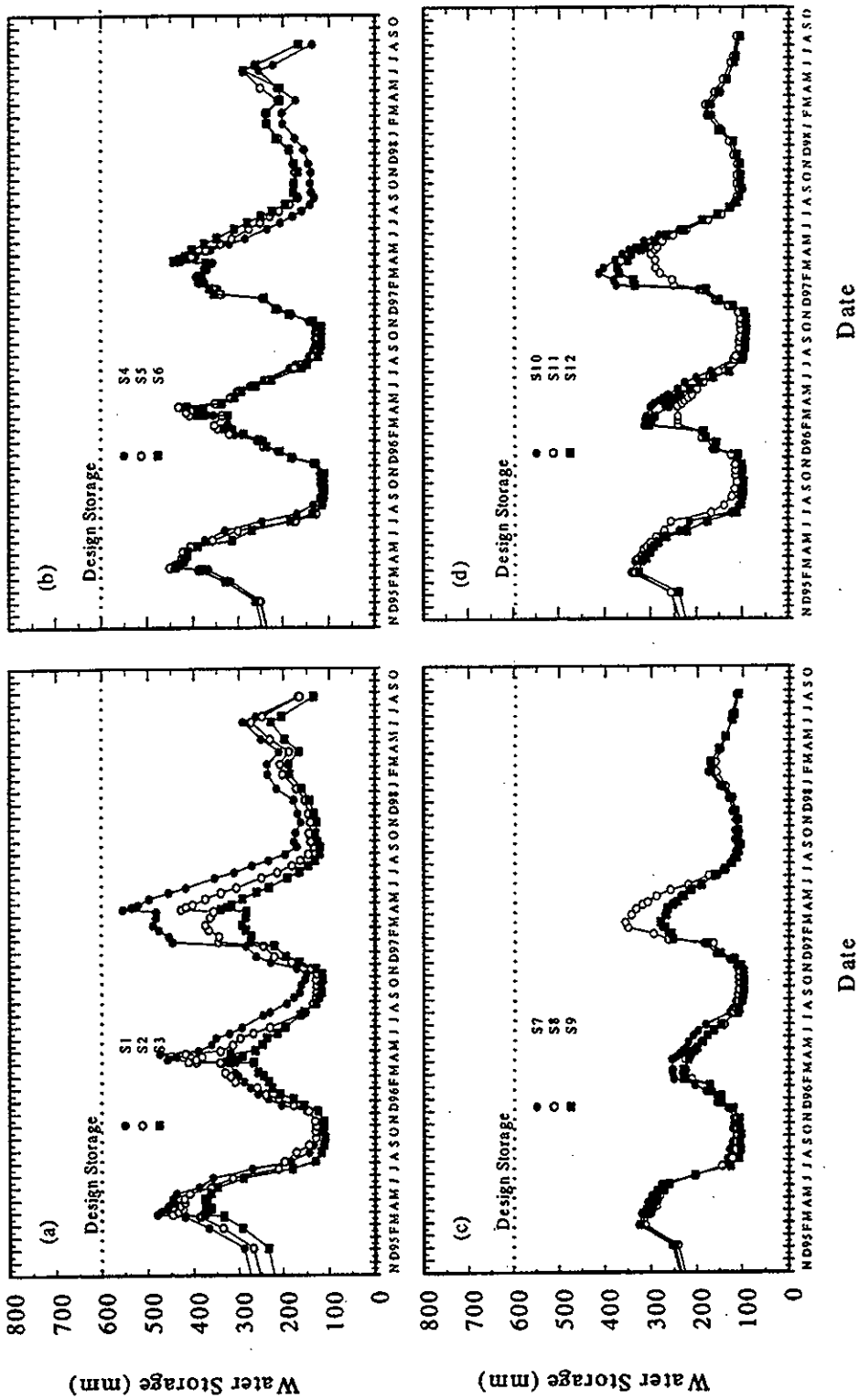

Figure 3-5. Spatiotemporal Variations in Soil Water Content at the Bottom of the Silt-Loam Layer of the Irrigated Treatment of the Barrier. ([a] northern end of treatment, tube AA1 + AA5, and [b] southern end of treatment, tube AA2 + AA6).

(a)

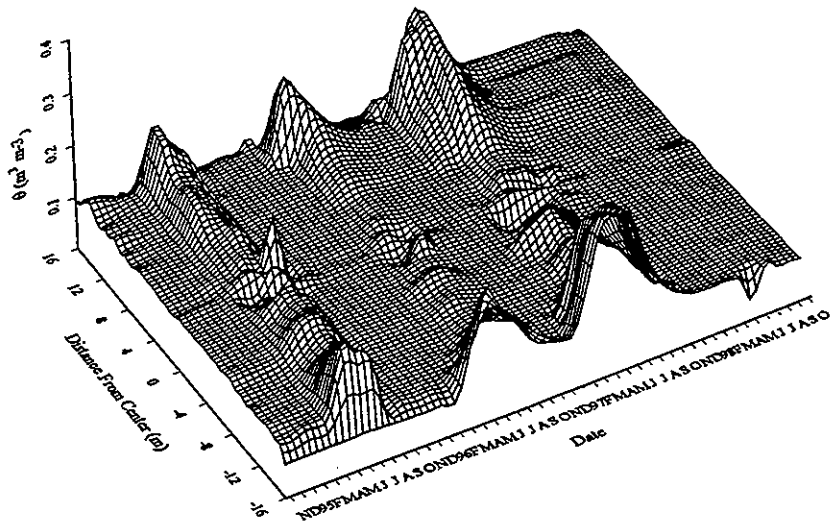

(b)

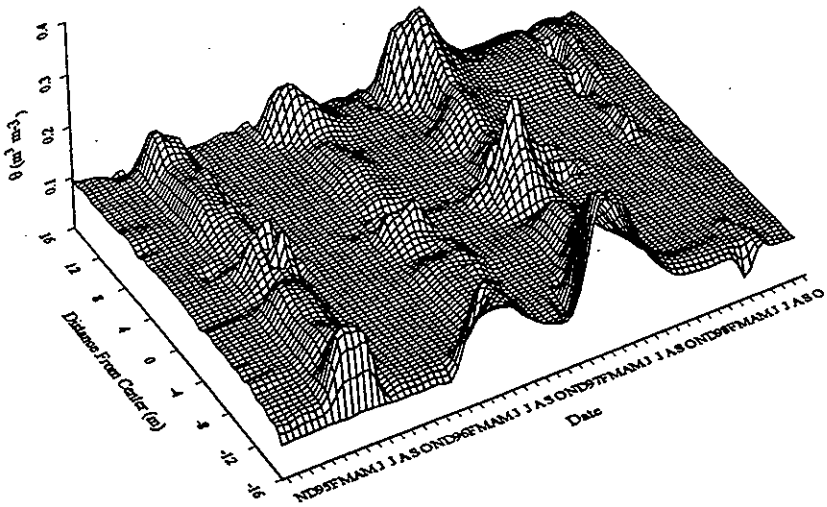

Figure 3-6. Spatiotemporal Variations in Soil Water Content at the Bottom of the Silt-Loam Layer of the Nonirrigated Treatment of the Barrier.
([a] northern end of treatment, tube AA3 + AA7, and [b] southern end of treatment, tube AA4 + AA8).

(a)

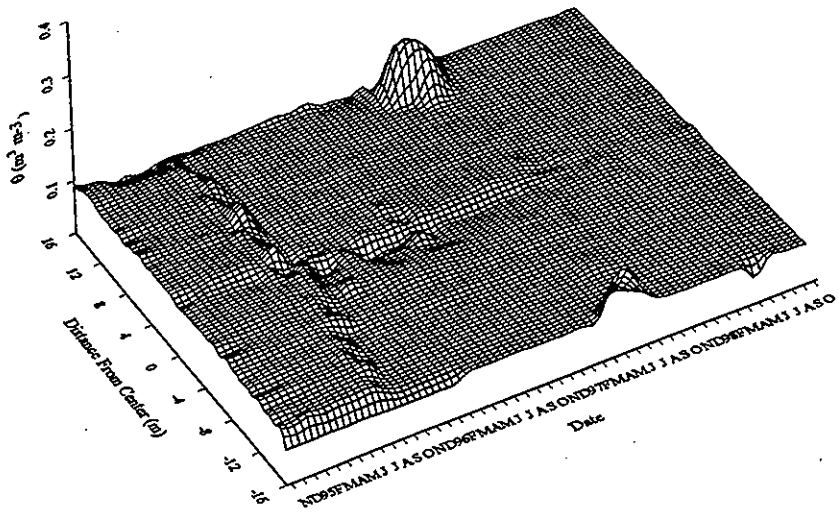

(b)

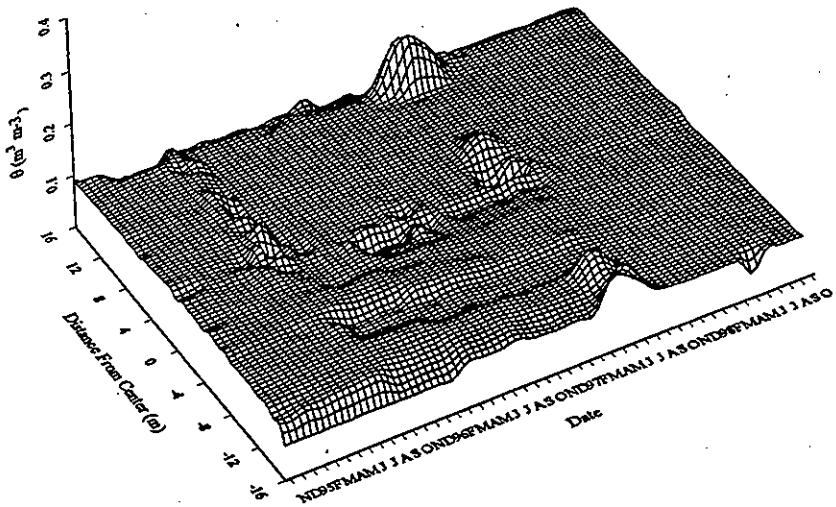

A better visual perspective of the temporal change in θ is obtained from two-dimensional plots of θ(t) along a transect of interest. Figure 3-7 shows a plot of θ(t) at 7 m (midpoint of the plot) and 14 m (outer edge of the plot) in each treatment. In November 1994, initial θ on the four plots was relatively similar, with a mean of 0.10 m^3 m^{-3} over all plots. Despite regular irrigations, no significant increase in θ was observed at the capillary break until just after the first simulated 1,000-year storm on March 26, 1995.

In general, accumulation of water was greatest at the northwest and northeast edges of the irrigated plots (tubes AA1 and AA5) and usually peaked by early May. These data also show that the decline in θ at the capillary break usually starts shortly after reaching its maximum value. There also appears to be a difference in the arrival time of the wetting front at tubes in the north and south ends of each plot, as well as a difference between the value of θ on the western (Figure 3-7a) and eastern (Figure 3-7b) plots. These differences are most likely due to differences in the snow and water accumulation during the winter and spring..

Figures 3-7(c) and 3-7(d) show that on the nonirrigated section, θ declined during the first 10 months of monitoring, after which it remained relatively constant. The first real increase in θ occurred following the winter of WY 1997. Water content reached as high as 0.30 m^3 m^{-3}, which for the Warden silt-loam soil, corresponds to a matric potential of about -186 cm of water. The saturated θ for the Warden silt loam is 0.49 m^3 m^{-3}, so the soil was never saturated. Nevertheless, these observations may have implications on final design, as the elevated water content appears to have originated at the edge of the barrier, in the transition plot.

The occurrence of infiltration along the sloped interface between the silt-loam layers and the side slopes could impact long-term performance. In very wet years, infiltration along the edges (e.g., edge effect) could lead to lateral migration along the capillary break. Although the soil remained unsaturated, there is a possibility of water crossing the capillary break by preferential flow due to fingering. Nevertheless, the data show that by the end of October of each year, θ is usually back to pre-winter levels, reflecting the pattern observed in water storage in the silt-loam profile. Thus, in normal years, the accumulation of water at the base of the silt-loam profile appears controllable simply by ET. However, in extremely wet winters like in WY 1997, accumulation of water at the base of the sloped interface could cause a decrease in the matric suction to a point where water could cross the capillary break. In the absence of a drainage collection system in a final barrier design, water crossing the capillary break would eventually be diverted by the asphalt layer, increasing the amount available for infiltration along the edge of the asphalt layer. The amount of water that infiltrates past the silt-loam layer could be reduced by modifying the design of the sloped interface such that the slope was away from the base of the silt-loam layer rather than toward it, as is now the case. Such a modification would increase the storage capacity along the edge of the silt-loam layer.

3.2.1.3.2 Drainage. Figure 3-8 shows a plot of cumulative drainage (vertical drainage onto the asphalt layer diverted laterally to collection vaults) from each of the water collection zones through September 30, 1998. Table 3-6 summarizes the amount of water drained from each surface plot and shows the relationship to precipitation. In interpreting these data, it is assumed that the direction of flow is vertically downward through the upper layers and horizontal in the

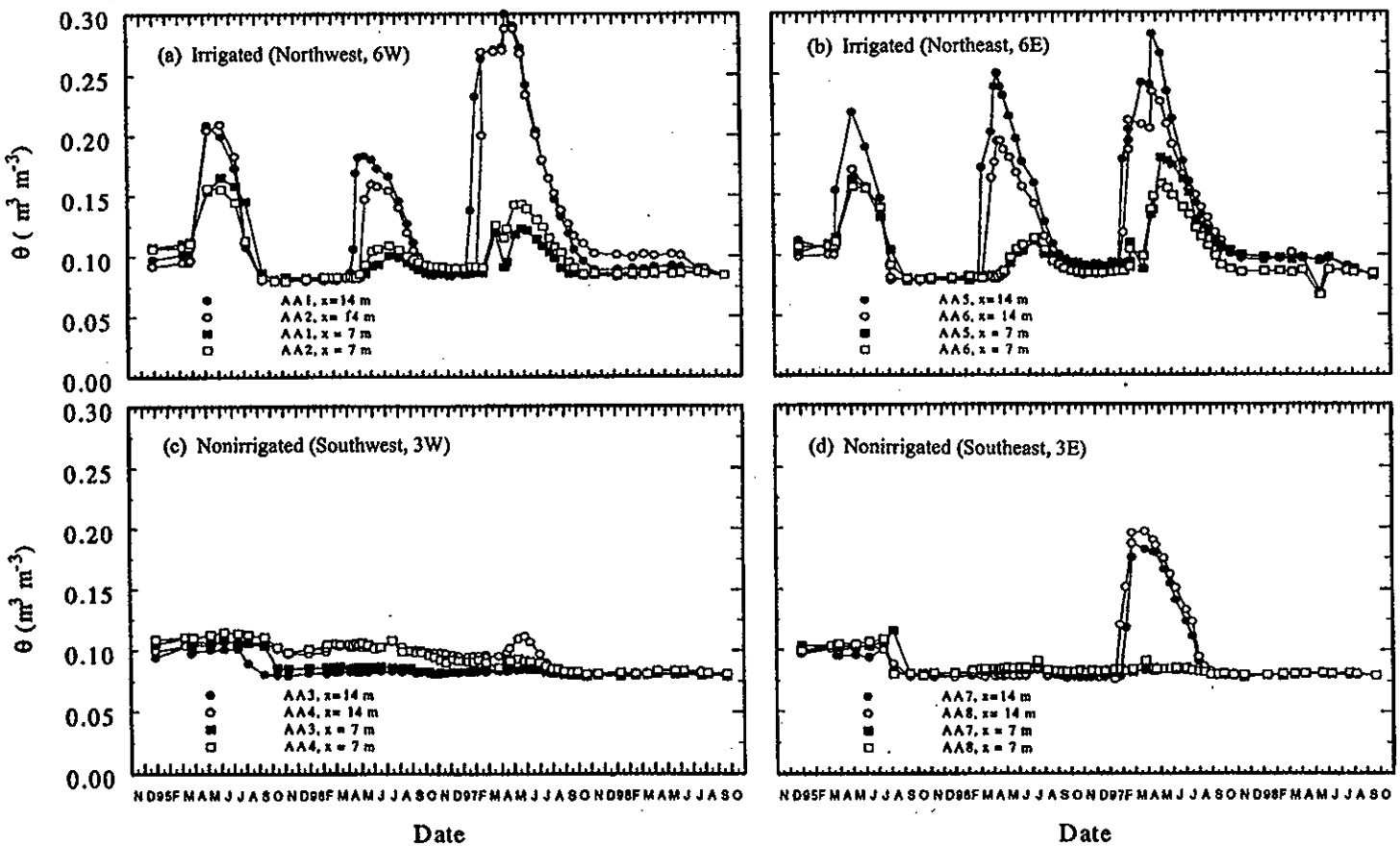

Figure 3-7. A Comparison of Temporal Variations in Soil Water Content Along Two Transects at the Bottom of Silt-Loam Layer of the Barrier.
(Data represent water content θ (t) at 7 m and 14 m from the center of each plot.)

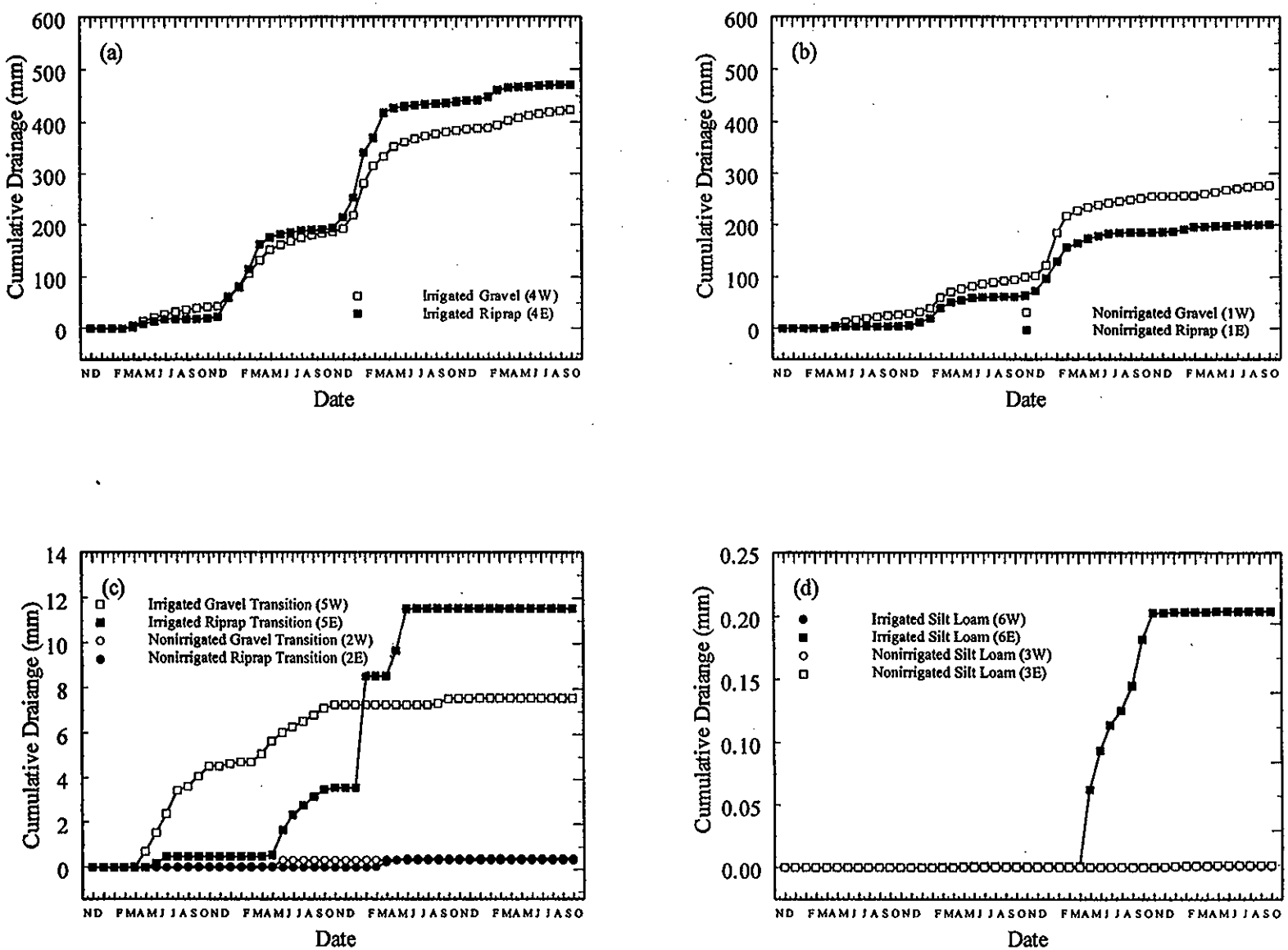

Figure 3-8. Cumulative Drainage from the 12 Collection Zones on the Asphalt Pad. ([a] irrigated side-slope plots, 4W, 4E; [b] nonirrigated side-slope plots, 1W, 1E; [c] transition plots 5W, 5E, 2W, 2E; and [d] silt-loam plots 6W, 6E, 3W, 3E.)

Table 3-6. Amounts of Water Diverted by the Asphalt Pad (Drainage) at the Prototype Barrier and the Relationship to Precipitation During the Period WY 1995 Through WY 1998.

Treatment[a]		WY 1995		WY 1996		WY 1997		WY 1998		WY 1995 - WY 1998	
Precip.	Plot	D (mm)	% P	D (mm)	% P	D (mm)	% P	D(mm)	% P	D (mm)	% P
3X[b]	Gravel (4W)[c]	$4.24 \cdot 10^{1}$	14.7	$1.40 \cdot 10^{2}$	28.6	$1.88 \cdot 10^{2}$	38.0	$3.95 \cdot 10^{2}$	26.9	$4.24 \cdot 10^{2}$	29.4
	Trans. (5W)	$4.54 \cdot 10^{0}$	0.93	$2.58 \cdot 10^{0}$	0.55	$2.81 \cdot 10^{-1}$	0.06	$3.74 \cdot 10^{-3}$	0.00	$7.57 \cdot 10^{0}$	0.525
	Soil (6W)	$3.68 \cdot 10^{-5}$	0.00	$1.74 \cdot 10^{-2}$	0.00	$1.10 \cdot 10^{-4}$	0.0001	$1.32 \cdot 10^{-3}$	0.00	$1.89 \cdot 10^{-2}$	0.001
	Soil (6E)	$1.3 \cdot 10^{-8}$	0.00	$1.33 \cdot 10^{-3}$	0.00	$1.81 \cdot 10^{-1}$	0.00	$1.23 \cdot 10^{-3}$	0.00	$2.04 \cdot 10^{-1}$	0.014
	Trans. (5E)	$4.88 \cdot 10^{-8}$	0.00	$2.99 \cdot 10^{0}$	0.62	$7.97 \cdot 10^{0}$	1.58	$9.70 \cdot 10^{-4}$	0.00	$1.15 \cdot 10^{-5}$	0.802
	Basalt (4E)[c]	$1.97 \cdot 10^{1}$	6.86	$1.68 \cdot 10^{2}$	34.7	$2.22 \cdot 10^{2}$	44.5	$3.14 \cdot 10^{1}$	21.4	$4.71 \cdot 10^{2}$	32.7
1X[b]	Gravel (1W)	$2.65 \cdot 10^{1}$	9.20	$6.60 \cdot 10^{1}$	30.6	$1.48 \cdot 10^{2}$	52.2	$2.18 \cdot 10^{1}$	14.9	$2.77 \cdot 10^{2}$	29.6
	Trans. (2W)	$4.51 \cdot 10^{-2}$	0.02	$2.77 \cdot 10^{-1}$	0.12	$5.91 \cdot 10^{-4}$	0.00	$4.47 \cdot 10^{-3}$	0.00	$3.28 \cdot 10^{-1}$	0.035
	Soil (3W)	$3.26 \cdot 10^{-5}$	0.00	$3.26 \cdot 10^{-5}$	0.00	$1.96 \cdot 10^{-4}$	0.0	$1.00 \cdot 10^{-3}$	0.00	$1.29 \cdot 10^{-3}$	0.000
	Soil (3E)	$2.10 \cdot 10^{-2}$	0.00	$6.75 \cdot 10^{-2}$	0.03	$1.44 \cdot 10^{-4}$	0.00	$1.59 \cdot 10^{-3}$	0.00	$8.94 \cdot 10^{-2}$	0.010
	Trans. (2E)	$3.62 \cdot 10^{-4}$	0.00	$2.29 \cdot 10^{-3}$	0.00	$3.85 \cdot 10^{-1}$	0.13	$4.20 \cdot 10^{-3}$	0.00	$3.92 \cdot 10^{-1}$	0.042
	Basalt (1E)	$3.71 \cdot 10^{0}$	1.29	$5.63 \cdot 10^{1}$	25.3	$1.12 \cdot 10^{2}$	38.4	$1.49 \cdot 10^{1}$	10.1	$2.00 \cdot 10^{2}$	21.4

[a] Abbreviations in this column: Precip = precipitation; 3X = irrigated at 3 times LTA; 1X = ambient; trans. = transition zone.

[b] Drainage in millimeters of water can be converted to a volume in liters by multiplying D(mm) by 322 on the main plots and by 92 on the transition plots.

[c] The gravel and basalt slopes did not start receiving irrigation until WY 1996, although some additional water might have been added during testing of the irrigation system. For these calculations, it is assumed that precipitation is equivalent to that of the nonirrigated plots.

drainage gravel overlying the asphalt layer. In reality, flow is likely to be near vertical near in the middle plots of the barrier (e.g., plots 6W, 6E, 3W, 3E) and a combination of vertical and horizontal near the edges (plots 5E, 5W, 2E, 2W).

Except for the winter of 1997-1998, the amount of drainage from the irrigated gravel slope was similar to that of the irrigated riprap slope. Over the four water years on the irrigated treatment, the gravel slope (4W) drained 423.9 mm of water, or 29% of the precipitation, compared to 470.5 mm of water, or 33% of precipitation drained by the riprap slope (4E). The nonirrigated treatment shows a completely different picture. Over the same period, the riprap (1E) drained 200.4 mm of water (21% of precipitation), compared to 277 mm of water (30% of precipitation) drained by the gravel (1W). The 77-mm difference is equivalent to about 20 mm yr^{-1} of additional water available for infiltration at the edge if a gravel side slope was chosen over a riprap slope. Both plots were exposed to the same quantity of precipitation.

At present, it is not known why the gravel slope drains more than the riprap slope (Ward and Gee 1998). To better understand the difference in performance, data were analyzed on a monthly basis to identify any controlling factors. The analysis shows that in both side-slope configurations, drainage is seasonably dependent, characterized by a decline in the spring and summer and an increase in the winter. Based on these observations, a hypothesis has been formulated to describe the drainage mechanism.

The hypothesis is that advective airflow reduces drainage on the basalt side slope. Each spring (March, April, May) drainage is relatively high, as cool temperatures and relatively high humidity do not provide ideal conditions for evaporation from the side slopes. In the summer months (June, July, August) higher temperatures and lower humidity lead to more ideal conditions and the rate of water loss increases, causing a corresponding decrease in drainage. As the data show, drainage from the gravel is relatively consistent throughout the year; the reduction in drainage is most noticeable on the riprap slopes. This is due to the open structure resulting from the loose packing of 25-cm blocks, as well as to higher thermal gradients in the dark-colored basalt riprap. In the fall (September, October, November) lower temperatures again reduce the evaporation potential, and the drainage from the riprap increases. This trend continues through the winter months (December, January, and February) until the spring warmup causes another reversal in drainage amounts.

These observations may impact the final choice of the side-slope configuration and the construction material. The riprap slope not only occupies a smaller footprint, but also has clear advantages in controlling the amount of water available for drainage. In final barriers, this water would be discharged along the edge of the asphalt layer, and any reduction would reduce the possibility for underflow and deep transport of the buried wastes. Further optimization of the design could reduce drainage to near zero amounts throughout the year.

Apart from small seasonal discharges from the silt-loam-covered plots that have been attributed to condensation, no drainage from the soil-covered plots has occurred. The exception is the irrigated northeast plot (6E) that drained consistently between late April and October 1997. The total amount of water drained through October 31, 1997 was 65.4 L or 0.20 mm. The silt-loam cover was designed with a storage capacity of 600 mm of water, more than three times the LTA for the Hanford Site. A precursor for drainage from the silt-loam profile is water storage in

excess of the 600-mm storage capacity. Because water storage never exceeded the design capacity, the drainage from 6E raised a question about the source of this water.

There is evidence to suggest that the water came from the transition zone. The current design of the transition zone results in an inward-sloping interface between the fine soil layer and the protective slope (see Figure 1-3 and Appendix A). Under very wet conditions, such as those that occurred in the winter of WY 1997, water ponds along the outer edge of silt-loam plots because of the elevated access road around the top perimeter of the barrier. The water tends to move diagonally downward, along the interface, due to the capillary break formed by the fine-over-coarse soil sequence. Water then accumulates at the base of the transition zone and drains through the silt-loam collection zones. Such a scenario would occur without causing a detectable change in water storage simply because of the positioning of the vertical access tubes used to monitor water storage. The nearest vertical tube to the zone of interest is 3 m away; to avoid the possible bias caused by textural discontinuity at 2 m, the maximum depth to which θ is measured is 1.85 m.

These observations may be important to the design of final barriers. The ponding that occurs at the edges of the barrier would be eliminated in a design that does not have an access road. However, water would eventually be discharged along the edge of the asphalt layer. Another option is to increase the storage capacity of the transition zone. With the present design, the inward sloping interface reduces the storage capacity, particularly at the base. A design with an outward slope would eliminate this problem if constructability constraints could be overcome.

3.2.1.3.3 Performance of the asphalt layer. Figure 3-9 shows a plot of soil water content at depths of 1, 2, and 3 m beneath the asphalt. Figures 3-9(a), 3-9(c), and 3-9(e) represent θ as measured in the north tube (Tube BA1) that intersects the uncurbed section of the asphalt, while Figures 3-9(b), 3-9(d), and 3-9(f) show the distribution under the curbed section. In these plots, the $x = 0$ ordinate occurs along the center line of the barrier (under the silt-loam plots), while $x = 50$ m is to the east of the barrier. The edge of the asphalt occurs at 32 m.

The general trend is characterized by a temporal cycle in θ, which is observed at all three depths. This trend is similar to that observed in water storage measured in the silt-loam surface, only lagged in time. The response is less pronounced on the curbed section than on the uncurbed section. Such a temporal dependence is expected because all water diverted by the asphalt layer is shed to the surrounding soil in the uncurbed region, where it is subject to evaporation and plant uptake. The area east of the riprap is sparsely covered with vegetation (Ward et al. 1997).

There is also a widening of the wetted region with depth, but this is due mainly to the configuration of the access tubes. The access tubes were installed at 1-m increments below the asphalt, but because of the 2:1 east slope, each tube exits about 2 m to the east of the tube above it. The zone of measurement therefore increases with depth.

The initial condition showed a slightly wetted area extending about 1 m under the asphalt at the 3-m depth. Water content declined to about 0.10 $m^3\ m^{-3}$ in May 1995 and has remained unchanged. While there have been dramatic changes in θ along the edge of the asphalt layer and

Figure 3-9. Spatiotemporal Variations in Soil Water Content Under the Asphalt Layer. (Page 1)

(Uncurbed asphalt tube [a] BA1 at 1 m and curbed asphalt tube [b] BA2 at 1 m.)

(a)

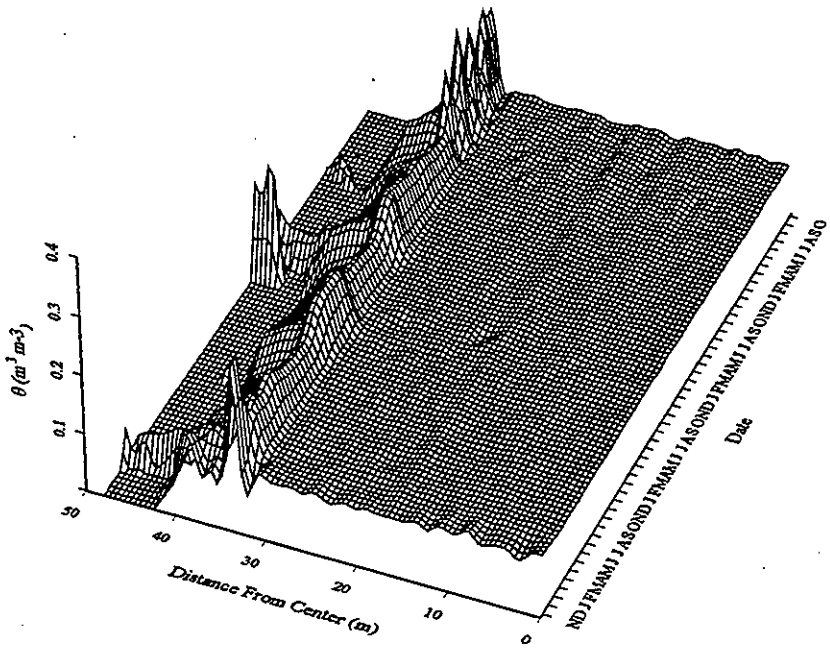

(b)

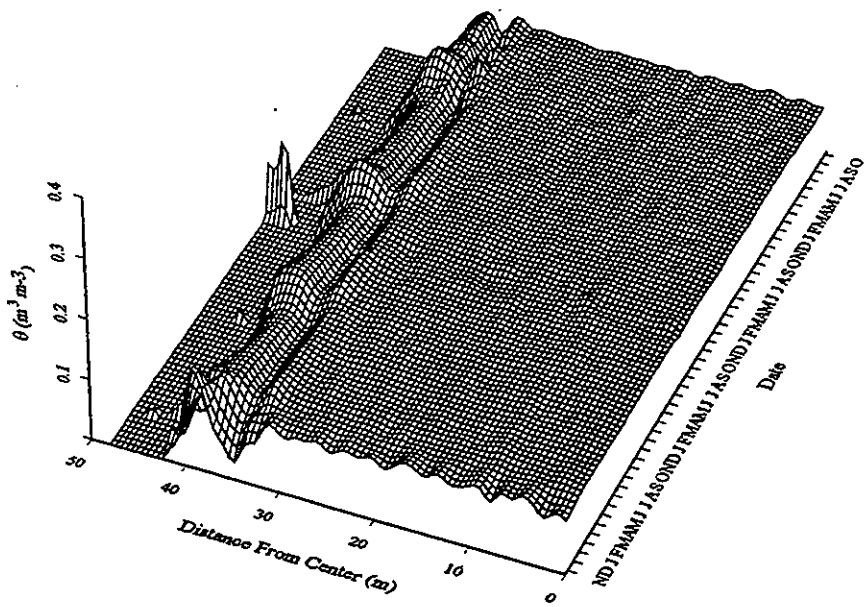

Figure 3-9. Spatiotemporal Variations in Soil Water Content Under the Asphalt Layer. (Page 2)

(Uncurbed asphalt tube [c] BA3 at 2 m and curbed asphalt tube [d] BA4 at 2 m.)

(c)

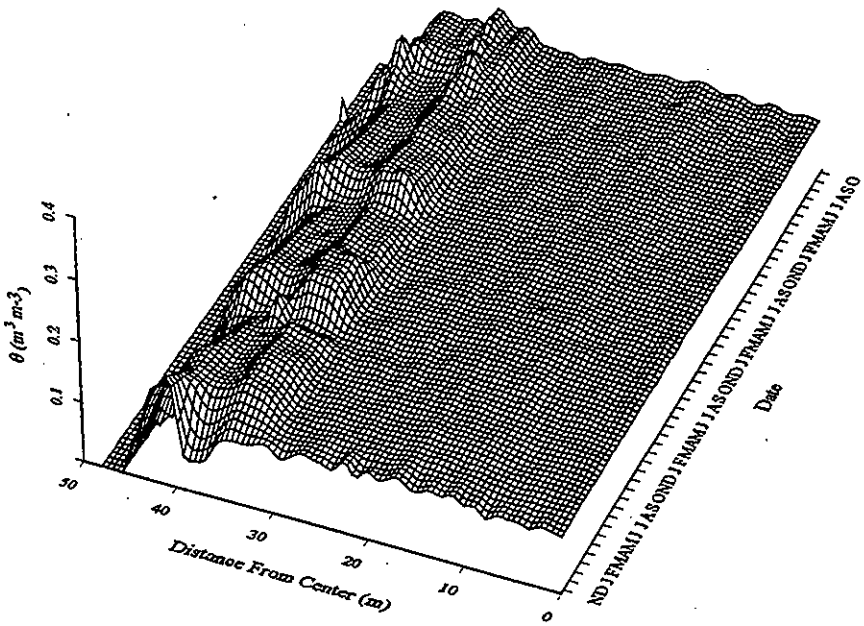

(d)

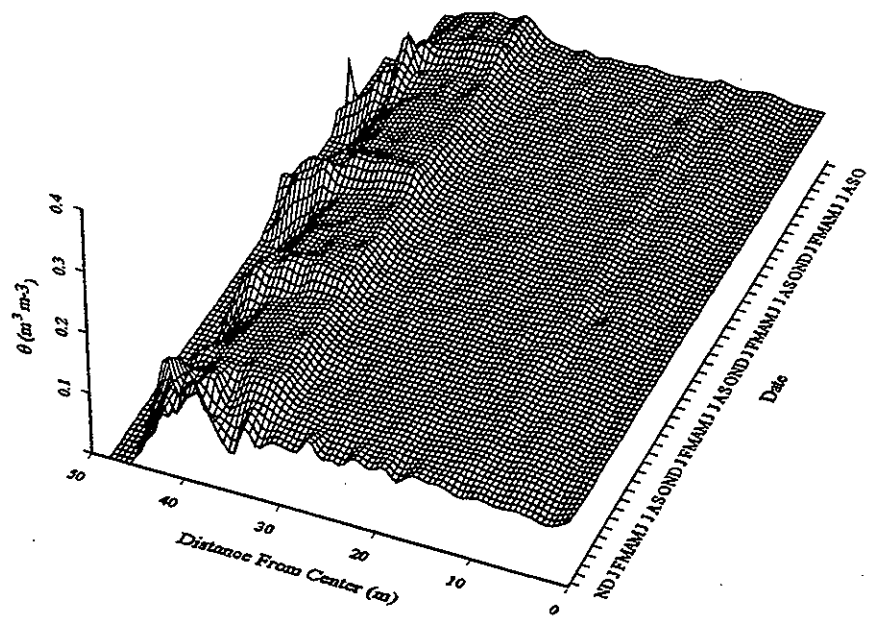

Figure 3-9. Spatiotemporal Variations in Soil Water Content Under the Asphalt Layer. (Page 3)

(Uncurbed asphalt tube [e] BA5 at 3 m and curbed asphalt tube [f] BA6 at 3 m.)

(e)

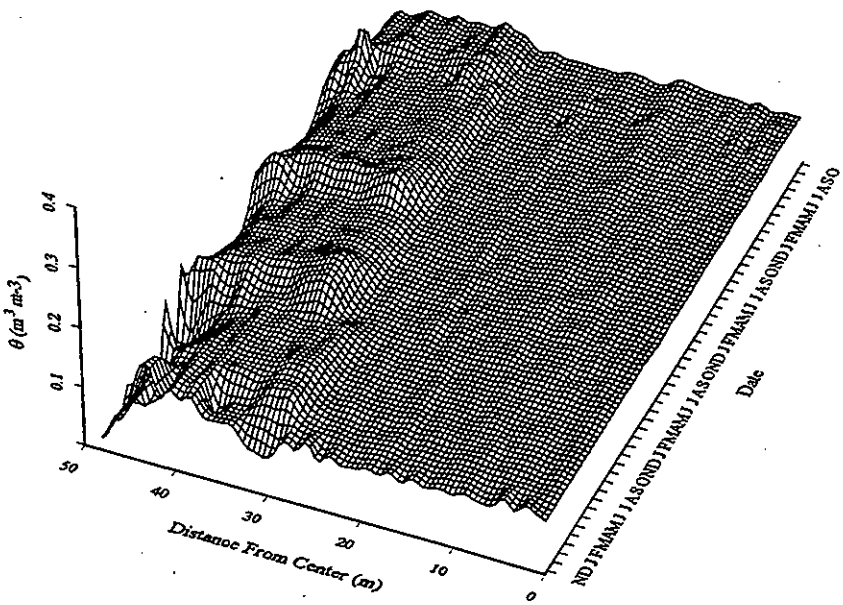

(f)

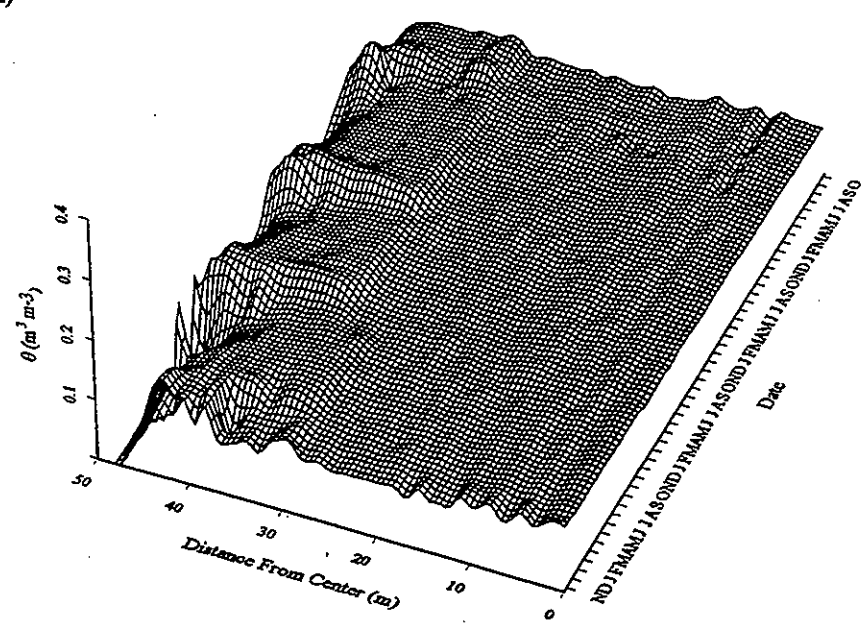

to the east where the water is shed, these changes have not extended very far under the asphalt. At all three depths, changes in θ have not extended more than 2 m under the asphalt, and even then θ has never increased beyond 0.15 m^3 m^{-3}.

The neutron probe measurements were complemented with data from the basin lysimeter installed directly under the asphalt layer. During the first year, a series of leak tests were conducted to determine the integrity of the lysimeter. To date, the volume of water recovered from the lysimeter is equal to the amount added in the tests.

Based on horizontal below-asphalt measures of θ and the lysimeter data, there is no evidence to indicate that water has infiltrated through the asphalt pad. Water content has remained essentially unchanged at 0.10 m^3 m^{-3} over the 4 years, and no leakage has been recovered from the pan lysimeter.

3.2.1.3.4 Surface runoff. Runoff was observed two times during the test period. The first observation was during the first simulated 1,000-year storm event on March 26, 1995 (WY 1995). After the application of 70 mm of water over an 8-hour period to the newly vegetated surface, 1.79 ± 0.11 mm of runoff was measured (Gee et al. 1995). During the next 2 years, none of the natural or simulated storms generated any surface runoff. The trend of no runoff was broken in the winter of WY 1997 when a 36.3 mm of runoff was measured. The runoff was attributed to rapid snowmelt on frozen ground (in December and January). By March 1997 there was no runoff, even during the simulated 1,000-year storm application.

In general, surface runoff occurs when the hydraulic conductivity of the soil is exceeded by the rainfall intensity, or under rapid snowmelt conditions. Previous erosion tests on Warden silt loam (the fine soil used in construction of the barrier) show that when unprotected, the soil is very susceptible to runoff. However, factors shown to reduce runoff include the presence of vegetation and low antecedent moisture (Gilmore and Walters 1993). In those studies, a 1-hour rainstorm with an intensity of 1,536 mm d^{-1} on gravel-amended plots at an antecedent water content of 0.016 g g^{-1} and on gravel-free plots at an antecedent water content of 0.056 g g^{-1} generated runoff equal to 1% of precipitation.

During the first simulated 1,000-year storm, soil cover was minimal, the antecedent moisture was relatively high, and runoff was 2.5% of precipitation (Gee et al. 1995). A well-developed vegetative cover and relatively low intensity of natural rainstorms (25 mm d^{-1} or less) reduced runoff to zero amounts in subsequent years, even during the simulated storms (Gee et al. 1996, Ward et al. 1997). December 1996 was by far the wettest month ever recorded at the Hanford Site with a total of 93.7 mm of precipitation (358% of normal). Rainfall intensity reached 35 mm d^{-1}, still two orders of magnitude smaller than the intensity shown to generate runoff on the test plots. However, a combination of rapid snowmelt and frozen surface soils created conditions conducive to runoff.

The 4 years of runoff monitoring show that, in the absence of a well-established vegetative cover, the inclusion of a pea gravel can keep runoff to less than 3% of the applied precipitation. An established vegetative cover on admix essentially eliminates runoff, except under frozen soil conditions. The impact of this type of runoff is discussed further in Section 3.2.2.2.

3.2.1.3.5 Evapotranspiration. Data collected during the treatability test were used to calculate water loss by ET for each silt-loam-covered plot of the two precipitation treatments. An overall determination of ET for WY 1995-1998 was also made. The water balance, including the calculated ET, is summarized in Table 3-7. The ET on the irrigated plots was significantly different from that on the nonirrigated plots over the 4 years of measurement. No significant differences between plots were found in either of the treatments.

A ratio of ET to total precipitation (P) provides a simple estimate of the efficiency of plant water uptake. A ratio greater than 1.0 suggests that the plants are removing all of the applied water as well as old water stored in the soil profile. A value less than 1.0 suggests that the plants are removing less water than is applied. There was an obvious decline in the ET-P ratio over the testing period. The decline was greater on the irrigated treatment. The irrigated section showed a ratio of 1.2 in WY 1995, but only 0.98 in WY 1996 and 0.88 in WY 1997. On the nonirrigated treatment, ET-P ratios were 1.3 in WY 1995, 1.0 in WY 1996, and 0.97 in WY 1997. The reduction observed from WY 1995 to WY 1996 may be related partly to the change in the plant population at the barrier. In WY 1996, no *Salsola kali* (tumbleweed) was found at the barrier, compared to WY 1995 when a healthy stand was in place. Under wetter conditions, plants on both treatments transpired more water, although it was a smaller percentage of the total precipitation.

Given the consistently higher ratios on the nonirrigated section, the nonirrigated plants appear to be more efficient at recycling water to the atmosphere. Nevertheless, these data show that the native plant species can easily recycle almost twice the LTA precipitation and will handle more than three times this amount, although probably only over short periods.

3.2.1.3.6 Summary. Four years of testing and monitoring for water balance evaluation at the prototype Hanford Barrier has been completed. This study demonstrates the effectiveness of the barrier in controlling infiltration to underlying wastes.

By the end of WY 1998, the irrigated treatment had received a total of 1,609 mm of water. The nonirrigated treatment had received 936 mm of water, about 1.8 times the LTA precipitation for the Hanford Site. Over the same period, 673 mm of irrigation water was applied. Water storage repeated the temporal cycle observed in the first year in which water storage was maximized in late winter followed by a rapid decline to reach a minimum at the end of October. By the end of September 1998, water storage on all of the plots had been reduced to levels similar to the three previous years. The lower limit of water storage was independent of precipitation treatment, a confirmation that the native plant species can use all water, at least in the short term. The 600 mm of design storage provided sufficient storage capacity for three times the LTA precipitation, including simulated 1,000-year return extreme precipitation events.

In the absence of a well-established vegetative cover, runoff from the barrier was less than 3% of the applied precipitation and was virtually eliminated after the vegetation was established. With an established vegetative cover, runoff occurred only under frozen soil conditions. Overall, the barrier performed according to design specifications, shedding water toward the edges to be diverted via the transition zones and side slopes rather than allowing accumulation on the surface.

Table 3-7. Water Balance Summary for the Hanford Prototype Barrier.

Treatment[a]		Water Year (WY)[b]	W_1 (mm)	W_2 (mm)	ΔW (mm)	P (mm)	I (mm)	R (mm)	D (mm)	ET (mm)
Precip.	Plot									
3X	6W	WY 1995	243.53	124.10	-119.43	287.27	350.60	1.78	3.68×10^{-5}	755.52
		WY 1996	124.10	132.10	8.00	224.28	247.35	0.00	1.74×10^{-2}	463.61
		WY 1997	132.10	144.27	12.17	289.81	224.92	36.30	1.10×10^{-4}	466.26
		WY 1998	144.27	156.5	12.3	146.81	200.00	0.00	1.32×10^{-3}	334.51
		WY 1995-1998	243.53	156.5	-87.03	948.43	1022.87	38.08	1.89×10^{-2}	997.36
	6E	WY 1995	233.43	114.47	-118.96	287.27	350.60	1.78	1.3×10^{-8}	755.06
		WY 1996	114.47	123.50	9.03	224.28	247.35	0.00	1.33×10^{-3}	462.60
		WY 1997	123.50	160.87	37.37	289.81	224.92	36.30	1.81×10^{-1}	440.86
		WY 1998	160.87	157.3	-3.57	146.81	200.00	0.00	1.23×10^{-3}	350.38
		WY 1995-1998	233.43	157.3	-76.13	948.43	1022.87	38.08	2.04×10^{-1}	986.28
1X	3W	WY 1995	225.67	112.33	-113.33	287.27	150.00	0.00	3.26×10^{-5}	550.60
		WY 1996	112.33	104.34	-7.99	224.28	0.00	0.00	3.26×10^{-5}	232.28
		WY 1997	104.34	112.47	8.13	289.81	0.00	0.00	1.96×10^{-4}	281.68
		WY 1998	112.47	112.5	0.03	146.81	0.00	0.00	1.00×10^{-3}	146.78
		WY 1995-1998	225.67	112.5	-113.17	948.43	150.00	0.00	1.29×10^{-3}	1061.60
	3E	WY 1995	229.60	106.15	-123.45	287.27	150.00	0.00	2.10×10^{-2}	560.70
		WY 1996	106.15	100.40	-5.75	224.28	0.00	0.00	6.75×10^{-2}	229.97
		WY 1997	100.40	109.37	8.97	289.81	0.00	0.00	1.44×10^{-4}	280.75
		WY 1998	109.37	110.7	1.33	146.81	0.00	0.00	1.59×10^{-3}	145.44
		WY 1995-1998	229.60	110.7	-118.90	948.43	150.00	0.00	8.94×10^{-2}	1067.24

[a]Abbreviations in this column: Precip = precipitation; 3X = irrigated at 3 times the long-term average; 1X = nonirrigated.

[b]Start and end dates for the WY used in these calculations were determined by the start and end dates for water storage measurements, W_1 and W_2, respectively. In WY 1995, W_1 and W_2 were September 30, 1994 through October 24, 1995; in WY 1996, W_1 and W_2 were October 24, 1997 through October 23, 1996; in WY 1997, W_1 and W_2 were October 23, 1996 through October 25, 1997; in WY 1998 W_1 and W_2 were October 25, 1997 through September 24, 1998.

Horizontal neutron measurements of water content at the 2-m depth in the silt loam show a seasonal cycling similar to that observed in the silt-loam profile. At the 2-m depth, water content changes were greatest along the edges of the barrier, exceeding 0.30 $m^3 m^{-3}$ on the northwest (6W) irrigated plot. Lateral migration of moisture on the northeast section was particularly heavy during the last winter. A proposed hypothesis suggests that the accumulation of water along the edges of the soil plots was a result of rapid infiltration along the sloped interface of the transition zones, with subsequent migration in the region of the capillary break. The below-asphalt measurements also showed a temporal cycling near the edge of the asphalt, but there were no changes in water content beneath any of the silt-loam-covered plots. Based on the horizontally measured water content and lysimeter data, there is no evidence to show that water has penetrated the asphalt pad.

The two side-slope configurations drained different amounts and at different rates. Under ambient conditions, the riprap side slope produced less drainage per year than the gravel slope; it is hypothesized that the difference is due to a greater advection potential in the riprap. Under elevated precipitation, both configurations generally produced similar amounts of drainage. None of the silt-loam plots, except for the irrigated northeast plot (6E), produced any drainage during the last year. The northeast plot started to drain in April 1997, generating 0.204 mm of water by the end of September 1998. Water storage measurements do not support this observation (of drainage). The water draining from 6E is believed to be water that infiltrated along the sloped interface of the adjacent transition zone. This drainage is water that crossed the capillary break and was diverted by the asphalt layer, as planned for in the design. Nevertheless, 0.204 mm of drainage from the silt-loam plot over the 4-year test period is significantly less than the 0.5 mm yr^{-1} drainage criterion set for the overall barrier system.

The upper silt-loam layers were able to store more than three times the LTA, but essentially all of the water was removed by ET. However, water balance evaluation shows that plants on the irrigated treatment were less efficient at recycling water by ET, suggesting that the native shrubs may be adversely affected by high levels of precipitation. Expressed as a percentage of precipitation, ET declined over the last 4 years, with the greater decline occurring on the irrigated treatment. The nonirrigated plants appear to be more efficient at recycling water to the atmosphere. Nevertheless, evaluation of the water balance shows that native plant species can easily recycle almost twice the LTA precipitation and will handle more than three times this amount, although probably only over short periods.

3.2.2 Water and Wind Erosion

3.2.2.1 Rainfall Characteristics. The important influences on erosivity are the amount and intensity of rainfall. During the 3 years of erosion monitoring, rainfall data were analyzed to establish the timing of the most erosive rains. The rains recorded at the barrier have been generally of low erosivity with EIs ranging from 4 units to 25. The average annual EI for the area around and including the Hanford Site is 20 (Wischmeier and Smith 1978). During the most vulnerable stage of the barrier's life (sparse vegetative cover), the most erosive precipitation event was the simulated 1,000-year storm in March 1995. The calculated EI for the simulated storm was 20.6, a value that exceeds the mean reported for the site. It should be noted that the simulated storms did not represent the most erosive events because the raindrop size and intensity remained constant (8.5 mm hr^{-1}) over time. The intensity of natural storms tends to

follow a bell-shaped curve, and drop sizes are variable. The first storm event resulted in 2 mm of runoff, just over 2% of the total applied amount. However, it has been shown that even under more erosive conditions (precipitation exceeding 60 mm hr^{-1}), runoff and sediment yield were effectively controlled by soils amended with pea gravel (Gilmore and Walters 1993). This rate exceeds those calculated for extreme events at the Hanford Site. Extreme value analysis of site precipitation records shows rates of 20.6 mm hr^{-1} for the 100-year return storm and 28.2 mm hr^{-1} for the 1,000-year return storm.

3.2.2.2 Surface runoff and sediment yield. During the first simulated 1,000-year storm, runoff occurred in increasing amounts after 5 hours of irrigation (Gee et al. 1995). During that test a runoff volume of 1.79 ± 0.11 mm was recorded. During that same test, sediment collection started at around 7 g L^{-1} and decreased with time to 1 g L^{-1} by the end of the test. This pattern of sediment yield (i.e., high initial concentrations falling off with time) is consistent with the results obtained from the erosion test plots with little or no vegetation at McGee Ranch.

Field tests showed that unprotected silt loam is very susceptible to rainsplash erosion and does not contain enough coarse material to initiate the development of surface armor (Gilmore and Walters 1993). Use of bare silt-loam-gravel admixes reduced the rate of erosion, but soil loss continued throughout the tests. In contrast, silt-loam-gravel admix, combined with a vegetative cover, brought about the greatest reduction in sediment yield; it is estimated that such a combination could reduce sediment yield by 10 to 100 times (Gilmore and Walters 1993).

Following the first year in which sediment loss occurred, the intensity of rainstorms occurring at the barrier were generally less than 25 mm d^{-1} and, as such, did not generate any runoff or sediment yield. Following the first runoff event, no runoff or soil loss was observed until January 1997. A combination of rain and snowmelt and frozen surface soil led to sporadic runoff events. Runoff occurred from both the irrigated and nonirrigated plots. Most of the water accumulated along the eastern and western edges of the barrier, with the greatest accumulation at the northeast and southeast corners. This accumulation led to significant increases in water stored in the profile, near the transition zone (e.g., S1, S2 in Figure 3-4a). However, no soil loss was observed.

Overall, erosion control on the barrier has performed according to design specifications. The vegetated soil cover reduces soil loss and, under unfavorable conditions, the gentle 2% slope encourages the shedding of water toward the edges to be diverted via the transition zones and side slopes rather than allowing accumulation on the surface. The fact that the only loss of soil occurred during a simulated storm event on essentially bare soil suggests that potential for soil loss has decreased as the plant cover developed. Results from the tests at McGee Ranch and the first year of barrier testing show that in the event of the barrier temporarily losing its vegetative cover, the gravel admix can effectively minimize runoff and sediment yield. The potential for runoff and soil will always exist; however, as the barrier ages, the amount of soil loss expected will continue to decrease, especially if the surface remains covered with vegetation.

3.2.2.3 Near-Surface Soil Bulk Density. Near-surface soil bulk density, ρ_b, was measured periodically during WY 1995 through WY 1997. During that period, ρ_b has shown a consistent decrease (Ward et al. 1997). The mean surface dry bulk density, $\overline{\rho}_b$, as measured in December 1994 was 1,879 ± 67 kg m^{-3}. By September 1997 measured $\overline{\rho}_b$, excluding the buffer

zones, was 1,695 ± 47 kg m^{-3}. The Student's t-test confirms that $\overline{\rho}_b$ in WY 1997 was significantly smaller ($\alpha = 0.05$) than in WY 1995. It is hypothesized that the decline in ρ_b is due to the effect of increased root biomass and the depositions of organic matter near the surface. To test this hypothesis, the WY 1997 data were further analyzed to detect differences in $\overline{\rho}_b$ between the two treatments and between silt-loam plots within a treatment. Results of these tests show a significantly higher $\overline{\rho}_b$ (1,718 ± 45 kg m^{-3}) on the nonirrigated treatment compared to the irrigated treatment, where $\overline{\rho}_b$ was only 1,673 ± 39 kg m^{-3}. Differences between silt-loam plots within the treatments were not significant at $\alpha = 0.05$.

These results show a negative correlation between dry density and precipitation regime. Such a relationship could result from an increase in root biomass, bioturbation, and soil organic matter content under elevated precipitation. Analysis of soil samples for organic carbon content showed that mean %C on the irrigated treatment was 2.6 ± 0.11%, compared to 2.0 ± 0.40% in the control sample and 2.0 ± 0.10% on the nonirrigated treatment. The %C on the irrigated treatment was significantly larger than that on the control and nonirrigated treatments, but no difference was found between the nonirrigated and control treatments.

It is clear that the establishment of vegetation on the barrier led to a significant reduction in near-surface (≤0.20 m) bulk density. Based on the results, it seems likely that in a wetter climate enhanced plant growth would lead to higher organic C and a lower bulk density, both of which have been shown to enhance infiltration and water storage capacity. However, as shown by the results from the nonirrigated section, elevated organic matter and reduced bulk densities are benefits rather than prerequisites for successful performance.

3.2.2.4 Water Erosion Summary. The erosivity of the major natural storm events has been generally less than the average annual EI for the Hanford Site and considerably less than events that caused soil erosion in the past. The simulated 1,000-year storm events were characterized by a constant intensity, unlike natural events. Consequently, predictions cannot be made based on the results obtained during such tests. Nevertheless, results from the first year of barrier testing show that even with a low percentage of surface plant cover, the gravel admix can reduce runoff and sediment yield. A well-established vegetative cover virtually eliminated runoff and sediment yield in subsequent years. Four major storm events were observed during the winter of WY 1997, generating a total of 36.3 mm of surface runoff, but no soil loss was observed. The 2% slope of the surface promotes adequate runoff without inducing excessive erosional forces. Based on 4 years of erosion monitoring, the erodibility of the soil appears to have declined significantly, thereby making the soil less vulnerable to water erosion.

3.2.2.5 Wind Stress Characteristics. Boundary layer data collected in WY 1995 through WY 1997 were used to track mean and peak-gust wind speed on the barrier from which erosive stresses were calculated. Over the length of the test, the mean wind speed at the barrier was 3.1 m s^{-1} on the elevated surface and 2.5 m s^{-1} adjacent to the barrier, compared to a normal wind speed of 3.4 m s^{-1} for the Hanford Site. Peak-gust wind speed showed a similar trend, being highest on the silt-loam surface at Stations 01 and 02 and lowest at Station 03. For example, in WY 1997, the mean peak gust at Station 01 was 11.3 ±± 1.9 m s^{-1} compared to 10.9 ±1.8 m s^{-1} at Station 02 and 11.1 ± 1.5 m s^{-1} at Station 03; the annual average peak-wind gust reported at the Hanford Site by the HMS is 11.6 m s^{-1}.

The difference in wind velocities between the stations at the barrier is partly due to edge effects and partly due to surface features that increase roughness. Because Station 03 is at a lower elevation (off the barrier's surface) and the native plants are somewhat taller, lower velocities can be expected, due to increased drag on the airflow. With the prevailing west-northwest or northwest wind direction, Station 02 is downwind of Station 01, and wind encounters increasing surface roughness as it moves toward Station 02. Downwind measurements are therefore more representative of the barrier as the airflow is more fully equilibrated with the vegetated surface.

For any given soil condition, the amount of soil that is transported by wind is controlled by the wind stress parameters, which depend partly on the wind velocity and partly on the roughness length. Therefore, an analysis of the change in wind stress parameters in moving from the wind tunnel to the field and in the field as the barrier aged provides an indication of the effectiveness of the surface vegetation in reducing the erosive stresses.

Roughness length is controlled mainly by vegetation, and soil is therefore almost immune to wind erosion when covered with vegetation. Before the surface was vegetated, the largest peak-gust wind speed recorded was 17.65 m s^{-1} measured at a height of 2 m on October 26, 1994 (Gee et al. 1995). Using Equation 2.5, a mean friction velocity, u_*, was calculated as 0.91 ± 0.002 m s^{-1}. After vegetation was established, the largest peak-gust wind speed recorded was 22.04 m s^{-1} on December 15, 1996 at Station 01. Malfunctioning anemometers at the lower levels prevented use of these data to estimate stress parameters. Instead, the boundary layer measurements taken 3 days earlier, when peak-gust wind speed at the 2-m elevation reached 18 m s^{-1} at Station 02, are used for the calculation. The resulting mean u_* on the surface was 1.78 ± 0.3 m s^{-1}. Figure 3-10 shows the boundary layer profiles from peak gusts measured in WY 1997. The mean u^* on the surface was 2.17 ± 0.04 m s^{-1}. These friction velocities show a significant increase over time, indicating an increase in surface roughness. The WY 1995 and WY 1996 results are also an order of magnitude lower than those reported in the literature. Sehmel (1980, 1984) reported u_* of 1.81 m s^{-1} at a height of 2 m above level desert surfaces. Ligotke (1993) reported u_* between 0.4 and 2.2 m s^{-1} for bare silt-loam admixtures in wind tunnel tests. The increase in u_* is related to an increase in the effectiveness of turbulent exchange over the surface and is consistent with increases in vegetative cover and plant height. The effect of plant cover on boundary layer profiles is clearer after calculating the mean roughness height, z_o.

The mean roughness height calculated from the WY 1997 data was 0.076 ± 0.006 m, compared to 0.041 ± 0.02 m in WY 1996 and 0.0013 ± 0.0001 m in WY 1994. Analysis of the WY 1997 results shows a higher value of z_o at Station 01 (0.082 m) than at Station 02 (0.070 m) in WY 1997. The two stations showed identical values of z_o in WY 1994. These results are somewhat higher than those reported in the literature. For level desert surfaces, Sehmel (1980, 1984) reported a typical surface roughness height of 0.0003 m at a height of 2 m above the surface. Ligotke (1993) calculated z_o of 0.0005 ± 0.0002 m in wind tunnel tests on bare surface construction materials. The higher values of z_o are related to the zero plane displacement, d, which is indicative of the mean level at which momentum is adsorbed by the individual elements of the plant community; the velocity can approach zero at an elevation of z_o + d and d would increase as the plants grew taller. The effect of increasing d is to reduce the erosive stress near the surface.

Figure 3-10. Peak Gust Wind Profiles Measured over the Elevated Surface of the Hanford Barrier on March 30, 1997.

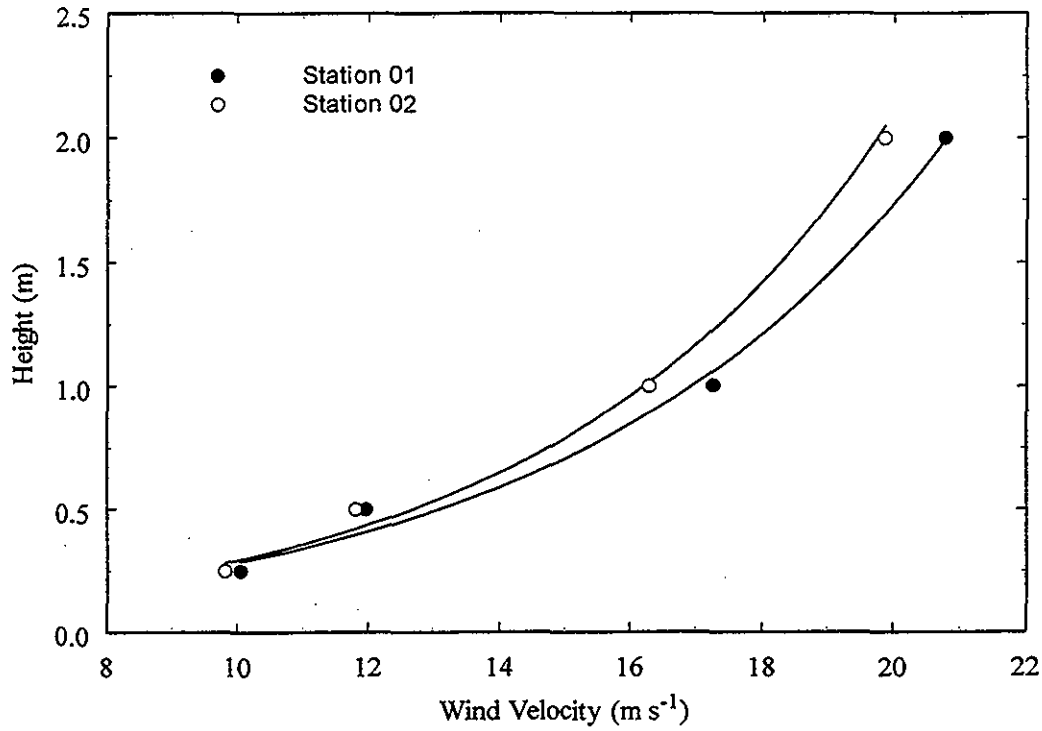

Because z_o is controlled mainly by surface vegetation, comparison of field and laboratory measurements without plants, or with plants having dissimilar characteristics, can be misleading. Ward et al. (1997) estimated plant height from z_o and compared the results with measured values. Mean plant height estimated from z_o at Stations 01 and 02 was 0.58 ±0.05 m, compared to 0.54 ± 0.11 m, obtained by averaging the height of *C. nauseosus* (gray rabbitbrush) and *A. tridentata* (big sagebrush) in the nonirrigated treatment.

If the results from Station 02 are excluded, because of its proximity to the edge of the barrier, and only the dominant *A. tridentata* is considered in the comparison, the results are even better. The plant height estimated from z_o becomes 0.63 m compared to 0.65 m measured on the nonirrigated treatment. A similar analysis for data collected soon after barrier construction, and before restoration, gives a z_o of 0.0012 m and *h* of 0.088 m on the surface. These values are comparable to those observed by Ligotke (1993).

The increase in u_* and the increase in z_o and *h* with time is consistent with an increase in plant cover and height and a corresponding decrease in the potential for wind erosion as the barrier aged. These results are supported by the data collected from dust traps installed on the barrier. The dust traps were monitored between August 29, 1994, and November 1, 1994. The traps provided information on the vertical distribution, quantity, and composition of soil blowing over the surface of the barrier. During the sampling period, the average mass of material collected from three traps ranged from 0.07 to 2.9 g. In eight of nine samples, the vertical profiles of

suspended material were similar, regardless of the intensity of the dust storms (Gee et al. 1995). The data were normalized by dividing the mass at each height by the total mass. The results are shown in Figure 3-11. The results show that the normalized shape of the vertical distribution of blowing soil over the surface was quite uniform. From this information, the total quantity of soil blown past the monitoring stations during the nine sampling periods was determined to have varied from 25 to 2,500 g per meter of width. During the monitoring period when the soil was bare, there were no abnormal winds (>2-year return period) and, as such, the amount of soil loss was relatively small.

Figure 3-11. Normalized Vertical Profile of Soil Mass Blowing Across the Barrier's Surface Between September 29, 1994 and November 1, 1994.

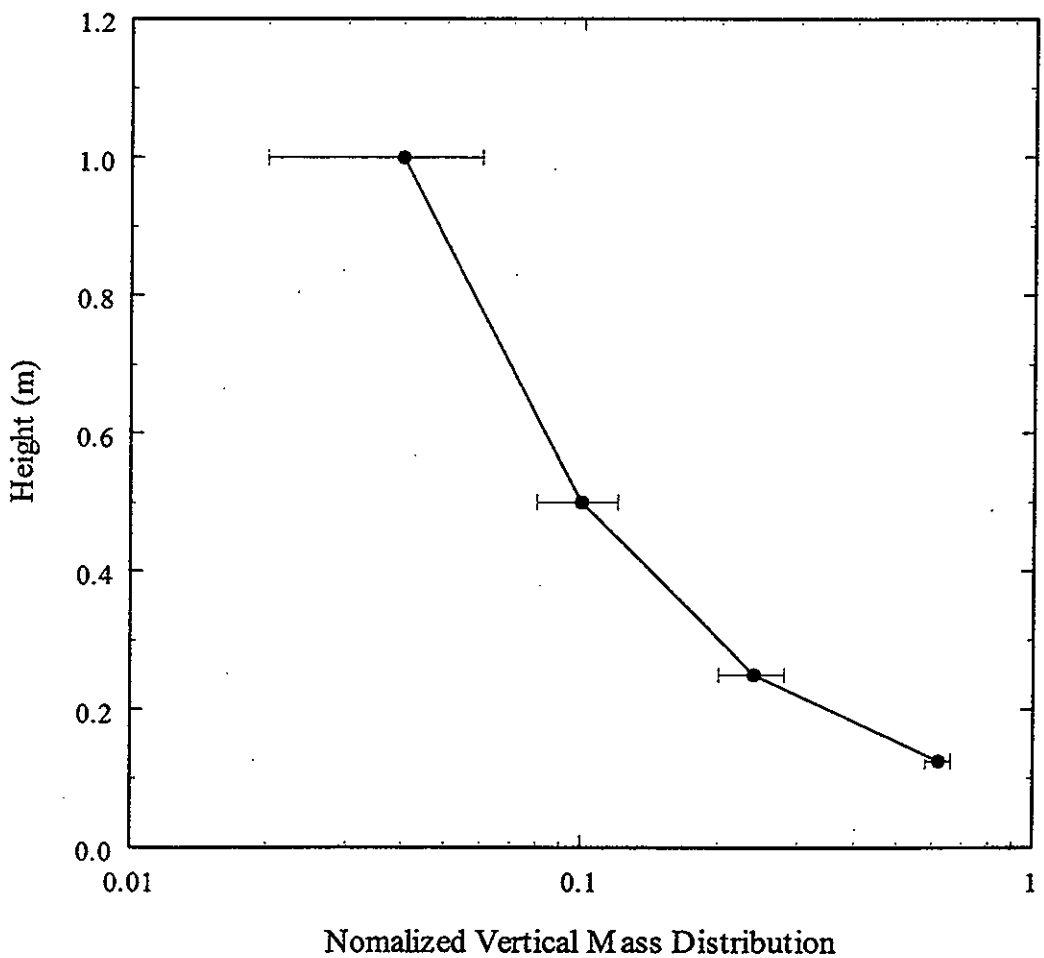

Figure 3-12 shows that the composition of the material collected in the dust traps was dominated by very fine sand and silt particles with a mean diameter smaller than 106 μm. Because of their small sizes, such particles have the greatest tendency to remain suspended once they are removed from the surface by wind. These particles pose little threat to causing further erosion. About 20% of the soil collected consisted of fine sand particles with diameters ranging from 106 to 500 μm. The greatest quantities were found at a height of 0.5 m above the surface. This size of particle is most likely to be transported by wind in saltation, traveling short distances with low-angle terminal impacts causing smaller silt-sized particles to be ejected from the surface. Therefore, this size of particle poses the greatest threat for causing wind erosion. In contrast, very small quantities (<1%) of sand grains with diameters greater than 500 μm were observed. This size of particle is generally transported by wind during creep sliding and rolling at or near the surface. Overall, the size distribution of the soil removed by wind was 89 ± 4% with diameters less than 106 μm; 10 ± 4% between 106 and 500 μm; and <1% greater than 500 μm.

Figure 3-12. Particle Size Distribution of Soil Material Collected in Dust Traps at the Barrier in WY 1995.

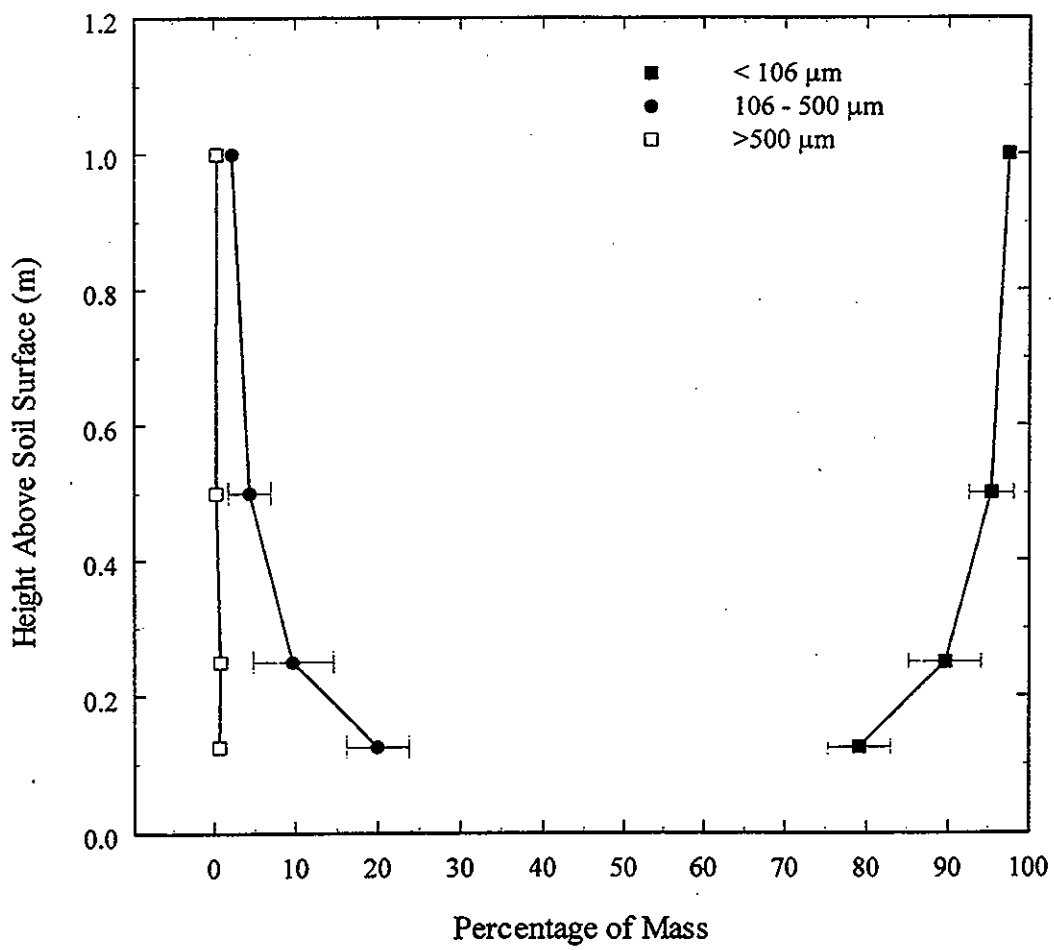

3.2.2.6 Surface Layer Composition. Near-surface (0 to 2 cm) and bulk gravel (0 to 10 cm) contents by weight on a dry weight basis from the first 3 years of testing are summarized in Table 3-8. In WY 1994, mean gravel content for the entire barrier was 16.2 ± 3.0% by weight. Mean gravel content on the irrigated treatment was 16.9 ± 4.0% by weight, which was not significantly different (α=0.05) from the 15.5 ± 1.0% observed on the nonirrigated treatment. In WY 1997, mean gravel content for the entire barrier was 13.4 ± 2.0% by weight, a significant decline from the WY 1994 value (α=0.05). The treatment differences between WY 1994 and WY 1997 were also significant, with the irrigated treatment showing the greatest decline in gravel content.

While changes in the composition of the admixture layer are not expected in the short term, near-surface (0 to 2 cm) changes are quite possible and can provide information on the ability of the silt-loam admixture to resist erosion. During deflationary periods, the pea gravel content at the surface is expected to increase and form an armor as soil particles are removed by wind. Under such conditions, the pea gravel content in the top few centimeters of soil could be expected to increase relative to its bulk distribution in the soil layer. During inflationary periods, a layer of soil that is largely free of pea gravel is expected to form on the surface and the gravel content in the top few centimeters of soil could be expected to decrease, relative to its bulk distribution in the soil layer.

Table 3-8. Mean % Pea Gravel Content ($\overline{G}$) and the Standard Deviation of the Mean ($\sigma_{\overline{G}}$) of Near-Surface (0-2 cm) and Bulk Samples (0-10 cm) Obtained from the Prototype Surface Barrier.

Plot	Depth (cm)	WY 1994[a]		WY 1995		WY 1996		WY 1997	
		$\overline{G}$ (%)	$\sigma_{\overline{G}}$ (%)	$\overline{G}$ (%)	$\sigma_{\overline{G}}$ (%)	$\overline{G}$ (%)	$\sigma_{\overline{G}}$ (%)	$\overline{G}$ (%)	$\sigma_{\overline{G}}$ (%)
NE	0-2	NA	NA	14.8	2.2	12.1	2.6	12.6	2.1
	0-10	16.8	4.0	12.6	1.4	12.6	1.9	14.2	2.2
NW	0-2	NA	NA	15.1	2.0	12.5	3.6	11.5	2.1
	0-10	NA	NA	12.6	1.2	12.8	1.8	12.6	2.5
Irrigated[b]	**0-2**	**NA**	**NA**	**14.9**	**2.1**	**12.3**	**3.2**	**12.0**	**2.2**
	0-10	**16.9**	**4.0**	**12.6**	**1.3**	**12.8**	**1.8**	**13.4**	**2.5**
SE	0-2	NA	NA	15.7	3.2	11.5	1.4	14.5	1.9
	0-10	NA	NA	13.6	1.0	13.2	0.9	13.3	0.9
SW	0-2	--	--	13.6	1.5	14.4	2.4	13.5	2.2
	0-10	15.5	1.0	12.5	1.1	13.3	1.0	13.4	1.4
Non-irrigated[c]	**0-2**	**--**	**--**	**14.6**	**2.7**	**12.9**	**2.5**	**14.0**	**2.1**
	0-10	**15.5**	**1.0**	**13.1**	**1.2**	**13.3**	**1.0**	**13.3**	**1.2**

NOTE: Gravel content is reported on a dry weight basis. Samples were taken in August of each year, except in WY 1995 when samples were taken in April.

[a]Construction was taking place during WY 1994; therefore, no testing or monitoring activities took place other than coring. Cores taken in WY 1994 were from 0- to 8-cm depth and were not differentiated into surface and bulk samples.

[b]Bolded rows contain averages from data in the preceding columns for Plots NE and NW.

[c]Bolded rows contain averages from data in the preceding columns for Plots SE and SW.

NA = not available

In WY 1997, mean gravel content in the 0- to 2-cm layer for the entire surface was 13.0 ± 2.3% by weight, which was unchanged from the WY 1995 values (14.8 ± 2.4%). The mean surface gravel content decreased from 14.9 ± 2.1% by weight in WY 1995 to 12.3 ± 3.2% by weight in WY 1997. The decrease in surface gravel (0 to 2 cm), particularly on the irrigated treatments, suggests gravel loss by either erosion or surface inflation. The erosivity of rainstorms at the barrier was insufficient to move pea gravel over any considerable distance and, therefore, rules out erosion. However, a measurable increase has occurred in the %C in the surface soil and an increase in plant debris on the surface, particularly in the irrigated treatment. These changes are most likely the cause of the apparent changes in pea gravel content. It is expected that most of the short-term changes will occur in the near-surface layers, with changes in bulk gravel content occurring only in the long term or after severe erosional stresses.

3.2.2.7 Wind Erosion Summary. Monitoring was performed to measure, evaluate, and document the effects of eolian stresses on the silt-loam surface of the barrier. Wind speeds on the elevated barrier surface can be 20% higher than at ground level. Therefore, the exposed, elevated, vegetated surface cover of the barrier is subjected to greater erosive stresses than the surrounding natural environment. The barrier was monitored for soil loss in WY 1994, a period representing worst-case surface conditions for wind erosion. The only measurable soil loss by wind erosion occurred in the first 3 months when the soil surface was bare. The total quantity of blowing material was determined to have varied between 25 and 2,500 g per meter of width. The removal was sufficient to initiate the formation of a pea gravel armor. The pea gravel armor, coupled with establishment of vegetation on the surface, essentially reduced the rate of soil loss to zero. The changes in the wind stress parameters over time and the associated decrease in soil loss are consistent with the evolution of a more stable barrier surface.

Wind stress parameters calculated from peak gusts were generally lower than the values from the literature and Pacific Northwest National Laboratory wind tunnel measurements, and are indicative of reduced stress near the surface. The increase in the roughness length over time is related to an increase in plant cover and plant height, both of which increase turbulent exchange over the barrier and reduce the erosive stress near the soil surface. Mean roughness height calculated from boundary layer theory was similar to that observed in wind tunnel experiments. Plant heights predicted from the theory were identical to field-measured values.

Mean gravel content (0 to 10 cm) in WY 1997 was significantly smaller than the WY 1994 value. No differences were found between plots within treatments or between the two treatments in WY 1997. However, the irrigated treatment showed the greatest decline from WY 1994. This result is a reflection of the effect of organic matter and plant debris on the composition of the surface layer (0- to 2-cm depth). These results indicate a stable surface that has undergone very little soil loss except during the first 3 months following construction. The vegetation was effective at protecting the soil from direct wind contact, one of the prerequisites for wind erosion.

In the design of erosion-resistant soil layers for field-scale barriers, an important issue is whether laboratory and wind tunnel tests can be extrapolated to the field. In extrapolating such results, other issues include (1) the practicality of deploying an admixture at the field scale and (2) whether a uniform admixture composition could be maintained throughout the life of the barrier. The results of the wind-erosion component of the treatability test show that field-measured stress parameters can allow more accurate predictions of wind velocity profiles above vegetated barrier surfaces than can be obtained from the literature and wind tunnel tests. There is also a clear indication that a 15% pea gravel admixture can be effectively deployed at the field scale and can successfully reduce the erodibility of vulnerable soils without impairing the water storage capacity or the establishment of vegetation.

3.2.3 Stability

3.2.3.1 Surface Elevation. Figure 3-13 shows topographic contour maps of the barrier surface on December 16, 1994, the first survey, and on September 4, 1997, the last survey, as well as the change in elevation over the same period. The data used to generate the December map were collected prior to establishment of vegetation on the barrier. A comparison of the December and September maps shows that the main features of the barrier (e.g., the 2% slope from the center toward the edges) remained unchanged between the two surveys. Figure 3-13(c) also shows that there was a general increase in elevation, ranging from 1.0 cm to 5.0 cm. The map also shows a few areas where an elevation decrease occurred. These areas are represented by the shaded hachured zones and correspond to decreases in elevation ranging from 1.0 to 4.0 cm.

The increase in elevation could be due to several factors. However, with topographical surveys being conducted only once per year, it is possible only to hypothesize as to the real cause. One possible cause is an increased plant root biomass in the silt-loam soil. Plant roots are usually much larger than the pores present in compact and relatively structureless soils. Such a structureless condition would have existed soon after construction of the prototype. However, as shown with many crop species, root development encourages soil granulation and the development of a fluffy, porous condition with a subsequent decrease in bulk density. Near-surface measurements of bulk density at the barrier have shown a decrease during the first 3 years of the treatability test. Plant root biomass data (addressed in Section 3.2.4.6) show higher mean root length densities on the northern irrigated section. Because there is no clear spatial pattern to the increases in elevation, these changes are likely not due entirely to plant root activity. Another possible cause is winter freeze-thaw cycles in the near surface. Winter freeze-thaw has been shown to cause pedoturbation, thereby gradually loosening soil and reducing the as-placed bulk density in the upper 30 to 60 cm of soil. Spatial patterns of soil water content, controlled by spatial variability of hydraulic properties and plant water uptake, would likely influence the pattern of elevation change as a result of freeze-thaw. Localized increases in elevation may also be attributable to other factors. For example, the largest increase in elevation over the 3 years of monitoring was in the area of coordinate 60 m north and 5 m east on the barrier. This increase was caused by excavation and backfill of the temporary runoff flume used in the March 1995 simulated 1,000-year storm event (Gee et al. 1996).

Figure 3-13. Surface Elevations at the Prototype Barrier.
([a] surface elevation, in meters, measured on December 16, 1994; [b] surface elevation, in meters, measured on September 2, 1997; and [c] the change in elevation between December 1994 September 1997. The contour interval is 0.025 m except for the difference map where it is 0.005 m.)

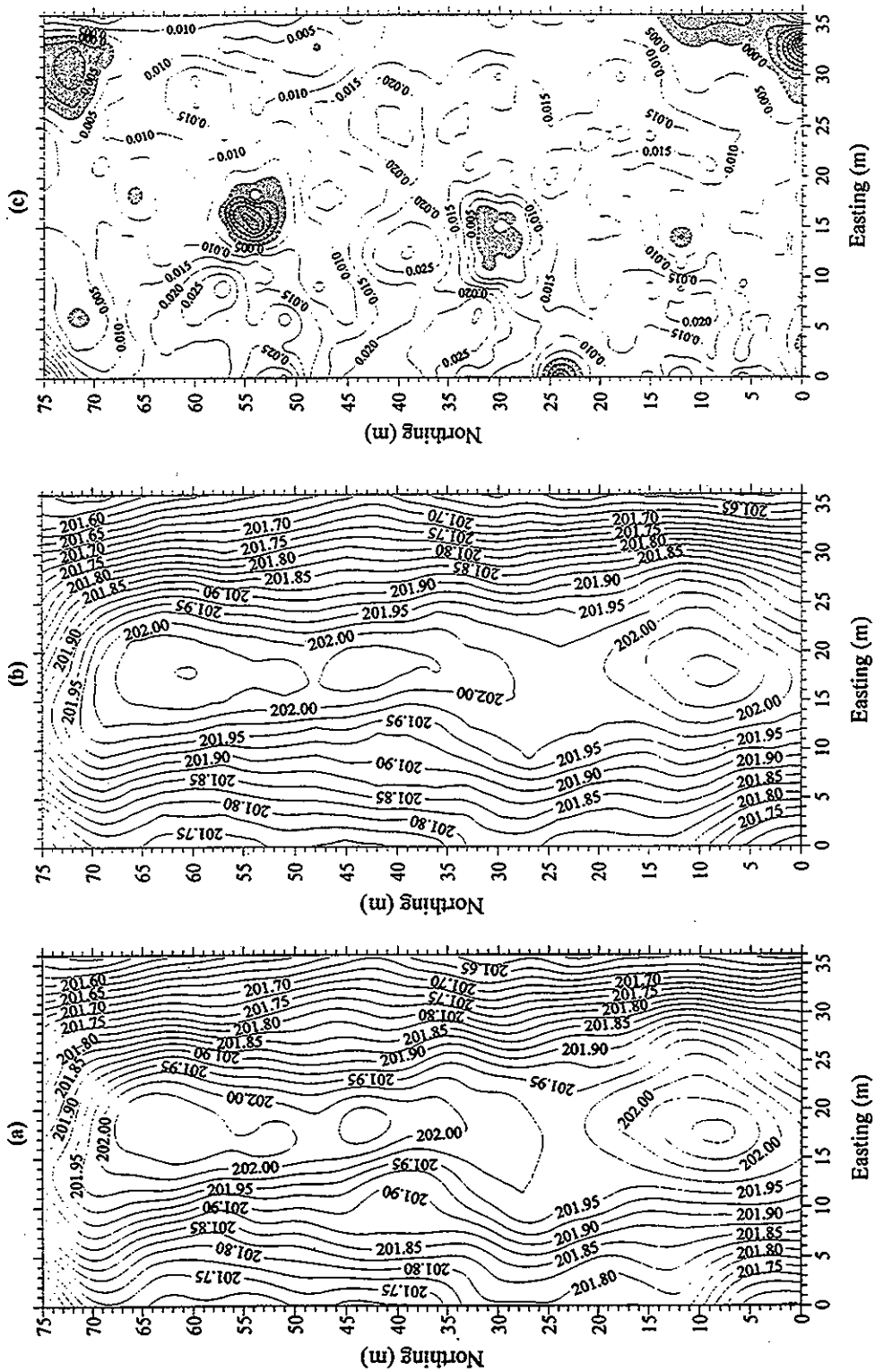

The largest amount of settlement occurred at the northeastern and southeastern corners of the silt-loam surface and has been ongoing since monitoring started (Gee et al. 1996). The observed settlement is difficult to explain without additional data. The creep gauge near these two locations shows no large-scale movement in the riprap side slope, and there are no other visible indicators that can explain this settlement. The smaller depression to the north is the location at which calibration of the neutron probe and other sensors took place in 1994. The calibration procedure involved the ponding of water on the surface and subsequent coring, activities that would have contributed to subsidence. The region near the 25-m coordinate north along the west edge is the original location of the runoff flume.

3.2.3.2 Settlement Gauge Movement. Figure 3-14 shows a plot of the settlement gauge elevation for the period WY 1995 through WY 1997. Recall that gauge DSG1 is near the crown of the barrier, whereas gauge DSG 2 is 14 m to the east. The general trend in these data is an increase in elevation. The greatest change in elevation occurred between the first survey in December 1994 and the third survey in January 1996. Both gauges remained relatively stable until September 1996, after which they both showed declines in elevation, with the bigger change occurring on DSG2. By the last survey, both gauges had increased from their original elevations.

When data are corrected for closure error of each survey, the overall increase in elevation between the first and last survey is statistically significant, although the rate of change varied in magnitude and statistical significance between sampling intervals. Over the monitoring period, the change in elevation on DSG1 was of 0.0089 m, equivalent to a mean rate of 3.27 mm yr^{-1}. The change at DS2G was slightly higher, 0.011 m, with an equivalent rate of 4.00 mm yr^{-1}.

These results are somewhat surprising and difficult to explain. The surface and near-surface soils consist of sands of fluvial and eolian origin. These materials do not characteristically exhibit significant expansion or compression behavior. While proper compaction of the subsoil during construction would largely eliminate the potential for settlement, some compression could still be caused by the weight of the barrier materials. Therefore, a decrease, rather than an increase, in elevation was expected to be the more likely response. A dishing effect on the asphalt layer was expected to be less than 3.0 cm and should have no impact on hydrologic performance of the barrier (Becker 1993). The differential increase in elevation between the two gauges, with the outer gauge increasing more, could lead to a dishing effect if it persisted.

The difficulty in interpreting the data, however, remains. Application of a large surcharge loading condition over a broad area will induce changes in the state of stress within a relatively large volume of soil and will produce a complex deformation response in the subgrade. Toward the center of the loaded area, the soil is in a state of true tri-axial confinement, whereas near the edges of the surcharge, confining stresses can be relieved. For uniform loading, the greatest vertical deformation always occurs at the center of the loaded area. In this case, loading was not uniform and the subsidence gauges were near the north edge of the barrier, which is near the periphery of the "pressure bulb" formed within the soil. Furthermore, the first measurements were taken in December 1994, long after the first placement of material and the time during which initial settlement would have taken place. Interpretation of the subgrade response data to distributed loads over large areas is generally a fairly complex problem, and the

Figure 3-14. Summary of Changes in Settlement Gauge Elevation Between November 1, 1994 and September 1997. (Error bars represent the total measurement error; DSG2 is located 14 m east of DSG1.)

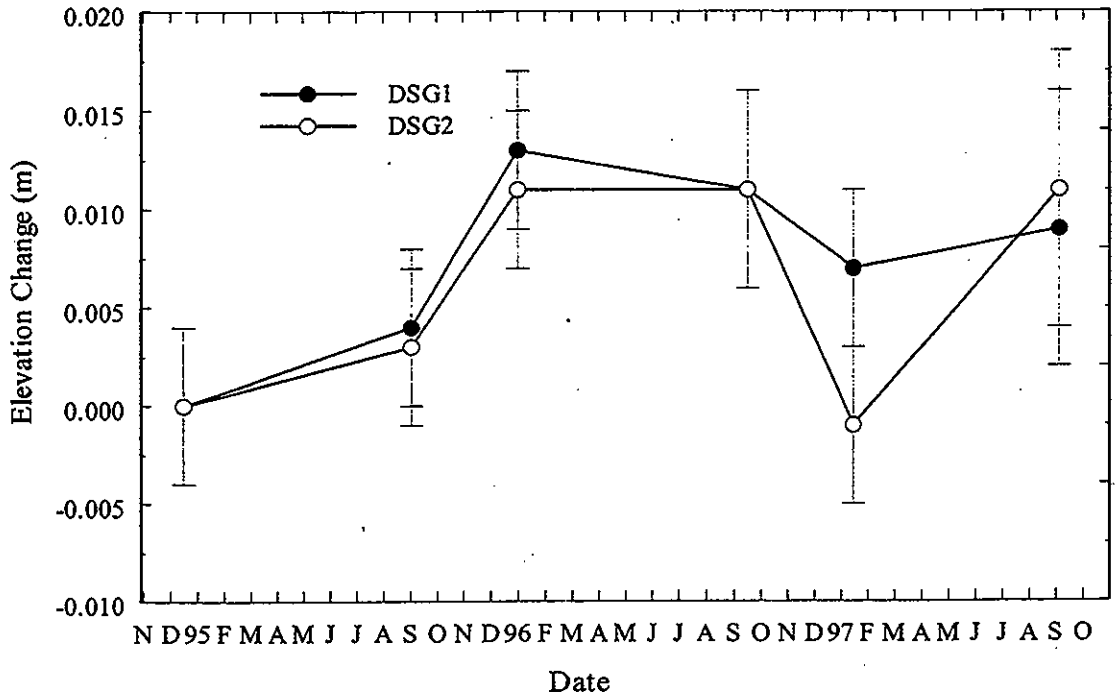

complexity is further increased by the factors discussed above. So far the rate of change, although highly variable, appears relatively small. Nevertheless, it is difficult to determine whether such a rate will be sustained. Additional monitoring will be necessary to document any movement of the asphalt.

3.2.3.3 Creep Gauge Movement. As shown in Figure 3-15, the change in location and elevation between the first survey in December 1994 and the second survey in September 1995 showed no clear pattern. This is indicative of random settling of the riprap slope (Ward et al. 1997). This sort of movement was usually observed between surveys. However, a plot of the total change between December 1994 and September 1997 shows a more clearly defined result.

Figure 3-16 shows the displacement vector for the creep gauges between the first and last surveys. Over the 3-year period, the preferred direction of gauge movement (Θ) was toward the east, although not all gauges showed statistically significant changes in spatial location or elevation. Gauges CG10a and CG10b, placed at upper and lower slope positions, respectively, showed no significant difference in displacement between gauges or between survey dates. The mean distance traveled between the two surveys was 0.014 ± 0.002 m in a generally northeasterly direction. If the measurement error is taken into consideration, it is clear that not all of the changes are significant (Ward et al. 1997). However, the movement shown by gauges CG1, CG4, CG9, and CG11 between the two survey dates was statistically significant, with CG1 showing the greatest movement of 0.036 ± 0.015 m in an easterly direction.

Figure 3-15. Creep Gauge Movement Between December 1994 and September 1995. (Elevation was measured by EDM; the resultant is in meters and the bearing is in radians).

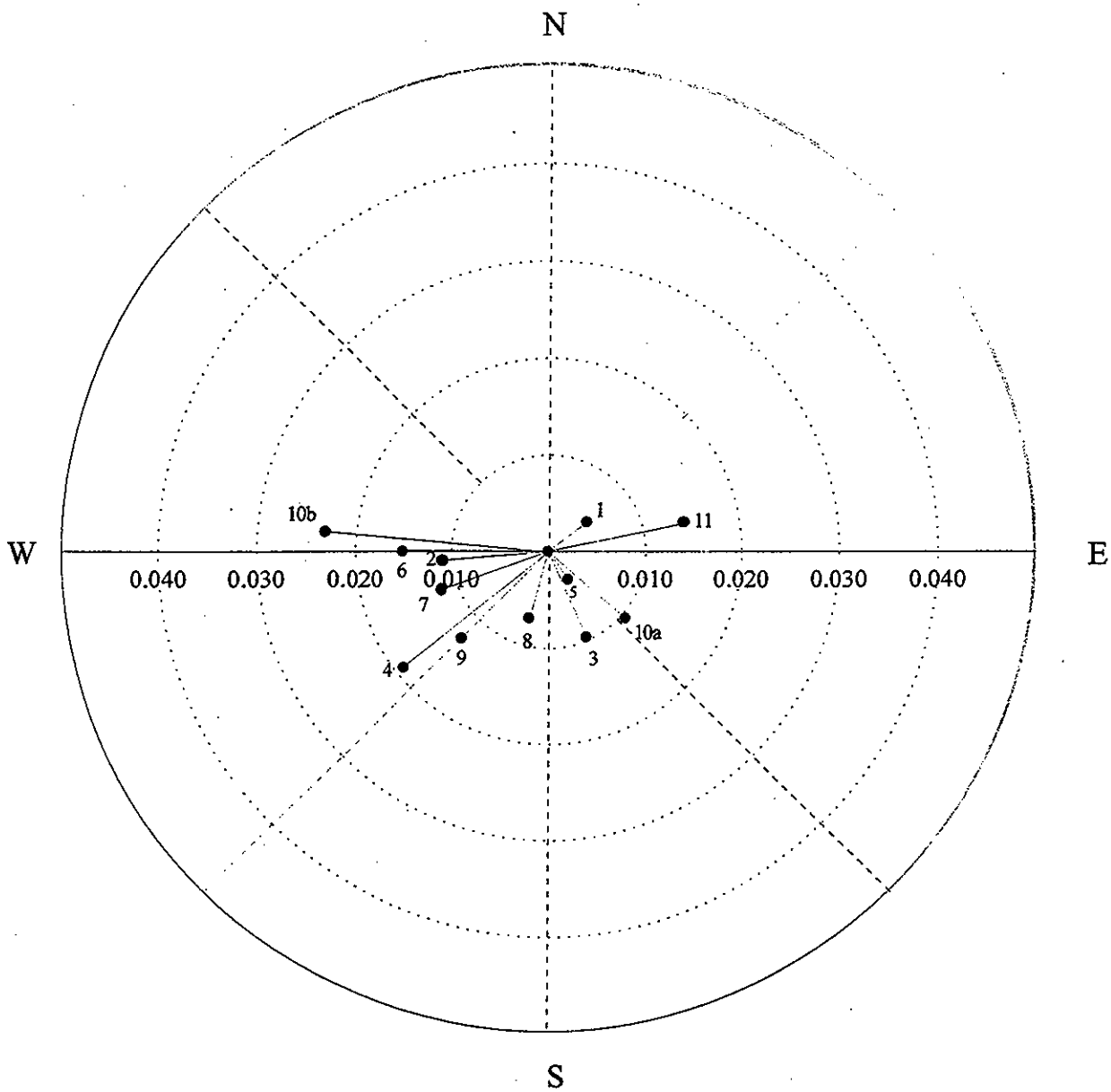

Figure 3-16. Creep Gauge Movement Between December 1994 and September 1997. (Elevation was measured by EDM; the resultant is in meters and the bearing is in radians).

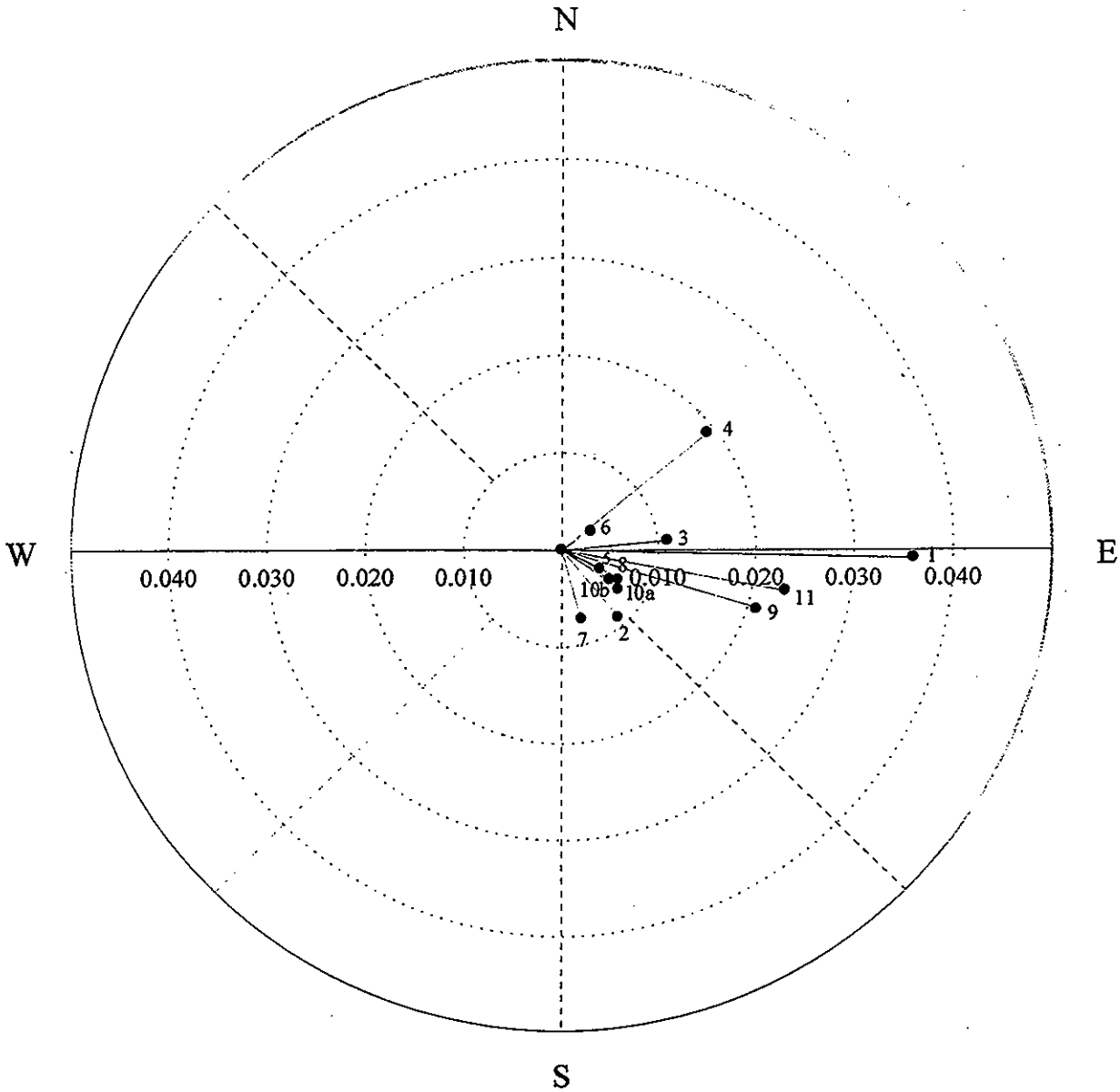

An analysis of the time course of creep gauge movement over the last 3 years shows a decrease in both the resultant and bearing between the first and second surveys (Ward et al. 1997). After the initial decline, they both increased and remained relatively constant. The variance in the resultant data was also relatively high, suggesting some randomness to the movement. However, the decrease in variance of the bearing estimates between the first and last surveys suggest a preferred easterly movement. Movement in an easterly direction is consistent with an outward and downward movement of the rock slope. However, visual observation and the magnitude of the measured changes show no evidence of side-slope failure. Thus, the small amount of displacement observed between December 1994 and September 1997 is probably due to settlement of the side slope into a more stable and compact arrangement. As with the settlement gauges, additional monitoring would be required to confirm or eliminate slope failure.

3.2.4 Vegetation

Plants and animals influence water and wind erosion and the hydrologic characteristics of landfill covers, such as the prototype barrier (Link et al. 1995a, 1995b). Vegetation of the barrier surface was done in the late fall of 1994, as discussed in Gee et al. (1995). Conclusions from the first 2 years of observations suggest that plants dry out the surface under most conditions, even with added water, and that plants virtually eliminate wind and water erosion (Gee et al. 1995, 1996; Ward et al. 1997). In WY 1997, studies of the biological component of the prototype barrier included extensive observations of plant and animal characteristics. This section summarizes data on vegetation characteristics including floristics composition, ground cover and spatial distribution, plant height, canopy leaf area, gas exchange rate, roots, shrub survivorship, and reproduction.

3.2.4.1 Plant Identification (Floristics). A species plant list was developed in WY 1995, WY 1996, and WY 1997. This list was compiled through several inspections each year. For identifications, Hitchcock and Cronquist (1973) was consulted. The species list is presented in Table 3-9 with documentation of the origination, occurrence, and life form of each species on the barrier surface.

The surface was planted in November 1994 with seedlings of *A. tridentata* (big sagebrush) and *C. nauseosus* (gray rabbitbrush) and then seeded with a mixture of native perennial grasses. This mixture included *Poa sandbergii* (Sandberg's bluegrass), *Agropyron dasystachyum* (thickspike wheatgrass), *Oryzopsis hymenoides* (Indian ricegrass), *Poa ampla* (Sherman's big bluegrass), *Stipa comata* (needle-and-thread grass), *Pseudoroegneria spicata* (bluebunch wheatgrass), and *Sitanion hystrix* (bottlebrush squirreltail).

A total of 38 species have been observed since WY 1995. Currently, 12 families are present of which *Brassicaceae, Compositae,* and *Poaceae* comprise 68% of the 38 species. In WY 1997, 57% of the species found were native to the western United States, and the rest were invasive aliens. Annuals comprise 46% of the species, and 54% are biennials or perennials. A prolific invasion of *Salsola kali* (tumbleweed) during the first year dominated the surface, but this plant species was mostly absent in subsequent years.

Table 3-9. Plant Species Observed on the Prototype Surface Barrier. (2 Sheets)

Scientific Name		Common Name	Species[a]	Presence (WY)			Life Form
Family	Species			1995	1996	1997	
Boraginaceae	*Amsinckia lycopsoides*	Devil's lettuce	N	X	X	X	Annual forb
Brassicaceae	*Cardaria draba*	Whitetop	I		X	X	Perennial forb
	Chorispora tenella	Blue mustard	I	X		X	Annual forb
	Descurainia pinnata	Western transymustard	N	X	X	X	Annual forb
	Draba verna	Spring whitlowgrass	I	X	X	X	Annual forb
	Sisymbrium altissimum	Jim Hill tumblemustard	I	X	X	X	Annual forb
Chenopodiaceae	*Chenopodium leptophyllum*	Slimleaf goosefoot	N	X	X	X	Annual forb
	Salsola kali	Russian thistle	I	X	X	X	Annual forb
Compositae	*Achillaea millifolium*	Yarrow	N	X		X	Perennial forb
	Ambrosia acanthicarpa	Bur ragweed	N	X		X	Perennial forb
	Artemisia tridentata	Big sagebrush	N, R	X	X	X	Perennial shrub
	Chrysothamnus nauseosus	Gray rabbitbrush	N, R	X	X	X	Perennial shrub
	Chrysothamnus viscidiflorus	Green rabbitbrush	N			X	Perennial shrub
	Conyza canadensis	Horseweed	N			X	Annual forb
	Lactuca serriola	Prickly lettuce	I	X	X	X	Annual forb
	Machaeranthera canescens	Hoary aster	N		X	X	Biennial, Perennial forb
	Tragopogon dubius	Yellow salsify	I		X	X	Annual forb
Convolvulaceae	*Convolvulus arvensis*	Field bindweed	I		X	X	Perennial forb
Geraniaceae	*Erodium cicutarium*	Storksbill	I	X	X	X	Annual forb
Hydrophyllaceae	*Phacelia linearis*	Threadleaf scorpionweed	N	X			Annual forb
Leguminosae	*Astragalus sp.*	Milkvetch	N			X	Perennial forb
	Lupinus pusillus	Low lupine	N			X	Annual forb
	Melilotus alba	White sweetclover	I		X	X	Annual forb
Malvaceae	*Sphaeralcea munroana*	Munro's globemallow	N		X	X	Perennial forb

Table 3-9. Plant Species Observed on the Prototype Surface Barrier. (2 Sheets)

Scientific Name		Common Name	Species[a]	Presence (WY)			Life Form
Family	Species			1995	1996	1997	
Onagraceae	*Epilobium paniculatum*	Tall willowherb	N		X	X	Annual forb
Poaceae	*Agropyron cristatum*	Creasted wheatgrass	I		X	X	Perennial grass
	Agropyron dasytachyum	Thickspike wheatgrass	N, R	X	X	X	Perennial grass
	Agropyron intermedium	Intermediate wheatgrass	I		X	X	Perennial grass
	Bromus tectorum	Cheatgrass	I	X	X	X	Annual grass
	Oryzopsis hymenoides	Indian ricegrass	N, R	X	X	X	Perennial grass
	Poa ampla	Sherman's big bluegrass	R	X	X	X	Perennial grass
	Poa bulbosa	Bulbous bluegrass	I	X	X	X	Perennial grass
	Poa sandbergii	Sandberg's bluegrass	N, R	X	X	X	Perennial grass
	Pseudoroegneria spicata	Bluebunch wheatgrass	N, R	X	X	X	Perennial grass
	Sitanion hystrix	Bottlebrush squirreltail	N, R	X			Perennial grass
	Stipa comata	Needle-and-thread grass	N, R	X		X	Perennial grass
	Triticum aestivum	Wheat	I	X			Annual grass
Verbenaceae	*Verbena bracteata*	Bracted verbena	N		X	X	Perennial forb

[a]N = Native plant species; I = invasive alien species; R = species hydroseeded.

The new species observed in WY 1997 include *Chrysothamnus viscidiflorus* (green rabbitbrush), *Conyza canadensis* (horseweed), *Lupinus pusillus* (low lupine), and an *Astragalus* (milkvetch) species (Table 3-3). Seeds of new species likely are carried to the surface by wind, dust devils, animals, and humans. All of the species present in WY 1996 were present again in WY 1997.

The variation of plants (number and type) on the soil surface has increased from WY 1995 through WY 1997. The number of annuals has varied from 12 to 16, while the number of perennials has increased from 11 in WY 1995 to 19 in WY 1997 (Figure 3-17).

The total number of species has increased from 24 to 35 in the same period. In WY 1995, 55% of the species were annuals. In contrast, only 44% and 46% of the species were annuals in WY 1996 and WY 1997, respectively. The continued increase in the number of perennials, compared with annuals, suggests the plant community will become increasingly dominated by perennials. A highly diverse mix of perennials is preferred because of their more efficient use of water.

Figure 3-17. Number of Annual and Perennial Species Including Total Species on the Barrier's Surface.

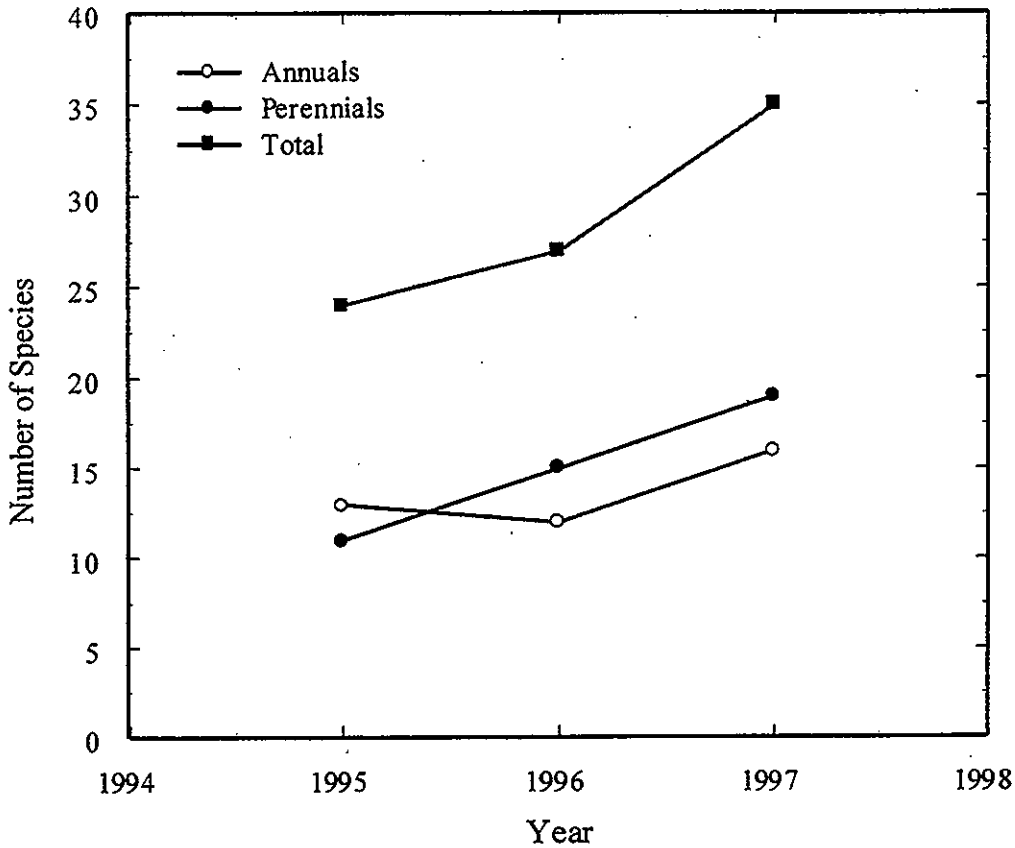

The plant community currently on the barrier is considered mature and diverse. It is similar in many respects to that of nearby natural plant communities. Similar native plant communities extract essentially all the available water annually from the soil profile (Link et al. 1990b, 1994), as does the community on the prototype surface barrier. The capability of the plants to remove water from the surface may remain as long as an appropriate mix of perennial and annual plants exists on the surface. When soils at the Hanford Site are disturbed, invasive species generally dominate, as long as an invasive seed source is in proximity. If soils are not grossly disturbed, the native community is likely to remain the dominant vegetative cover.

3.2.4.2 Plant Cover. Significant effects of the irrigation treatment and changes between WY 1996 and WY 1997 were observed for the cover data. These effects are discussed by treatments within years and by years within treatments. Cover data obtained in 1996 revealed significant effects of irrigation (Tables 3-10 and 3-11). Grass cover in the irrigated half was significantly greater than in the nonirrigated treatment, as indicated by the larger median value. Shrub cover was not significantly different between treatments. Based on *Z* scores (Table 3-11), herbaceous cover was significantly greater in the nonirrigated treatment, although median and mode values were not sufficiently sensitive to reveal the difference (Table 3-11). No significant difference was noted in litter cover.

Table 3-10. Median and Mode of the Percent Cover Classes.

Cover Class	Treatment	Water Year	Median	Mode
Grass	Irrigated	1996	25-50	5-25
		1997	50-75	50-75
	Nonirrigated	1996	5-25	5-25
		1997	25-50	25-50
Shrub	Irrigated	1996	0-5	0-5
		1997	25-50	25-50
	Nonirrigated	1996	0-5	0-5
		1997	25-50	25-50
Herbaceous	Irrigated	1996	0-5	0-5
		1997	0-5	0-5
	Nonirrigated	1996	0-5	0-5
		1997	0-5	0-5
Litter	Irrigated	1996	5-25	5-25
		1997	50-75	50-75
	Nonirrigated	1996	5-25	5-25
		1997	25-50	25-50
Bare	Irrigated	1996	5-25	5-25
		1997	5-25	25-50
	Nonirrigated	1996	5-25	5-25
		1997	25-50	25-50

Table 3-11. Mann-Whitney Test Results for Cover Class Comparisons Between Years Within Treatments and Between Treatments Within Year.

Water Year (1996-1997)			
Cover Class	**Treatment**	***Z* Score**	**Probability Level**
Grass	Irrigated	10.26	<0.00001
	Nonirrigated	12.58	<0.00001
Shrub	Irrigated	14.63	<0.00001
	Nonirrigated	14.55	<0.00001
Herbaceous	Irrigated	-6.05	<0.00001
	Nonirrigated	-8.94	<0.00001
Litter	Irrigated	14.07	<0.00001
	Nonirrigated	11.03	<0.00001
Bare	Irrigated	-0.17	0.8674
	Nonirrigated	2.18	0.0294
Treatment (Irrigated – Nonirrigated)			
Cover Class	**Water Year**	***Z* Score**	**Probability Level**
Grass	1996	9.04	<0.00001
	1997	10.72	<0.00001
Shrub	1996	-0.80	0.4252
	1997	-3.19	0.0014
Herbaceous	1996	-3.61	0.0003
	1997	0.99	0.3207
Litter	1996	0.47	0.6384
	1997	11.53	<0.00001
Bare	1996	-2.78	0.0055
	1997	-5.34	<0.0001

NOTE: The sign of the *Z* score represents the direction of change between comparisons. Refer to Table 3-5.

3.2.4.3 Plant Size. Data were collected for 4 years for *A. tridentata* (big sagebrush) and *C. nauseosus* (gray rabbitbrush). Observations were made on the height of *S. kali* (Russian thistle) and *A. dasystachyum* (thickspike wheatgrass) in each treatment, and the results are presented in Gee et al. (1996). Differences between treatments for height data (WY1995-1997) were assessed by comparing regression relationships in time using a linear test approach (Neter and Wasserman 1974).

Chrysothamnus nauseosus grew significantly taller over the first 3 years, and plants were taller in the irrigated treatment than in the nonirrigated treatment. Plants in the irrigated treatment increased from 37.8 to 54.1 cm, and those in the nonirrigated treatment increased from 31. 4 to 42.9 cm from WY 1995 to WY 1997. Linear regressions were significantly different for the two treatments ($F^* = 7.43 > F[0.95;2,61] = 3.15$; see the linear test approach in Neter and Wasserman [1974]). Although no height differences appeared between the treatments in any one year, when all data were combined, plants in the irrigated treatment were significantly taller than those plants in the nonirrigated treatment.

In WY 1998, the first year no irrigation was applied, *C. nauseosus* growth was almost equal (about 3 cm) between the two treatments. The formerly irrigated treatment had an average height of 57 cm, and the nonirrigated treatment had an average height of 45 cm (BHI 1998).

Artemisia tridentata grew significantly taller over the first 3 years, but appears to have been affected by irrigation. Plants in the irrigated treatment increased from 45 to 59 cm, and those in the nonirrigated treatment increased from 37 to 65 cm from WY 1995 to WY 1997. Linear regressions were not significantly different for the two treatments ($F^* = 3.03 < F^*[0.95;2,101]) = 3.10$; see Neter and Wasserman [1974]). No differences between the treatments were observed in any one year or when all data were combined. The data for the irrigated treatment suggest that, if irrigation were continued in the future, *A. tridentata* in the nonirrigated treatment may become significantly taller than those in the irrigated treatment. If the difference in size is used as an indicator of the potential to remove water, these results support that sustained elevated precipitation could reduce the efficiency of ET by *A. tridenta*. The effect of irrigation on plant behavior is better quantified by measuring the leaf area index.

In WY 1998, *A. tridentata* showed no additional growth over 1997 (BHI 1998). The average height recorded on the irrigated treatment was 59 cm. On the nonirrigated side, the plants had an average height of 63 cm. The 2-cm difference in height between WY 1997 and WY 1998 is not considered to be a significant change, but rather is associated with variability in the measurement method.

3.2.4.4 Plant Gas Exchange. Plant gas exchange data collected in 1995 and 1996 provide information on both transpiration and net photosynthesis. Such data are useful as an indication of the ability of shrubs to remove water from the surface. Comparisons are made for the effect of the irrigation treatment on gas exchange rates for *A. tridentata*. Previous gas exchange data collected for *C. nauseosus* indicate similar rates as for *A. tridentata* (Gee et al. 1996). Because of the similarity and the decreasing importance of *C. nauseosus* on the surface only, data for *A. tridentata* are presented in this report. These data are graphically presented with earlier data as in Gee et al. (1996) to interpret long-term trends in plant gas exchange.

Gas exchange data were obtained with a Li-Cor 6200 gas exchange system. Gas exchange data are collected by placing a chamber over stem tips and allowing water vapor and CO_2 to change over a few minutes. In 1997, a 10-cm-length of stem was placed in the chamber for plants in the ambient precipitation treatment, and a shorter piece, less than 5 cm long, was used in the irrigated treatment. The varying amounts of exposed leaf area were used to maintain a similar vapor pressure in the chamber between treatments. After observations were made, the stem was cut and the single-sided leaf area was measured using a Li-Cor 3100 Leaf Area Meter. All gas exchange observations were taken at mid-day and in full sun.

Transpiration rates increased from near 0.75 mmol m^{-2} s^{-1} in February to 19.7 mmol m^{-2} s^{-1} in late July in the ambient precipitation treatment. The irrigated treatment values were at a maximum of 14.2 mmol m^{-2} s^{-1} in June, dropping to 8.8 mmol m^{-2} s^{-1} in July. There were no differences between treatments on any of the 5 days ($p > 0.05$), except for July when the transpiration rate in the ambient precipitation treatment was significantly greater than in the irrigated treatment ($p = 0.033$). The higher rate of transpiration in the ambient precipitation treatment than in the irrigation treatment suggests that *A. tridentata* is under a hydration stress, apparently caused by too much water. As discussed in Gee et al. (1996), plants in the irrigated treatment had much higher pre-dawn xylem pressure potential values than those in the ambient precipitation treatment, an indication of no apparent water stress. Yet, there appears to be a restriction in the ability of water to move through *A. tridentata* when it is supplied with three times the normal precipitation. Perhaps excess water reduces the hydraulic conductivity of *A. tridentata,* leading to a reduction in transpiration rates. Combining these transpiration data with leaf area data for the surface allows the rates of water loss from the surface through *A. tridentata* to be estimated. This estimate assumes that transpiration rates of the entire shrub are similar to that of the stem tips used to collect the transpiration data. Estimates were computed by converting transpiration rates for day-of-year 169 (14.2 mmol m^{-2} s^{-1} - irrigated; 9.7 mmol m^{-2} s^{-1} - ambient) to the equivalent that would leave the surface for the entire leaf area (393 m^2 - irrigated; 955 m^2 - ambient) on the surface in 1 hour (20,090 mol h^{-1} - irrigated; 33,352 mol h^{-1} - ambient), and then converting this to the equivalent depth of water on the surface (0.46 mm h^{-1} - ambient; 0.28 mm h^{-1} - irrigated). These rates are only estimates of the true rate that is difficult to measure. The rates presented here are based on stem tips and are likely to be higher than rates for the entire canopy. This has been previously demonstrated for *Bromus tectorum* canopies. The rates observed in this study are probably near maximum values for the day, having been collected just prior to mid-day. Rates will be lower at other times of the day. A better estimate would be achieved by the use of whole plant gas exchange data collected over an entire day. The transpiration values obtained here should not be used to estimate the components of evapotranspiration because they are not representative of all the vegetation on the surface, nor are they representative of the time scale used in ET estimates for the surface.

Net photosynthetic rates increased from near 3 μmol m^{-2} s^{-1} in February to 19.7 μmol m^{-2} s^{-1} in the ambient precipitation treatment. In the irrigated treatment, values were at a maximum of 17.9 μmol m^{-2} s^{-1} in June, dropping to 10.1 μmol m^{-2} s^{-1} in July. There were no differences in treatments on any of the 5 days ($p > 0.05$).

3.2.4.5 Leaf Area and Leaf Area Index. Table 3-12 shows the estimated leaf area index for *A. tridentata* for both irrigated and nonirrigated treatments.

Table 3-12. Estimated Leaf Area Index of *Artemisia tridentata* in Each Treatment in WY 1997.

Treatment	Date	Leaf Area Index
Irrigated	April 16	0.198
	May 14	0.268
	June 17	0.303
Nonirrigated	April 16	0.460
	May 14	0.595
	June 17	0.737

The results of model predictions (Ward et al. 1997) indicate that leaf area for shrubs such as sagebrush changes significantly in the spring, nearly doubling in a period of 2 months (April to June) for the nonirrigated treatment, while increasing by less than 50% for the irrigated treatment. The data suggest that for sagebrush there may be suppression of growth due to elevated precipitation (irrigation).

3.2.4.6 Root Study. Root length density exhibits little pattern with depth other than a decrease near the bottom in WY 1997 (Figure 3-18). During WY 1995 and WY 1996, no attempt was made to distinguish live roots from dead roots. By WY 1997, dead roots became obvious, and both live and dead root length densities were quantified. These data are expressed as the ratio of dead to live root length density with depth. The mean ratio of dead to live root length density over depths and holes was significantly different with a ratio of 0.25 ± 0.08 in the irrigated treatment and 1.14 ± 0.24 in the nonirrigated treatment.

The mean root lengths found in irrigated and nonirrigated treatments were significantly different in years two (WY 1996) and three (WY 1997), corresponding to the higher plant cover and plant density found on the irrigated plots. In the third year (WY 1997), no roots were found at the bottom of the viewing zone (175 cm), but they were present in the previous 2 years. However, rooting for sagebrush to depths of at least 3 m has been observed in adjacent lysimeters in sandy or rocky soil. The apparent loss of roots at depth may be associated with the impact of continued irrigation treatment on the sagebrush, although it should be noted that mean root length density over depths and holes was significantly greater in the irrigated treatment than in the nonirrigated treatment in WY 1996 and WY 1997.

3.2.4.7 Survivorship. *Chrysothamnus nauseosus* (gray rabbitbrush) survivorship was significantly greater in the irrigated treatment than in the nonirrigated treatment (Figure 3-19). In contrast, survivorship of *A. tridentata* was significantly greater in the nonirrigated treatment than in the irrigated treatment. There has been a persistent loss of *A. tridentata* in the irrigated treatment. In WY 1997, survivorship dropped to 91%. After 3 years, survivorship of *A. tridentata* across treatments remains much greater than survivorship of *C. nauseosus*. Survivorship by shrub species was not assessed in WY 1998.

Figure 3-18. Mean Root Length Density as a Function of Depth in WY 1995, WY 1996, and WY 1997.
([a] nonirrigated treatment, and [b] irrigated treatment.)

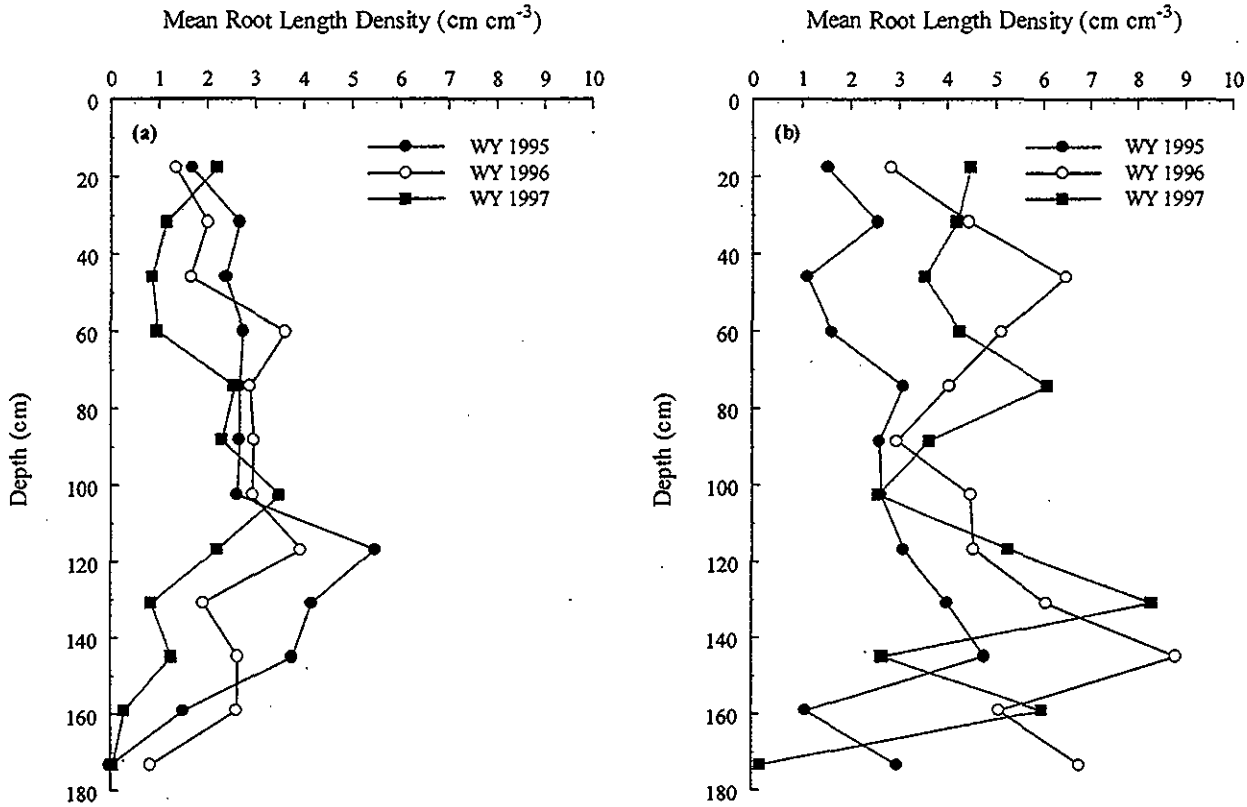

Figure 3-19. Mean Survivorship for *Artemisia tridentata* and *Chrysothamnus nauseosus* in WY 1995, WY 1996, and WY 1997 for the Nonirrigated and Irrigated Treatments. (Error bars are one standard error of the mean. Means with differing letters within years and species are significantly different.)

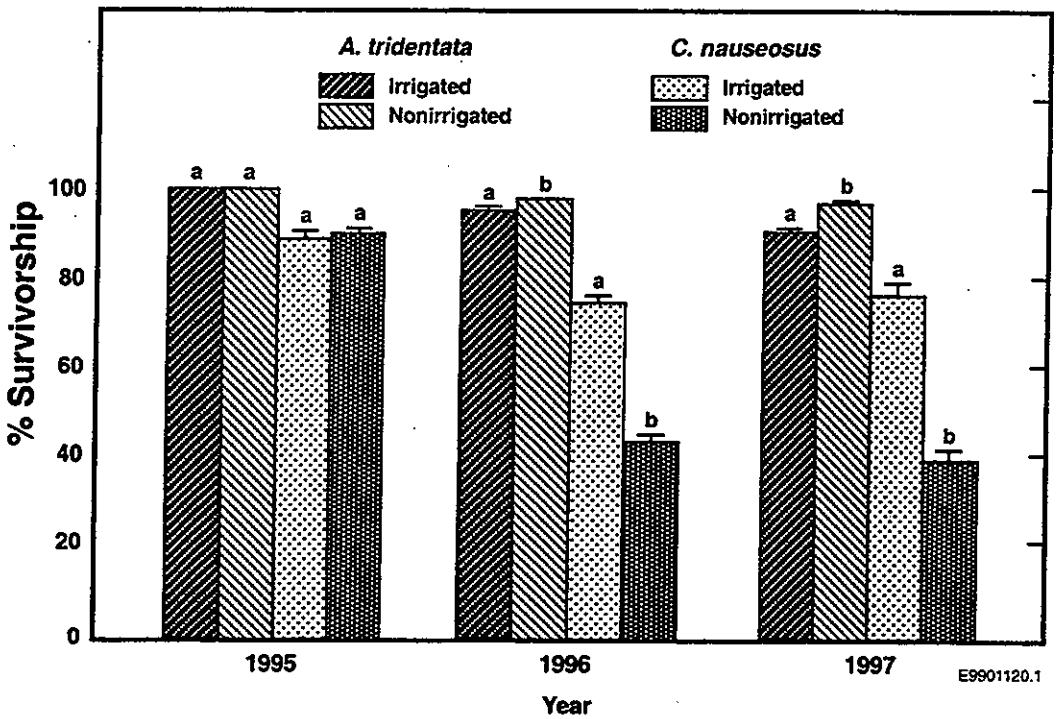

3.2.4.8 Reproduction. The percentage of *A. tridentata* with mature seed heads in the irrigated treatment was significantly ($p = 0.009$) lower than in the nonirrigated treatment (Table 3-13). The irrigated treatment had only 62.3% of the *A. tridentata* shrubs with mature seed heads, and the nonirrigated treatment had 80.6%. This result is another indication that *A. tridentata* is less viable on this surface with three times normal precipitation than with nonirrigated precipitation (Gee et al. 1996).

Table 3-13. Percentage of *Artemisia tridentata* Shrubs with Mature Seed Heads in the Irrigated and Nonirrigated Treatments.

Treatment	Mean %	SE
Irrigated	62.3	3.7
Nonirrigated	80.6	3.8

Observations were also made of seedling establishment of *A. tridentata* (sagebrush) and *C. nauseosus* (rabbitbrush) in WY 1997. In late spring, numerous seedlings of both species occurred in both treatments. By late summer, most of the seedlings had perished. Even so, a significant number of *A. tridentata* (sagebrush) seedlings were at least 1 year old and were up to 5 cm tall. Germination of new shrubs is expected to continue over the next several years.

3.2.5 Animal Intrusion

Animal evidence on the surface was casually noted in WY 1995 and quantified in WY 1996 through WY 1998. In WY 1996, animal evidence (feces and holes) was found in 20% of the quadrants in the nonirrigated half of the barrier and in 8% of the quadrants in the irrigated half. Nine holes were observed on the surface. In WY 1997, feces were present in 93% of the quadrants in the nonirrigated half of the barrier and in 69% of the quadrants in the irrigated half. Animal evidence consisted almost exclusively of rabbit feces. The vertical depth of two holes/depressions on the surface was measured and found to be shallow; one hole was 7.5 cm deep and the other 8 cm deep. These were the largest holes/depressions (<10 cm in diameter) found on the surface and may not have been animal related.

In WY 1998, rabbit feces were seen on virtually all quadrants. In addition, one observation of coyote feces on the barrier surface was made, and deer tracks and beds were evident at the west base of the barrier. Shallow mouse burrows and harvester ant mounds were commonly observed on the lower half of the gravel side slope. In the northwest corner of the base, pocket gopher activity was observed. On the barrier surface, 11 mouse burrows (2.54 to 3.81 cm diameter and 2.54 to 25.4 cm deep) and 4 ant mounds (5.0 to 7.6 cm in height and diameter) were observed. The surface ant burrows were not made by harvester ants (species unknown).

In both treatments, animal evidence increased from WY 1996 to WY 1998. Evidence was much stronger and easier to observe in the nonirrigated half during both years, compared with the irrigated half of the barrier. There appeared to be an association between animal evidence and litter cover. It is possible that animal evidence is truly the same in each treatment but, because of the greater vegetative and litter cover in the irrigated half, the ability to observe the evidence is reduced.

Holes burrowed into the surface were little changed between WY 1996 through WY 1998. Holes dug by burrowing animals are much more common in undisturbed areas (Link et al. 1995b). As a result, burrowing activity is likely to increase as the ecosystem becomes more similar to that of undisturbed areas (Ward et al. 1997).

3.2.6 Summary of Vegetation and Animal Intrusion Observations

The establishment of a viable and highly diverse plant community on the soil surface continues to have significant impact on the function of the barrier after 4 years of testing. The complete coverage of the soil by deep-rooted plants is responsible for the annual drying of the soil profile, even with three times normal precipitation. The plant community has accommodated the excess precipitation with more vegetative matter. In addition, the plants have virtually eliminated evidence of wind and water erosion. In contrast, the lack of vegetation on the side slopes makes them vulnerable to water intrusion, as attested by the high rates of measured drainage for both the riprap and the clean gravel side slopes. While designed to accommodate the lack of vegetation, by using low-permeability asphalt layers to shed water, the impact of bare sides must be accounted for in determining the overall performance of abovegrade barriers and their relationship with surrounding waste sites. The lack of fine soil on either side slope minimized its water-holding capacity and kept the seedbed surface dry so that seed germination and plant

establishment was minimized. Bare surfaces or sparse vegetation will likely dominate the side slopes for many years to come; thus, high rates of drainage from the side slopes are expected to persist.

Animal intrusion during the past 4 years appeared to have little impact on barrier performance. Animal intrusion impacts on future barrier performance are also expected to be minimal. The cover is thick enough and designed well enough (with redundant layers, etc.) that animal intrusion should never be a problem under any reasonable scenario. The first 4 years of testing support this hypothesis. The animal intrusion activities were documented by primary (direct) observation of animal burrowing animals and also by secondary observation of other animal activity such as the observation of presence (by documenting the presence of animal feces). While the burrowing is the only clear evidence of animal impacts on barrier performance, the presence of animals as identified by feces count also provided some indication of the biotic activity at the site, which could result ultimately in changes of vegetation type and composition as animals become vectors for the spreading of seed sources or modify the vegetative compositions by foraging and other activities.

3.3 DEVIATIONS FROM TEST PLAN/COMPARISON OF TEST OBJECTIVES

Several deviations were made from the test plan (DOE-RL 1993b) and are documented below.

1. Sand Dune Test. This planned test included the creation of an artificial sane dune with monitoring the impacts of surface erosion, plant community viability, and soil water balance. This test was deemed not necessary since it became evident that the barrier surface, as designed, was stable and effective in controlling erosion while supporting plant establishment and providing an adequate water storage capacity.

2. Erosive Impacts After Artificial Wildfire. Plans were also made to look at the increased susceptibility of the barrier surface to erosion following a fire (Gee et al. 1993b). However, this test was not considered necessary. During the first 3 months after construction, the surface of the barrier was bare and conditions were worst case for wind erosion. This period could be considered equivalent to a post-fire condition. Soil loss by wind was sufficient to initiate the formation of a pea gravel armor, thereby stabilizing the surface and curtailing any further soil loss.

3.4 QUALITY ASSURANCE

The prototype barrier testing has been operated under the Quality Assurance (QA) plan OHE-002, Rev. 6, a Pacific Northwest National Laboratory-controlled document located in the project files and with each task leader. This plan contains guidance for the quality of testing data collected on the prototype surface barrier. Specific test procedures are identified in the QA plan and include procedures for irrigation applications, dosing siphon measurements, and a series of water content measurements and related analysis. Data reduction related to drainage and water balance measurements are emphasized in the test plan and the QA plan. Data from water infiltration, water storage measurements, wind and water erosion, and biointrusion tasks are collected and input into laboratory record books and into data loggers and electronic data files.

These files are formatted for subsequent graphical display and analysis. Detailed records are kept and hardcopy files are maintained at the task level. A CD-ROM, compiling electronic data records, was prepared and is in the project file (PNNL 1999).

Procedures that are specific to the prototype barrier project include the following:

- PNL-PSB-2.0 Procedure for Operational Use of Prototype Barrier Linear Irrigation Equipment.
- PNL-PSB-4.0 Procedure for Routine Maintenance and Calibration of Dosing Siphons at the Prototype Surface Barrier.
- PNL-PSB-5.0 Procedure for Surface Composition Analysis of the Prototype Surface Barrier.
- PNL-PSB-9.0 Procedure for Calibration of Precipitation Meter Load Cells at the Prototype Surface Barrier.
- PNL-PSB-10.0 Procedure for Measuring Soil Moisture Using the Neutron Probe in the Neutron Access Tube Vertical and Horizontal Arrays.
- PNL-PSB-11.0 Soil Sampling and Testing Procedure for Verification of Hydrologic Performance at the Hanford Prototype Surface Barrier.

Data analysis focused on quantifying barrier performance. Quantification of water balance was made on selected test areas and, combined with wind and water erosion and biotic intrusion measurements, have been reported in status and letter reports on an annual basis (Gee et al. 1995, 1996; Ward et al. 1997).

4.0 CONCLUSIONS AND RECOMMENDATIONS

Four years (FY 1995-1998) of performance testing and monitoring have been successfully completed on a prototype of the Hanford Barrier constructed in FY 1994 over the 216-B-57 Crib in the 200-BP-1 Operable Unit. The principal barrier performance parameters evaluated during the test included water balance within the barrier under ambient and extreme precipitation conditions, surface wind and water erosion, stability of the barrier foundation, surface and riprap side slope, surface vegetation dynamics, and animal intrusion. In addition, constructability and cost data were collected. Using irrigation techniques, extreme precipitation conditions were simulated by applying water up to three times normal, including 1,000-year storms. All test objectives defined in Section 2.1 have been successfully achieved.

Results of the treatability test have demonstrated the effectiveness of the Hanford Barrier and associated design elements. General conclusions regarding the constructability, cost, and performance of the Hanford Barrier include the following:

- Construction of the prototype Hanford Barrier was easily completed using standard construction equipment. No construction issues were identified that would compromise overall barrier performance.

- The approximate unit cost of the barrier (excluding testing and monitoring tasks) was $\$320/m^2$. Extrapolation of these unit costs for estimates of larger barriers, and/or mass construction of barriers, should take into account economy-of-scale factors.

- Hydraulic conductivity testing results concluded that the asphalt layer performed better than the 1×10^{-7} cm s^{-1} low-permeability (recommended maximum) soil layer in the RCRA barrier design.

- Essentially no drainage of water through the barrier silt-loam layers was observed under ambient and extreme (three times normal including 1,000-year storms) precipitation conditions. The upper silt-loam layers and capillary barrier functioned to effectively store precipitation for subsequent removal by ET, thereby preventing drainage. As expected, drainage did occur from the gravel and riprap side slopes, but was effectively diverted by the sloped asphalt layer. No change in water content or drainage was observed under the asphalt layer except at its very edge.

- Surface water runoff generated under extreme precipitation conditions was minimal except under frozen soil conditions.

- Native vegetation was established quickly on the barrier surface and effectively extracts water from the 2-m-thick silt-loam profile, even under extreme precipitation conditions. The complete coverage by deep-rooted perennials effectively dries out the soil.

Under elevated precipitation, the plant community has adapted to the additional water with increased biomass. However, there was some evidence of a shift in vegetation from shrub-dominated to more shallow-rooted, grass-dominated species under elevated precipitation. During periods of sustained elevated precipitation, such a shift in plant species could have an impact on the depth of water extraction.

Both sagebrush and rabbitbrush seedlings survived and flourished, with sagebrush persisting with an overall 90% survival rate. Rabbitbrush survival was over 70% on irrigated areas, but declined to less than 40% on the nonirrigated areas. The initial irrigation treatment and wet winter (above normal precipitation) was likely responsible for the high rate of survival.

- As a result of the vegetative cover and the 15 wt% pea gravel admix in the upper silt-loam layer, there was no measurable loss of surface soil from wind or water erosion after the first year of testing. The relatively short, gentle (2%) surface slope promotes runoff (which was minimal) without significant erosion.

- No significant settlements or side-slope movements were observed during the test period. Overall, the surface of the barrier uniformly increased in elevation, most likely due to an increase in plant root biomass and/or freeze-thawing.

- Observations of animal intrusion on the barrier surface were minor with no impact on barrier performance. Animal use has generally increased each year.

Testing of the Hanford Barrier supports the 200-BP-1 Operable Unit RI/FS process, as well as the 200 Areas in general where surface barriers have been identified as a viable remedial action alternative (DOE-RL 1999). Conceptual surface barrier designs, including the Hanford Barrier, have been established through a feasibility study process (DOE-RL 1996, 1999). A graded approach to cover design has been developed whereby a limited number of barrier designs satisfy the requirements of a broad range of waste sites. Selection of a graded barrier would be dependent on the level of protection required by a waste site as well as regulatory requirements. Although the application of the Hanford Barrier itself is expected to be limited in the 200 Areas, the Hanford Barrier test results are applicable to other, more modest surface barrier designs because they share common design concepts and components (e.g., capillary break). The remedial design process will be streamlined by having a thoroughly tested set of surface barrier design elements from which site-specific definitive designs can be prepared.

Based on the successful results and lessons learned over the past 4 years of treatability testing, the following recommendations are provided that address (1) remediation of the 200-BP-1 Operable Unit and (2) optimization of select barrier design components.

Treatability test objectives (Section 2.1) have been achieved or exceeded by the 4 years of testing, and no further treatability testing to support the 200-BP-1 RI/FS process is needed.

A sufficient performance baseline has been established on the effectiveness of the barrier and its components. As a result, operable unit-specific recommendations include the following:

- Use of the existing prototype Hanford Barrier as a final remedy for the 216-B-57 Crib and implementation of a post-closure care and monitoring program for the waste site. A continued but reduced level of monitoring of the Hanford Barrier is recommended to support other Hanford Site programs that may require longer term records of barrier performance.

- Adoption of a surface barrier using the graded barrier approach for final remediation of the 216-BY Cribs consistent with the 200-BP-1 feasibility study preferred alternative (DOE-RL 1994b).

The following recommendations pertain to barrier design optimization and are based on field observations and lessons learned over the course of the treatability test. Although the observations were of the Hanford Barrier design, they can be applicable to guide the optimization of other graded barrier designs because of shared design elements.

- Silt Loam Thickness. A performance objective of the prototype barrier was to limit net drainage through the barrier profile to 0.5 mm yr^{-1}. Test results indicate that the water storage capacity of the upper silt-loam layers (600 mm) alone was sufficient to meet the 0.5 mm yr^{-1} criterion. The presence of a good vegetative cover of deep-rooted perennials and a capillary break beneath the silt loam was critical in achieving this level of performance. Because of the efficiency of the silt loam in limiting drainage, the asphalt layer functioned primarily to shunt drainage received from the side slopes.

  Treatability testing results suggest that some optimization of the silt-loam thickness may be appropriate depending on site-specific performance needs. Where a maximum degree of hydrologic protection for extended periods of time (1,000 years) is required, 600 mm of storage capacity (i.e., 2-m-thick vegetated silt-loam layer over a capillary break) is considered appropriate to accommodate potential long-term climatic changes and changes in vegetative cover to plant species that are less effective at water removal. For the Hanford Barrier design, no hydrologic performance credit would be given for the asphalt layer other than as backup protection should the performance of the vegetated silt loam deteriorate over the long term.

  Test results suggest that a silt-loam storage capacity of 400 mm (i.e., 1.3-m-thick vegetated silt-loam layer over a capillary break) could accommodate up to 1.8 times the LTA precipitation amount. This would provide a high degree of hydraulic performance for precipitation conditions up to the maximum amount of annual precipitation on record, which may be appropriate for periods of performance up to 500 years. Additional reductions in silt-loam water storage may be appropriate based on the level of hydraulic performance required at a particular site or the use of additional hydraulic barrier components such as an asphalt layer. Moisture breakthrough studies of the silt loam would provide supporting data to optimize silt-loam thickness. However, based on the observations of plant response to moisture availability, potential impacts to the plant

community and resulting water balance dynamics should be addressed when considering reductions to the silt-loam thickness.

- Transition Zone Design. The transition surface soil plot overlies an area where the silt-loam profile transitions horizontally into the side slopes and consists of a diagonally oriented capillary break. The presence of a sloped capillary break in this zone can facilitate the movement of water from the transition zone into the silt loam as observed in surface plot 6E in WY 1997. Because of the potential negative impact on the silt-loam water balance under extreme precipitation conditions, consideration should be given to optimizing the configuration of the transition zones (e.g., tapering the edge of the silt-loam layer toward the side slopes) addressing both water-balance performance and constructability aspects.

- Side-Slope Drainage. Significant drainage (22% to 34% of precipitation) occurred through the side slopes under both ambient and elevated precipitation levels for both the gravel and riprap end treatments. Neither slide-slope treatment supported vegetation, which enhances water intrusion. In the case of the prototype Hanford Barrier tested, asphalt curbing conveyed the drainage away from the waste site. These observations imply that without proper edge curbing, particularly for large surface barriers, significant amounts of water may infiltrate locally along the edge of the asphalt layer that could impact the waste site covered by the barrier or other adjacent waste sites. Impacts from this phenomenon need to be addressed in site-specific designs.

- Side-Slope Design. Under ambient precipitation conditions, the riprap side slope produced less drainage than the gravel side slope which is believed to be associated with a greater advection (wind-assisted drying) potential. The riprap slope benefited from the inclusion of fines, resulting from the blasting process, which increased the storage capacity enough to allow advection to cause drying. In addition, the riprap side slope supports a much steeper side slope (up to 1.5:1) resulting in less material, a smaller footprint, and less slide-slope drainage. Based on these findings, a riprap side slope is the preferred configuration for a nonvegetated side slope. The inclusion of fines to optimize storage without reducing the advective potential is worth considering.

  Creep gauge measurements showed a small degree of outward and downward movement in the riprap side slope. Not all of the displacements that occurred over the test period were considered to be statistically significant. Nevertheless, continued monitoring is warranted to better assess changes in displacement rates over time and overall long-term stability.

- Surface Perimeter Access Road. A gravel road was constructed around the perimeter of the barrier surface to provide access for prototype testing and monitoring activities. Because the road was slightly elevated, water runoff was impaired and some ponding occurred at the edge under extreme precipitation conditions. In a typical surface barrier application, there is no need for such an access road, and it could be eliminated. The need to reconfigure the existing prototype barrier to optimize runoff should be evaluated.

- Asphalt Layer. The composite asphalt layer of the Hanford Barrier consists of a 15-cm-thick low-permeability asphalt layer top coated with fluid-applied asphalt. The hot spray-applied asphaltic coating was added to the design because it is a highly resilient and flexible coating with favorable constructability attributes that provides additional assurance against leakage through the asphalt layer over the long term.

  The top coating was found to be disproportionately expensive (12% of construction costs) and difficult to apply. A preliminary stability analysis of the prototype barrier indicated that the viscous properties also make it the weakest layer in the prototype barrier and most prone to creep. In addition, the penetration of the overlying gravel layer into the topcoat may compromise the integrity of the topcoat as a hydraulic barrier (Daniel 1994a). Without the topcoat, laboratory and field hydraulic testing of the asphalt layer has demonstrated that the permeability of the asphalt alone met the standard RCRA low-permeability soil criteria of 10^{-7} cm s^{-1}, which is a recommended maximum value. Furthermore, in the case of the Hanford Barrier design, asphalt performance was not needed beneath the silt-loam layer because of the effectiveness of the silt loam in limiting drainage. Any potential incremental benefit the topcoat provides may be outweighed by constructability problems, excessive cost, and performance concerns that remain unresolved. It appears appropriate to eliminate the fluid-applied asphalt coating, particularly for more modest surface barrier designs and those that do not require gas control.

- Moisture Measurements. The neutron method was the chosen method for measuring soil water content. The method was found to be very reliable but relatively labor intensive. Should additional water content monitoring be warranted (i.e., for post-closure monitoring), alternate reliable methods should be evaluated that are conducive to automation.

- Vegetative Cover. The establishment of a viable and highly diverse plant community on the silt-loam surface continues to have significant impact on the function of the barrier after 4 years of testing. The complete coverage of the soil by deep-rooted plants is responsible for the annual drying of the soil profile, even with three times normal precipitation. Both species of shrubs, rabbitbrush and sagebrush, were sensitive to sustained elevated precipitation, and the dominance of shallow-rooted grasses in one section of the barrier reduced the efficiency of the water recycling process. The ideal plant community to optimize silt-loam performance is one composed of grasses and native, deep-rooted perennial shrubs, preferably sagebrush. Artificial seeding of grasses and planting of shrub seedlings in the late fall and winter is recommended to enhance early establishment of preferred plants and to limit the invasion of undesirable species.

  In contrast, the lack of vegetation on the side slopes limits drying as attested by the high rates of measured drainage for both the riprap and the gravel side slopes. The lack of fine soil on either side slope minimized its water-holding capacity and kept the seedbed surface dry so that seed germination and plant establishment was minimized. Bare surfaces or sparse vegetation will likely dominate the side slopes for many years to come; thus, drainage from the side slopes is expected to persist. While designed to accommodate the lack of vegetation, by using a low-permeability asphalt layer to shed

water, the impact of side-slope drainage must be accounted for in determining the overall performance of abovegrade barriers and their relationship with surrounding waste sites.

- Erosional Control Components. In the upper silt-loam layer, the 15 wt% pea gravel admix effectively optimized erosional control without affecting plant establishment or recycling of water. After the simulated 1,000-year rainfall event, even in the absence of a well-established plant cover, surface runoff was held to less than 3% of the applied precipitation, and sediment yield was minimized. Deflation was limited to the first 3 months after construction, and the initial soil loss was sufficient to initiate surface armoring. These results show that the silt-loam-gravel admix offers effective control of erosional stresses and should be used in future designs.

- Animal Intrusion. Although observations of animal intrusion were minor in nature, animal use did increase over the test period. It is reasonable to expect that animal use will continue to increase to some degree as the vegetative cover matures. As a result, animal intrusion inspections should continue to be performed annually.

Test results considered to be directly applicable to the other graded barrier designs include ease of construction, asphalt permeability results, the general hydrologic effectiveness of the silt-loam/capillary break component, the effectiveness of the silt-loam/pea gravel admix in limiting erosion, riprap as a preferred side-slope configuration, and the use of a diverse native plant cover of grasses and shrubs.

Several design issues have been previously identified in DOE-RL (1996, 1999) as priority topics for future barrier development work and are discussed in the following sections. As is the case with settlement and subsidence, previous recommendations have been updated to reflect the information gained from the treatability test. In addition, modeling and breakthrough data needs to support future barrier design efforts are discussed.

- Asphalt Durability Assessment. The durability of the low-permeability asphalt layer in the Hanford Barrier and the Modified RCRA Subtitle C Barrier remains a design issue. Preliminary information from analog studies of natural asphaltic materials (Waugh et al. 1994) indicates that asphaltic materials are likely to exhibit adequate durability for surface barriers with design life criteria of 500 or 1,000 years. An investigation is planned in FY 2000 to obtain defensible data on the long-term performance of asphaltic materials for surface barrier applications.

- Settlement and Subsidence. Settlement and subsidence refer to various forms of soil response to surcharge loading of the site surface. In the context of surface barriers, surcharge loading refers to the weight of the barrier materials. A general engineering study had been previously recommended by DOE-RL (1996) to address potential settlement and subsidence concerns associated with various types of waste sites in the 200 Areas. However, subgrade settlement measurements made as part of the 200-BP-1 treatability test have shown a minor response to the weight of the barrier at a typical waste site (i.e., crib). This is significant considering that the Hanford Barrier is the thickest of the three graded barrier designs and generates the highest surcharge loads.

Settlement and subsidence concerns are expected to be site-specific issues that can be addressed as part of the site-specific remedial design process that would include site-specific subgrade modification methods for eliminating subsidence potential when needed (e.g., solid waste burial grounds and timbered cribs).

- Material Availability. Material availability is an important consideration in deploying surface barriers. Materials specified in the graded barrier designs were generally perceived to be readily available, often on site. The McGee Ranch silt-loam borrow site used in the construction of the prototype Hanford Barrier was assumed as the source of fine soil in all designs. Under the current preferred use scenario identified in DOE (1999), the McGee Ranch silt may not be available for mining. A significant amount of effort has been given to characterizing the physical and hydraulic properties as well as material quantities of the McGee Ranch silt (Last et al. 1987, Lindberg and Lindsey 1993, Lindberg 1994, Skelly et al. 1994). If an alternate source of silt loam is needed, additional field and laboratory investigations needed to properly evaluate the alternative sources should be initiated. Of the various barrier components, the silt loam is expected to be the most sensitive material to source changes.

- Other Surface Barrier Performance Testing Needs. Full-scale field performance testing of previously untested designs (Modified RCRA C and D Barrier designs) was identified as a need to support implementation of the graded barrier approach (DOE-RL 1999). Construction of a Modified RCRA C Barrier over the 216-BY Cribs coupled with monitoring activities consistent with the 200-BP-1 feasibility study would help achieve this objective.

- Modeling Needs. The use of water balance models will be required to support future barrier design efforts and to evaluate long-term performance. Such models provide a means of rapidly evaluating design alternatives for optimization and demonstrating that regulatory or performance requirements will be met. Although the results from the treatability study of the Hanford Barrier can guide barrier design optimization, numerical tools are needed to quantitatively assess various design options in a holistic manner. It is recommended that available numerical models, such as UNSAT-H and HELP codes, be evaluated for their ability to simulate the hydrologic performance of graded barriers developed for the Hanford Site. An initial step in this evaluation should include a comparison of previous hydrologic simulations performed in DOE-RL (1996) to actual field data collected under the treatability test. Based on treatability test observations, two-dimensional modeling capabilities may be preferable to assess lateral hydraulic transport in the silt-loam layer at the capillary break. The overall purpose of the model evaluation would be to identify a preferred model for use in future barrier design efforts that would be accepted by the regulators. The preferred model could then be calibrated and verified against actual field data collected from the treatability test.

- Breakthrough Data Need. One significant parameter that was not determined from the treatability test was the total silt-loam water content at breakthrough (drainage through the silt loam). Although up to three times normal precipitation was applied to the barrier, the barrier was not sufficiently stressed for breakthrough to occur. It is recommended that breakthrough (field capacity) data be obtained as a function of bulk density and soil thickness to support model calibration and barrier design optimization (i.e., silt-loam thickness). Field capacity data can be obtained through either laboratory or field techniques.

5.0 REFERENCES

ASTM, 1990, *Standard Test Method for Field Measurement of Infiltration Rate Using a Double-Ring Infiltrometer with a Sealed-Inner Ring*, ASTM D5093-90, American Society for Testing and Materials, West Conshohocken, Pennsylvania.

Becker, E., 1994, "Prototype Barrier at 200-BP-1 Operable Unit," Letter Report for Project W-236, in *Prototype Hanford Barrier: Design Basis Document*, BHI-00007, Bechtel Hanford, Inc., Richland, Washington.

BHI, 1995, *Construction Quality Assurance Report for the Prototype Surface Barrier*, BHI-00432, Bechtel Hanford, Inc., Richland, Washington.

BHI, 1998, *Biotic Evaluation of Hanford Prototype Barrier*, Interoffice Memorandum 061792 to G. B. Mitchem, dated September 10, 1998, from S. G. Weiss, Bechtel Hanford, Inc., Richland, Washington.

Buckland, S. T., C. D. Campbell, L. A. Mackie-Dawson, G. W. Horgan, and E. I. Duff, 1993, "A Method for Counting Roots Observed in Minirhizotrons and Their Theoretical Conversion to Root Length Density," in *Plant and Soil*, 153, 1-9.

Comprehensive Environmental Response, Compensation, and Liability Act of 1980, 42 U.S.C. 9601 et seq., as amended.

Daniel, D. E., 1994a, *Preliminary Stability Analyses for Prototype Surface Barrier – 200 East Area*, Letter Report to N. R. Wing, Correspondence number 004803, dated August 28, 1994.

Daniel, D. E., 1994b, "Surface Barriers: Problems, Solutions, and Future Needs," G. W. Gee and N. R. Wing (eds.), pp. 441-487, in *In-Situ Remediation: Scientific Basis for Current and Future Technologies*, Battelle Press, Columbus, Ohio.

Daniel, D. E., B. A. Gross, R.C. Bachus, C. H. Benson, J. Boschuck, Jr., S. Dutta, L. G. Everett, H. Freeman, G. W. Gee, E. Kavazanjian, Jr., R. M. Koerner, R. E. Landreth, W. E. Limbach, S. Melchior, R. W. Ridky, P. R. Schroeder, K. Skahn, J. C. Stormont, A. Street, F. C. Walberg, and T. F. Zimmie, 1996, "Caps," in R. R. Rumer and J. K. Mitchell (eds.), pp. 119-140, *Assessment of Barrier Containment Technologies*, International Containment Technology Workshop, August 1995, Baltimore, Maryland.

Daubenmire, R., 1959, "A Canopy-Coverage Method of Vegetational Analysis," in *Northwest Sci.*, 33:43-64.

DOE, 1987, *Final Environmental Impact Statement for Disposal of Hanford Defense High-Level, Transuranic and Tank Wastes*, DOE/EIS-0113, U.S. Department of Energy, Washington, D.C.

DOE, 1998, *Revised Draft Hanford Remedial Action – Environmental Impact Statement and Comprehensive Land Use Plan*, DOE/EIS-0222D, U.S. Department of Energy, Washington, D.C.

DOE-RL, 1990, *Remedial Investigation/Feasibility Study Work Plan for the 200-BP-1 Operable Unit, Hanford Site, Richland, Washington*, DOE/RL-88-32, Rev. 1, U.S. Department of Energy, Richland Operations Office, Richland, Washington.

DOE-RL, 1993a, *Phase I Remedial Investigation Report for the 200-BP-1 Operable Unit*, DOE/RL-92-70, Rev. 0, U.S. Department of Energy, Richland Operations Office, Richland, Washington.

DOE-RL, 1993b, *Treatability Test Plan for the 200-BP-1 Prototype Surface Barrier*, DOE/RL-93-27, Rev. 0. U.S. Department of Energy, Richland Operations Office, Richland, Washington.

DOE-RL, 1994a, *Construction Report for the 200-BP-1 Prototype Surface Barrier*, DOE/RL-94-76, Rev. 1, U.S. Department of Energy, Richland Operations Office, Richland, Washington.

DOE-RL, 1994b, *Feasibility Study Report for the 200-BP-1 Operable Unit*, DOE/RL-93-35, Rev. 1, U.S. Department of Energy, Richland Operations Office, Richland, Washington.

DOE-RL, 1996, *Focused Feasibility Study of Engineered Barrier for Waste Management Units in the 200 Areas*, DOE/RL-93-33, Rev. 1, U.S. Department of Energy, Richland Operations Office, Richland, Washington.

DOE-RL, 1999, *200 Areas Remedial Investigation/Feasibility Study Implementation Plan – Environmental Restoration Program*, DOE/RL-98-28, Rev. 0, U.S. Department of Energy, Richland Operations Office, Richland, Washington.

Frueh, W. T. and J. W. Hopmans, 1997, "Soil Moisture Calibration of a TDR Multilevel Probe in Gravelly Soils," in *Soil Sci.*, 162(8):554-565.

Fryrear, D. W., 1986, "A Field Dust Sampler," in *J. Soil and Water Conservation*, 41(2):117-120.

Gardner, W. H., 1986, "Water Content," p. 493-544, in *Methods of Soil Analysis, Part 1. Physical and Mineralogical Methods*, Agronomy Monograph No. 9 (2nd Edition), American Society of Agronomy, Madison, Wisconsin.

Gee, G. W., D. G. Felmy, L. L. Downs, J. C. Ritter, M. D. Campbell, M. J. Fayer, R. R. Kirkham, and S. O. Link, 1993a, *Field Lysimeter Test Facility Status Report IV: FY 1993*, PNL-8911, Pacific Northwest Laboratory, Richland, Washington.

Gee, G. W., L. L. Cadwell, H. D. Freeman, M. W. Ligotke, S. O. Link, R. A. Romine, and W. H. Walters, Jr., 1993b, *Testing and Monitoring Plan for the Permanent Isolation Surface Barrier Prototype*, PNL-8391, Pacific Northwest Laboratory, Richland, Washington.

Gee, G. W., H. D. Freeman, W. H. Walters, Jr., M. W. Ligotke, M. D. Campbell, A. L. Ward, S. O. Link, S. K. Smith, B. G. Gilmore, and R. A. Romine, 1994, *Hanford Prototype Surface Barrier Status Report: FY 1994,* PNL-10275, Pacific Northwest Laboratory, Richland, Washington.

Gee, G. W., A. L. Ward, B. G. Gilmore, M. W. Ligotke, and S. O. Link, 1995, *Hanford Prototype-Barrier Status Report: FY 1995,* Pacific Northwest National Laboratory, Richland, Washington.

Gee, G. W., A. L. Ward, B. G. Gilmore, S. O. Link, G. W. Dennis, and T. K. O'Neil, 1996, *Hanford Prototype-Barrier Status Report: FY 1996*, PNNL-11367, Pacific Northwest National Laboratory, Richland, Washington.

Gilmore, B. G. and W. H. Walters, 1993, *Water Erosion Field Tests for Hanford Protective Barriers: FY 1992 Status Report*, PNL-8949, Pacific Northwest Laboratory, Richland, Washington.

Green, R. E., L. R. Ahuja, and S. K. Chong, 1986, "Hydraulic Conductivity, Diffusivity and Sorptivity of Unsaturated Soils: Field Methods," in A. Klute (ed.), *Methods of Soil Analysis, Part 1,* Agronomy Monograph Series No. 9 (2nd edition), American Society of Agronomy, Madison Wisconsin, p. 771-798.

Hitchcock, C. L. and A. Cronquist, 1973, *Flora of the Pacific Northwest*, University of Washington Press, Seattle, Washington.

Hoitink, D. J. and K. W. Burk, 1995, *Climatological Data Summary 1996, With Historical Data*, PNL-11471, Pacific Northwest Laboratory, Richland, Washington.

Hook, W. R. and N. J. Livingston, 1996, "Errors in Converting Time Domain Reflectometry Measurements of Propagation Velocity to Estimates of Soil Moisture Content," in *Soil Sci. Soc. Am. J.*, 60:35-41.

Hook, W. R ., N. J. Livingston, and Z. J. Sun, 1992, "Remote Diode Shorting Improves Measurement of Soil Water by Time Domain Reflectometry," in *Soil Sci. Soc. Am. J.*, 56:1384-1391.

Hudson, N., 1981, *Soil Conservation*, English Language Book Society, London, England.

Last, G. V., M. A. Glennon, M. A. Young, and G. W. Gee, 1987, *Protective Barrier Materials Analysis: Fine Soil Site Characterization*, PNL-6314, Pacific Northwest Laboratory, Richland, Washington.

Ligotke, M. W., 1993, *Soil Erosion Rates Caused by Wind and Saltating Sand Stresses in a Wind Tunnel*, PNL-8478, Pacific Northwest Laboratory, Richland, Washington.

Lindberg, J. W. and K. A. Lindsey, 1993, *Reconnaissance Geology of the McGee Ranch Site: Phase I Characterization*, WHC-SD-EN-TI-098, Rev. 0, Westinghouse Hanford Company, Richland, Washington.

Lindberg, J. W., 1994, *Geology of the McGee Ranch Site, Area B: Phase II Characterization*, WHC-SD-EN-TI-206, Rev. 0, Westinghouse Hanford Company, Richland, Washington.

Link, S. O., G. W. Gee, M. E. Thiede, and P. A. Beedlow, 1990a, "Response of a Shrub-Steppe Ecosystem to Fire: Soil Water and Vegetational Change," in *Arid Soils Research and Rehabilitation*, 4:163-172.

Link, S. O., G. W Gee, and J. L. Downs, 1990b, "The Effect of Water Stress on Phenological and Ecophysiological Characteristics of Cheatgrass and Sandbergs's Bluegrass," in *J. Range Management*, 43:506-513.

Link, S. O., W. J. Waugh, J. L. Downs, M. E. Thiede, J. C. Chatters, and G. W. Gee, 1994, "Effects of Coppice Dune Topography and Vegetation on Soil Water Dynamics in a Cold-Desert Ecosystem," in *J. Arid Environments,* 27: 265-278.

Link, S. O., L. L. Cadwell, M. R. Sackschewsky, D. S. Landeen, and K. L. Petersen, 1995a, *The Role of Plants and Animals in Isolation Barriers: Hanford, Washington*, PNL-10788, Pacific Northwest Laboratory, Richland, Washington.

Link, S. O., N. R. Wing, and G. W. Gee, 1995b, "The Development of Permanent Isolation Barriers for Buried Wastes in Cool Deserts: Hanford, Washington," in *Journal of Arid Land Studies*, 4:215-224.

Myers, D. R. and D. A. Duranceau (eds.), 1994, *Prototype Hanford Surface Barrier: Design Basis Document,* BHI-00007, Rev. 00, Bechtel Hanford, Inc., Richland, Washington.

Neter, J. and W. Wasserman, 1974, *Applied Linear Statistical Models*, R. D. Irwin, Inc., Homewood, Illinois.

Petersen, K. L., J. C. Chatters, and W. J. Waugh, 1993, *Long-Term Climate Change Assessment Study Plan for the Hanford Site Permanent Isolation Barrier Development Program*, WHD-EP-0569, Rev. 1, Westinghouse Hanford Company, Richland, Washington.

PNNL, 1999, *Hanford Barrier (PSB) Data CD-ROM*, letter #068770, dated May 24, 1999, from G. W. Gee, Pacific Northwest National Laboratory, to C. D. Wittreich, Bechtel Hanford, Inc., Richland, Washington.

Resource Conservation and Recovery Act of 1976, 42 U.S.C. 6901 et seq., as amended.

Rosenburg, N. J., B. L. Blad, and S. B. Verma, 1983, *Microclimate, The Biological Environment*, John Wiley and Sons, New York, New York.

Sehmel, G. A., 1980, "Particle Resuspension: A Review," in *Environ Int.*, 4:107-122.

Sehmel, G. A., 1984, "Deposition and Resuspension," in *Atmos Sci and Power Prod*, DOE/TIC-27601, pp. 533-583, National Technical Information Center, Office of Scientific and Technical Information, Oak Ridge, Tennessee.

Seigal, 1956, *Nonparametric Statistics for the Behavioral Sciences*, McGraw-Hill Book Company, New York, New York.

Skelly, W. A., C. J. Chou, J. W. Lindberg, and D. J. Hoff, 1994, *Material Properties Data and Volume Estimate of Silt Loam at the NRDWL Reserve, McGee Ranch*, WHC-SD-EN-TI-218, Rev. 0, Westinghouse Hanford Company, Richland, Washington.

Stone, W. A., J. M. Thorp, O. P. Gifford, and D. J. Hoitink, 1983, *Climatological Summary for the Hanford Area*, PNL-4622, Pacific Northwest National Laboratory, Richland, Washington.

Szeicz, G., G. Endrodi, and S. Tajchman, 1969, "Aerodynamic and Surface Factors in Evaporation," in *Water Resour. Res.*, 5:380-394.

Upchurch, D. R. and J. T. Ritchie, 1983, "Root Observations Using a Video Recording System in Mini-Rhizotrons," in *Agronomy J.*, 75:1009-1015.

Walters, W. H., K. A. Hoover, and L. L. Cadwell, 1990, *Project Test Plan for Runoff and Erosion on Fine-Soil Barrier Surfaces and Rock-Covered Side Slopes*, PNL-6791, Pacific Northwest Laboratory, Richland, Washington.

Ward, A. L. and G. W. Gee, 1997, "Performance Evaluation of a Field-Scale Surface Barrier," in *J. Environ. Qual.*, 26:694-705.

Ward, A. L. and G. W. Gee, 1998, "The Relationship Between Side-Slope Configuration, Precipitation, and Peripheral Recharge from Above-Grade Capillary Barriers," in *EOS Transactions*, 79(45):H31F-04.

Ward, A. L, G. W. Gee, and S. O. Link, 1997, *Hanford Prototype-Barrier Status Report: FY 1997*, Pacific Northwest National Laboratory, Richland, Washington.

Waugh, W. J., J. C. Chatters, G. V. Last, B. N. Bjornstad, S. O. Link, and C. R. Hunter, 1994, *Barrier Analogs: Long-Term Performance Issues, Preliminary Studies, and Recommendations*, PNL-9004, Pacific Northwest Laboratory, Richland, Washington.

Wischmeier, W. H., D. D. Smith, and R. E. Uhland, 1958, "Evaluation of Factors in the Soil-Loss Equation," in *Agric. Eng.*, 39(8): 458-462

Wischmeier, W. H. and D. D. Smith, 1978, *Predicting Rainfall Erosion Losses - A Guide to Conservation Planning*, Agriculture Handbook 537, U.S. Department of Agriculture, Washington, D.C.

APPENDIX A

PROTOTYPE HANFORD BARRIER DRAWINGS AND AERIAL PHOTOGRAPH

Figure A-1. Plan and West-East Cross Section of the Prototype Hanford Barrier Highlighting the Asphalt Layer Water Collection Zones.

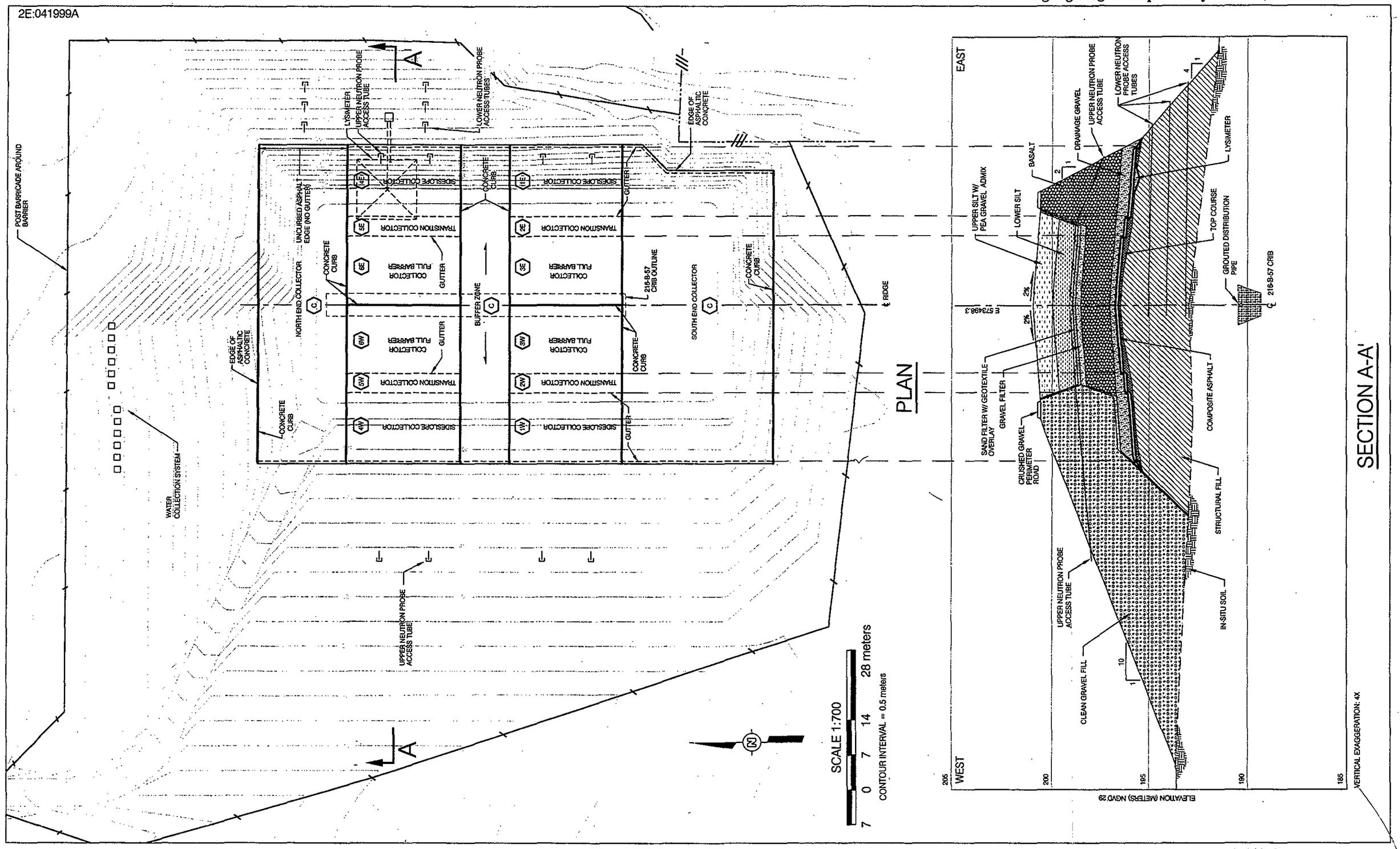

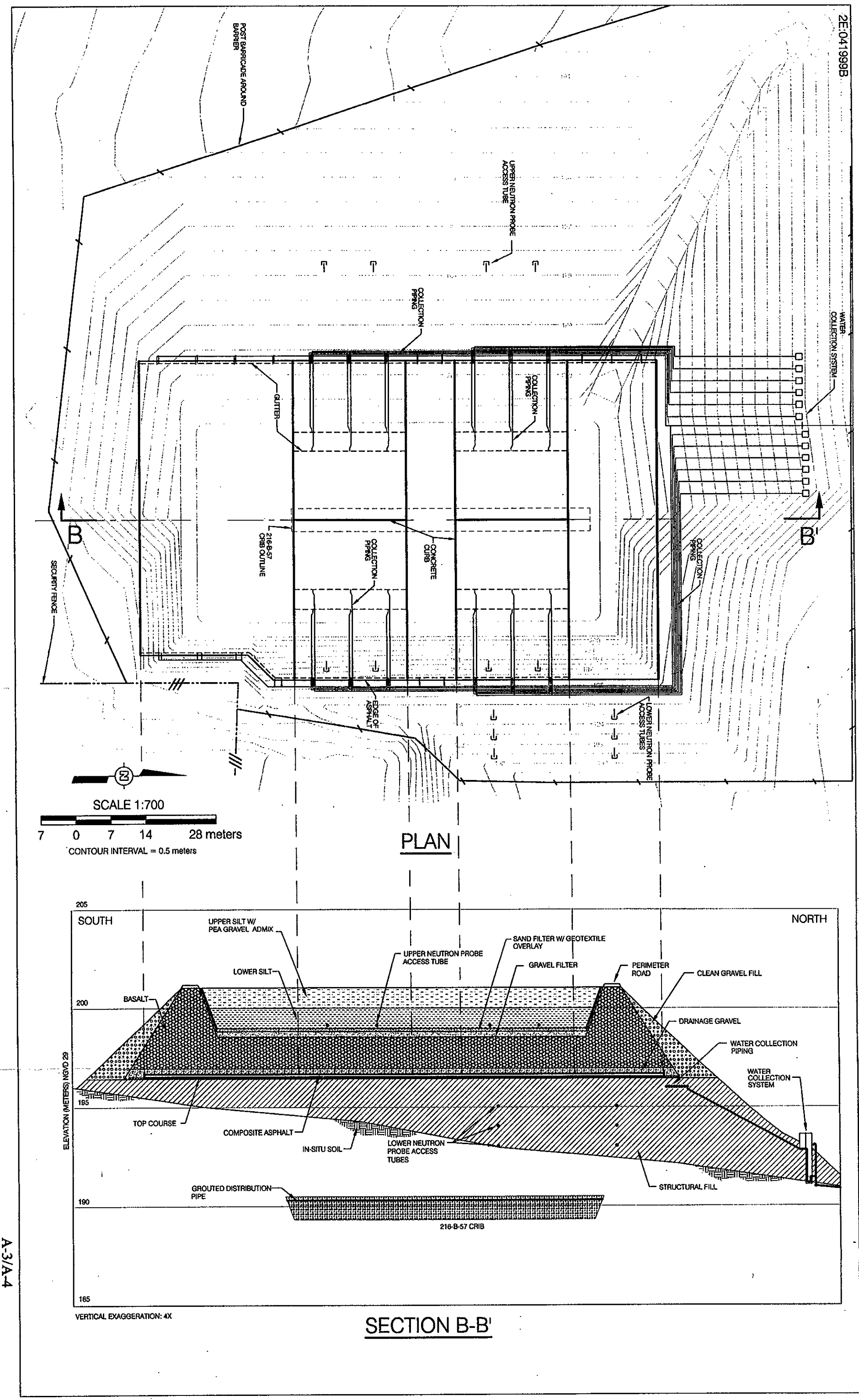

Figure A-2. Plan and North-South Cross Section of the Prototype Hanford Barrier Highlighting the Asphalt Drainage Collection System.

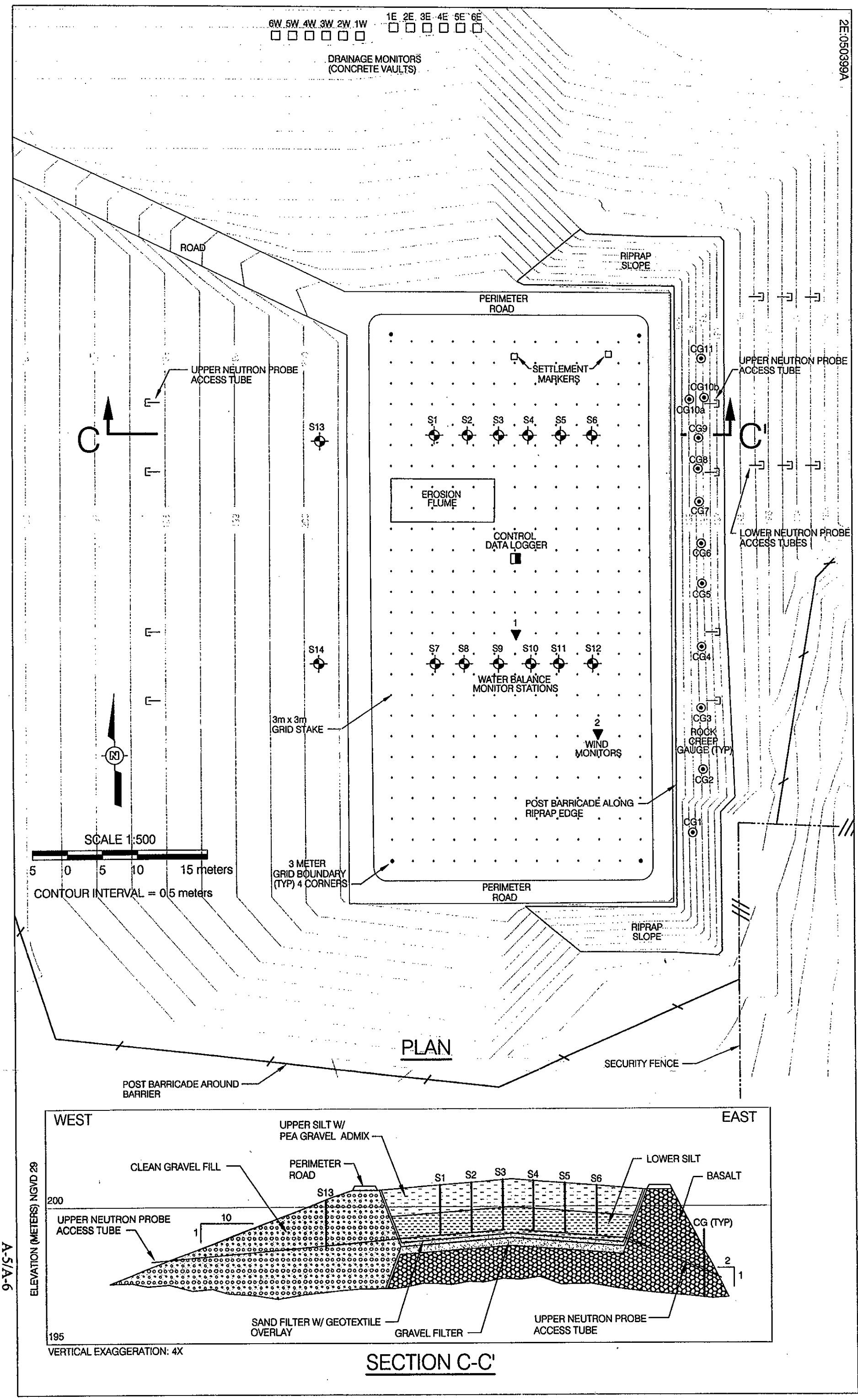

Figure A-3. Plan and East-West Cross Section of the Prototype Hanford Barrier and Surface Monitoring Stations.

Figure A-4. Aerial Photograph (September 1997) of the Prototype Hanford Barrier Taken on the North Side.

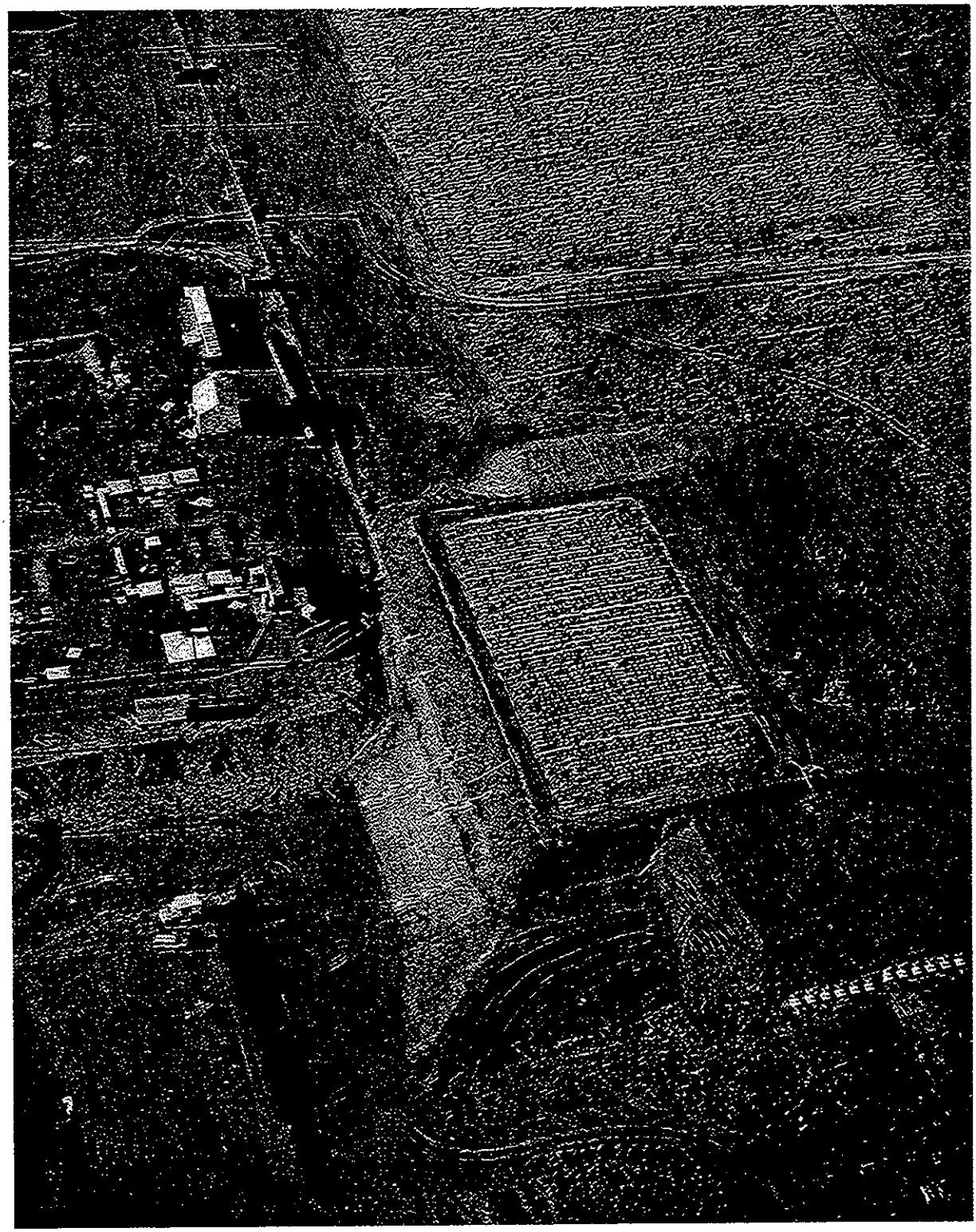

APPENDIX B

SUMMARY OF SOIL WATER STORAGE DATA FOR THE HANFORD BARRIER FOR WY 1995 THROUGH WY 1998

Table B-1. Soil Water Storage Data for the Hanford Barrier for WY 1995 Through WY 1998. (3 Pages)

Date	DOY	S1	S2	S3	S4	S5	S5	S7	S8	S9	S10	S11	S12
30-Sep-94	273	267.70	246.80	216.10	229.80	231.10	239.40	230.00	219.40	227.60	242.80	228.10	217.90
01-Nov-94	305	278.05	257.15	224.95	239.70	241.80	250.60	242.40	230.35	238.20	247.85	242.40	228.20
04-Jan-95	4	288.40	267.50	233.80	249.60	252.50	261.80	254.80	241.30	248.80	252.90	256.70	238.50
22-Feb-95	33	366.90	336.30	292.10	317.30	329.70	329.70	324.00	312.20	321.30	340.00	332.20	324.60
21-Mar-95	80	419.10	387.00	333.60	369.40	388.60	384.00	318.10	302.80	310.60	331.90	329.70	318.00
23-Mar-95	82	417.90	383.60	333.70	366.90	383.30	381.20	318.20	298.80	308.80	330.40	327.50	318.50
27-Mar-95	86	479.10	446.80	377.20	435.50	450.50	440.70	301.80	305.80	302.60	315.70	325.90	308.40
03-Apr-95	93	471.50	434.60	369.80	435.20	439.60	431.10	309.10	295.60	300.90	319.20	317.80	308.40
10-Apr-95	100	459.10	423.10	361.70	425.00	426.40	419.90	304.00	288.60	294.80	314.60	312.80	300.50
17-Apr-95	107	454.50	429.70	373.80	426.80	425.80	417.90	305.80	291.10	296.20	314.20	313.60	299.50
24-Apr-95	114	443.10	419.40	369.60	416.10	418.40	412.10	298.20	284.60	288.90	302.40	307.00	291.40
04-May-95	124	445.70	420.80	376.00	422.70	422.40	412.40	297.20	280.40	286.50	294.30	299.30	283.30
16-May-95	136	437.60	409.00	363.50	407.20	404.60	390.70	287.00	271.10	274.00	280.60	288.00	266.60
31-May-95	151	387.60	363.20	348.90	373.90	357.50	314.70	276.80	265.70	262.00	237.60	270.30	221.20
23-Jun-95	174	358.70	314.80	289.30	330.00	301.00	269.50	202.30	203.70	205.90	214.80	256.50	175.80
14-Jul-95	195	269.60	211.70	181.10	246.80	171.50	183.80	145.10	145.90	126.40	123.30	167.20	111.80
01-Aug-95	213	184.50	197.80	131.40	169.90	128.50	136.50	133.10	122.40	107.10	106.90	139.20	101.10
22-Aug-95	234	144.30	172.30	118.60	134.90	114.30	116.00	128.20	114.30	104.60	103.90	122.40	98.37
09-Sep-95	252	136.00	145.20	112.20	121.00	111.70	111.80	121.40	113.20	105.30	102.90	115.70	98.14
26-Sep-95	269	129.60	130.60	109.90	116.40	109.80	110.10	114.10	110.60	103.00	100.80	112.00	96.49
12-Oct-95	285	131.60	131.40	113.50	119.50	111.00	111.10	120.20	113.20	106.40	103.60	114.80	100.20
24-Oct-95	297	131.50	128.80	112.00	118.70	112.10	112.60	118.20	111.40	107.40	104.20	114.90	99.35
06-Nov-95	310	131.00	131.60	112.30	119.90	110.10	111.10	118.40	112.80	106.50	103.80	115.10	100.10
30-Nov-95	334	150.30	145.60	125.80	134.80	128.00	131.80	131.90	122.10	120.40	118.20	124.70	109.50
14-Dec-95	348	204.70	178.80	156.30	179.20	179.50	182.30	155.60	149.00	145.90	158.20	164.40	160.30
29-Dec-95	363	233.20	210.30	178.50	211.70	210.20	207.50	155.70	148.30	147.70	162.30	164.10	157.30
10-Jan-96	10	257.10	239.20	207.80	241.30	243.90	236.70	180.10	167.00	171.50	189.70	189.20	180.70
25-Jan-96	25	273.60	259.20	225.00	244.10	258.00	254.40	204.70	172.30	172.00	185.50	190.20	184.10
09-Feb-96	40	287.25	308.50	233.10	308.80	320.80	288.10	250.80	211.80	230.70	313.20	241.80	304.40
22-Feb-96	53	300.90	319.00	244.60	313.00	346.60	332.60	276.50	232.30	227.30	286.90	261.20	276.00
02-Mar-96	62	309.00	331.00	256.10	323.00	353.90	324.80	254.00	224.70	229.90	309.80	241.50	291.70
25-Mar-96	85	325.00	342.10	266.30	325.40	337.20	324.00	267.20	226.80	219.30	275.00	253.10	264.50
26-Mar-96	86	327.90	394.60	310.70	355.70	392.40	380.00	289.60	226.60	219.30	273.60	249.60	261.90

Table B-1. Soil Water Storage Data for the Hanford Barrier for WY 1995 Through WY 1998. (3 Pages)

Date	DOY	S1	S2	S3	S4	S5	S5	S7	S8	S9	S10	S11	S12
27-Mar-96	87	334.90	411.50	326.60	370.70	407.50	391.40	N/A	N/A	N/A	N/A	N/A	N/A
02-Apr-96	93	458.00	395.30	304.00	410.50	414.90	391.80	246.00	218.90	218.30	293.30	233.10	269.60
09-Apr-96	100	437.80	381.70	291.70	392.60	401.00	377.00	237.90	214.10	213.30	282.00	227.50	259.40
16-Apr-96	107	473.40	418.30	319.70	427.10	432.00	413.30	271.60	244.00	242.00	317.30	256.20	290.10
23-Apr-96	114	390.30	341.50	263.10	349.20	351.70	337.60	224.60	203.00	199.60	263.30	210.80	236.90
07-May-96	128	360.60	314.40	246.90	319.40	317.80	309.10	219.20	191.70	187.80	242.70	198.90	216.60
23-May-96	144	351.00	297.60	236.60	303.60	298.20	292.20	209.30	177.50	176.60	226.40	184.90	194.40
04-Jun-96	156	321.50	267.40	213.70	273.20	263.50	260.50	197.70	162.30	164.50	201.60	172.30	164.60
18-Jun-96	170	293.40	231.00	196.60	242.60	232.40	225.60	180.90	141.10	147.30	169.40	152.60	129.00
17-Jul-96	199	245.70	164.30	163.50	185.00	175.40	158.60	128.00	119.20	110.70	120.10	117.90	100.50
25-Jul-96	207	230.60	153.70	155.20	172.70	161.70	148.70	122.50	115.10	108.10	115.50	115.30	98.77
14-Aug-96	227	192.90	136.60	130.30	143.20	134.30	124.90	115.20	110.40	102.10	107.40	108.30	94.57
28-Aug-96	241	177.90	130.50	123.20	136.20	126.00	120.50	111.30	108.60	100.20	105.10	107.40	94.72
09-Sep-96	253	165.30	128.90	117.70	131.20	122.30	117.70	109.90	107.00	99.21	104.10	105.30	93.00
26-Sep-96	270	161.40	129.40	118.80	131.00	125.70	118.20	108.50	104.80	99.18	103.20	103.90	92.15
09-Oct-96	283	153.60	129.80	115.80	130.50	122.60	117.60	108.80	105.90	98.96	102.10	105.10	92.92
23-Oct-96	297	150.80	128.50	117.00	129.20	123.30	118.00	108.20	106.20	98.61	104.10	104.50	92.59
05-Nov-96	310	170.90	140.60	129.90	143.80	140.00	135.80	113.80	108.10	104.30	108.80	110.10	97.02
21-Nov-96	326	227.50	182.70	165.90	185.00	182.30	186.30	129.10	120.10	118.30	132.10	132.00	121.10
05-Dec-96	340	260.60	220.60	195.10	216.50	211.60	217.50	158.40	150.60	147.90	159.90	156.70	151.90
30-Dec-96	365	284.30	245.10	220.80	247.60	244.90	241.70	184.60	164.60	177.70	196.40	187.50	180.40
10-Jan-97	10	446.40	346.50	273.50	337.90	341.70	354.30	260.30	263.20	253.30	374.90	251.30	334.80
23-Jan-97	23	453.50	344.50	272.00	347.10	356.30	365.20	262.30	294.40	257.00	380.90	254.70	338.40
07-Feb-97	38	475.90	367.00	284.30	375.40	389.30	385.50	275.20	349.20	271.20	413.90	280.00	370.00
20-Feb-97	51	488.80	374.80	293.80	380.50	392.60	388.40	279.00	356.00	279.50	404.30	290.50	372.40
10-Mar-97	69	482.80	364.40	284.90	368.00	376.60	373.70	270.10	343.00	268.10	378.10	291.20	350.40
25-Mar-97	84	481.70	356.80	283.20	357.70	370.10	372.10	265.00	332.00	264.70	361.70	299.60	341.90
29-Mar-97	88	554.60	427.80	341.20	426.30	430.80	442.10	N/A	N/A	N/A	N/A	N/A	N/A
04-Apr-97	94	535.60	417.40	327.00	413.70	423.10	429.60	256.10	318.30	253.20	346.00	290.90	322.50
10-Apr-97	100	521.40	403.00	316.80	393.90	403.80	417.50	249.40	307.60	244.20	331.90	287.00	311.90
24-Apr-97	114	497.30	374.60	291.90	361.80	372.50	402.40	235.50	288.70	229.90	314.40	275.30	292.40
09-May-97	129	454.50	340.20	259.80	320.20	340.30	376.70	218.00	259.40	213.60	281.80	252.70	266.10
21-May-97	141	417.20	305.70	232.60	284.50	315.10	349.00	193.00	220.50	190.90	238.10	223.10	229.00

Table B-1. Soil Water Storage Data for the Hanford Barrier for WY 1995 Through WY 1998. (3 Pages)

Date	DOY	S1	S2	S3	S4	S5	S5	S7	S8	S9	S10	S11	S12
13-Jun-97	164	354.30	248.90	191.20	235.30	276.50	310.60	156.00	174.20	161.70	183.80	175.00	188.80
27-Jun-97	178	311.40	213.50	165.90	206.10	251.40	280.50	136.70	143.00	140.40	149.00	145.20	155.50
12-Jul-97	193	270.30	181.60	146.60	179.90	229.00	249.70	127.40	125.60	123.90	124.70	127.70	128.60
25-Jul-97	206	233.40	163.00	131.10	159.60	208.50	224.00	119.50	117.20	113.80	114.50	117.40	113.80
09-Aug-97	221	195.80	145.90	121.80	141.50	186.00	195.20	115.20	111.60	109.40	106.40	111.70	106.90
26-Aug-97	238	170.30	134.60	119.00	132.20	168.00	170.80	111.10	108.40	104.90	104.50	108.50	100.90
29-Sep-97	238	173.30	144.20	131.00	141.70	178.10	175.90	116.40	112.20	109.50	107.20	112.70	105.20
25-Oct-97	272	162.50	142.30	128.00	140.30	173.70	168.60	115.90	111.50	110.00	109.40	112.40	106.30
14-Nov-97	318	169.50	146.10	135.30	145.80	178.50	176.50	122.40	116.80	116.80	114.80	120.30	112.80
17-Dec-97	351	168.60	165.70	135.30	137.90	166.60	167.40	114.30	113.60	109.60	111.00	114.30	106.90
22-Jan-98	22	216.00	172.20	161.70	174.50	211.20	216.70	150.00	137.20	144.00	146.20	151.80	154.70
18-Feb-98	49	235.80	202.00	187.10	201.50	238.40	237.50	174.70	157.90	169.70	168.40	180.00	177.50
14-Mar-98	73	236.30	207.30	188.90	203.40	240.00	237.20	172.10	159.20	170.10	169.50	182.60	176.20
14-Apr-98	104	209.60	187.90	167.30	172.80	212.40	207.50	149.20	148.60	152.40	149.50	162.70	154.30
14-May-98	134	250.25	229.90	197.75	213.45	251.25	207.50	137.65	135.85	137.75	135.75	144.60	136.70
24-Jun-98	175	290.90	271.90	228.20	254.10	290.10	289.00	126.10	123.10	123.10	122.00	126.50	119.10
07-Jul-98	188	261.10	247.30	204.30	222.50	263.60	261.40	123.70	119.90	118.20	118.30	122.20	115.10
24-Aug-98	236	168.60	165.70	135.30	137.90	166.60	167.40	114.30	113.60	109.60	111.00	114.30	106.90

APPENDIX C

SUMMARY OF DRAINAGE DATA FOR THE HANFORD BARRIER FOR WY 1995 THROUGH WY 1998

Table C-1. Drainage Data for the Hanford Barrier for WY 1995 Through WY 1998. (2 Pages)

Date	Σ 1E	Σ 2E	Σ 3E	Σ4E	Σ 5E	Σ 6E	Σ 6W	Σ 5W	Σ4W	Σ 3W	Σ 2W	Σ 1W
30-Sep-94	1.00E-09	1.00E-09	1.00E-09	1.00E-09	1.00E-09	1.00E-09	1.00E-09	1.00E-09	1.00E-09	1.00E-09	1.00E-09	1.00E-09
31-Oct-94	2.00E-09	2.00E-09	2.00E-09	2.00E-09	2.00E-09	2.00E-09	2.00E-09	2.00E-09	2.00E-09	2.00E-09	2.00E-09	2.00E-09
30-Nov-94	3.00E-09	3.00E-09	3.00E-09	3.00E-09	3.00E-09	3.00E-09	3.00E-09	3.00E-09	3.00E-09	3.00E-09	3.00E-09	3.00E-09
31-Dec-94	4.00E-09	4.00E-09	4.00E-09	4.00E-09	4.00E-09	4.00E-09	4.00E-09	4.00E-09	4.00E-09	4.00E-09	4.00E-09	4.00E-09
31-Jan-95	5.00E-09	5.00E-09	5.00E-09	5.00E-09	5.00E-09	5.00E-09	5.00E-09	5.00E-09	5.00E-09	5.00E-09	5.00E-09	5.00E-09
28-Feb-95	6.00E-09	6.00E-09	6.00E-09	6.00E-09	6.00E-09	6.00E-09	6.00E-09	6.00E-09	6.00E-09	6.00E-09	6.00E-09	6.00E-09
31-Mar-95	7.00E-09	3.62E-04	7.00E-09	2.12E+00	7.00E-09	7.00E-09	3.68E-05	2.11E-02	4.92E+00	3.26E-05	1.48E-04	7.00E-09
30-Apr-95	2.20E+00	3.62E-04	8.00E-09	9.13E+00	8.00E-09	8.00E-09	3.68E-05	7.08E-01	1.45E+01	3.26E-05	1.48E-04	3.94E+00
31-May-95	3.15E+00	3.62E-04	9.00E-09	1.42E+01	1.89E-01	9.00E-09	3.68E-05	1.54E+00	2.14E+01	3.26E-05	1.48E-04	1.27E+01
30-Jun-95	3.35E+00	3.62E-04	1.88E-02	1.84E+01	4.89E-01	1.00E-08	3.68E-05	2.38E+00	2.76E+01	3.26E-05	4.88E-03	1.64E+01
31-Jul-95	3.36E+00	3.62E-04	2.01E-02	1.88E+01	4.89E-01	1.10E-08	3.68E-05	3.44E+00	3.27E+01	3.26E-05	2.73E-02	1.96E+01
31-Aug-95	3.36E+00	3.62E-04	2.01E-02	1.88E+01	4.89E-01	1.20E-08	3.68E-05	3.61E+00	3.68E+01	3.26E-05	4.51E-02	2.23E+01
30-Sep-95	3.43E+00	3.62E-04	2.01E-02	1.93E+01	4.89E-01	1.30E-08	3.68E-05	4.07E+00	3.99E+01	3.26E-05	4.51E-02	2.47E+01
31-Oct-95	3.71E+00	3.62E-04	2.01E-02	1.97E+01	4.89E-01	1.40E-08	3.68E-05	4.53E+00	4.24E+01	3.26E-05	4.51E-02	2.65E+01
30-Nov-95	5.21E+00	6.04E-04	2.01E-02	2.26E+01	4.89E-01	7.16E-05	3.68E-05	4.54E+00	4.42E+01	3.26E-05	4.51E-02	2.87E+01
31-Dec-95	1.18E+01	7.25E-04	2.01E-02	5.98E+01	4.89E-01	1.07E-04	3.68E-05	4.64E+00	6.28E+01	6.53E-05	4.51E-02	3.23E+01
31-Jan-96	1.96E+01	7.25E-04	2.01E-02	8.18E+01	4.89E-01	1.07E-04	3.68E-05	4.71E+00	8.01E+01	6.53E-05	4.51E-02	3.88E+01
29-Feb-96	3.96E+01	1.33E-03	2.01E-02	1.15E+02	4.89E-01	3.94E-04	3.68E-05	4.72E+00	1.07E+02	6.53E-05	4.51E-02	6.02E+01
31-Mar-96	5.11E+01	1.45E-03	2.01E-02	1.63E+02	4.89E-01	3.94E-04	1.74E-02	5.10E+00	1.33E+02	6.53E-05	4.51E-02	7.09E+01
30-Apr-96	5.46E+01	1.45E-03	2.03E-02	1.76E+02	5.54E-01	1.40E-03	1.74E-02	5.66E+00	1.53E+02	6.53E-05	4.60E-02	7.75E+01
31-May-96	5.95E+01	2.42E-03	8.75E-02	1.82E+02	1.67E+00	1.40E-03	1.74E-02	6.03E+00	1.62E+02	6.53E-05	3.22E-01	8.26E+01
30-Jun-96	6.12E+01	2.90E-03	8.77E-02	1.86E+02	2.34E+00	1.40E-03	1.74E-02	6.29E+00	1.69E+02	6.53E-05	3.22E-01	8.64E+01
31-Jul-96	6.18E+01	2.90E-03	8.77E-02	1.89E+02	2.76E+00	1.40E-03	1.74E-02	6.52E+00	1.75E+02	6.53E-05	3.22E-01	8.97E+01
31-Aug-96	6.19E+01	2.90E-03	8.77E-02	1.90E+02	3.15E+00	1.40E-03	1.74E-02	6.80E+00	1.80E+02	6.53E-05	3.22E-01	9.25E+01
30-Sep-96	6.19E+01	2.90E-03	8.77E-02	1.90E+02	3.48E+00	1.40E-03	1.74E-02	7.12E+00	1.84E+02	6.53E-05	3.22E-01	9.47E+01
31-Oct-96	6.42E+01	2.90E-03	8.77E-02	1.94E+02	3.56E+00	1.40E-03	1.74E-02	7.26E+00	1.86E+02	6.53E-05	3.22E-01	1.00E+02
30-Nov-96	7.37E+01	3.02E-03	8.77E-02	2.15E+02	3.56E+00	1.43E-03	1.75E-02	7.26E+00	1.93E+02	9.79E-05	3.23E-01	1.03E+02
31-Dec-96	9.74E+01	3.26E-03	8.77E-02	2.52E+02	3.57E+00	1.47E-03	1.75E-02	7.27E+00	2.19E+02	1.31E-04	3.23E-01	1.23E+02

Table C-1. Drainage Data for the Hanford Barrier for WY 1995 Through WY 1998. (2 Pages)

Date	Σ 1E	Σ 2E	Σ 3E	Σ4E	Σ 5E	Σ 6E	Σ 6W	Σ 5W	Σ4W	Σ 3W	Σ 2W	Σ 1W
31-Jan-97	1.30E+02	3.26E-03	8.78E-02	3.41E+02	8.54E+00	1.50E-03	1.76E-02	7.27E+00	2.81E+02	2.61E-04	3.23E-01	1.85E+02
28-Feb-97	1.57E+02	2.35E-02	8.78E-02	3.70E+02	8.54E+00	1.50E-03	1.76E-02	7.27E+00	3.16E+02	2.61E-04	3.23E-01	2.17E+02
31-Mar-97	1.65E+02	2.37E-01	8.78E-02	4.18E+02	8.54E+00	1.50E-03	1.76E-02	7.27E+00	3.34E+02	2.61E-04	3.23E-01	2.27E+02
30-Apr-97	1.74E+02	3.32E-01	8.78E-02	4.27E+02	9.67E+00	6.26E-02	1.76E-02	7.27E+00	3.53E+02	2.94E-04	3.23E-01	2.34E+02
31-May-97	1.79E+02	3.86E-01	8.78E-02	4.30E+02	1.15E+01	9.42E-02	1.76E-02	7.27E+00	3.62E+02	2.94E-04	3.23E-01	2.39E+02
30-Jun-97	1.83E+02	3.88E-01	8.78E-02	4.33E+02	1.15E+01	1.14E-01	1.76E-02	7.27E+00	3.68E+02	2.94E-04	3.23E-01	2.43E+02
31-Jul-97	1.85E+02	3.88E-01	8.78E-02	4.34E+02	1.15E+01	1.26E-01	1.76E-02	7.27E+00	3.73E+02	2.94E-04	3.23E-01	2.46E+02
31-Aug-97	1.85E+02	3.88E-01	8.78E-02	4.35E+02	1.15E+01	1.46E-01	1.76E-02	7.33E+00	3.78E+02	2.94E-04	3.23E-01	2.49E+02
30-Sep-97	1.85E+02	3.88E-01	8.78E-02	4.36E+02	1.15E+01	1.82E-01	1.76E-02	7.55E+00	3.81E+02	2.94E-04	3.23E-01	2.51E+02
31-Oct-97	1.86E+02	3.88E-01	8.78E-02	4.39E+02	1.15E+01	2.03E-01	1.76E-02	7.56E+00	3.84E+02	2.94E-04	3.23E-01	2.55E+02
30-Nov-97	1.87E+02	3.88E-01	8.82E-02	4.41E+02	1.15E+01	2.03E-01	1.76E-02	7.56E+00	3.87E+02	3.24E-04	3.23E-01	2.56E+02
31-Dec-97	1.87E+02	3.90E-01	8.87E-02	4.42E+02	1.15E+01	2.04E-01	1.82E-02	7.56E+00	3.88E+02	6.74E-04	3.25E-01	2.56E+02
31-Jan-98	1.91E+02	3.91E-01	8.90E-02	4.48E+02	1.15E+01	2.04E-01	1.85E-02	7.56E+00	3.90E+02	9.95E-04	3.27E-01	2.56E+02
28-Feb-98	1.95E+02	3.91E-01	8.90E-02	4.61E+02	1.15E+01	2.04E-01	1.85E-02	7.56E+00	3.95E+02	9.95E-04	3.27E-01	2.57E+02
31-Mar-98	1.97E+02	3.91E-01	8.90E-02	4.65E+02	1.15E+01	2.04E-01	1.85E-02	7.56E+00	4.03E+02	9.95E-04	3.27E-01	2.60E+02
30-Apr-98	1.97E+02	3.92E-01	8.94E-02	4.67E+02	1.15E+01	2.04E-01	1.89E-02	7.57E+00	4.09E+02	1.29E-03	3.28E-01	2.64E+02
31-May-98	1.98E+02	3.92E-01	8.94E-02	4.67E+02	1.15E+01	2.04E-01	1.89E-02	7.57E+00	4.13E+02	1.29E-03	3.28E-01	2.68E+02
30-Jun-98	1.99E+02	3.92E-01	8.94E-02	4.69E+02	1.15E+01	2.04E-01	1.89E-02	7.57E+00	4.16E+02	1.29E-03	3.28E-01	2.71E+02
31-Jul-98	2.00E+02	3.92E-01	8.94E-02	4.70E+02	1.15E+01	2.04E-01	1.89E-02	7.57E+00	4.19E+02	1.29E-03	3.28E-01	2.73E+02
31-Aug-98	2.00E+02	3.92E-01	8.94E-02	4.71E+02	1.15E+01	2.04E-01	1.89E-02	7.57E+00	4.22E+02	1.29E-03	3.28E-01	2.76E+02
30-Sep-98	2.00E+02	3.92E-01	8.94E-02	4.71E+02	1.15E+01	2.04E-01	1.89E-02	7.57E+00	4.24E+02	1.29E-03	3.28E-01	2.77E+02

DISTRIBUTION

U.S. Department of Energy,
Richland Operations Office

B. L. Foley (5)	H0-12

ERC Team

M. A. Buckmaster, BHI	X9-10
R. Boutin, BHI	H0-19
F. M. Corpuz, BHI	X9-06
K. R. Fecht, BHI	H0-02
B. H. Ford, BHI (2)	H0-21
R. P. Henckel, BHI	S3-21
G. B. Mitchem, BHI	H0-17
S. E. Parnell, CHI	H9-01
S. W. Petersen, BHI (2)	H0-02
C. D. Wittreich, CHI (10)	H9-03
Document and Information Services (3)	H0-09
DOE-RL Public Reading Room	H2-53
Hanford Technical Library	P8-55

Pacific Northwest National Laboratory

G. W. Gee (10)	K9-33
T. L. Stewart	K9-18
A. L. Ward (2)	K9-33

PHMC

F. M. Mann	R1-04
A. J. Knepp	H0-02
W. A. Skelly	H3-26
M. I. Wood	H6-06